January 2018

Predictable Reliability In Inter-Vehicle Communications

Chuan Li
Wayne State University, chuan@wayne.edu

PREDICTABLE RELIABILITY IN INTER-VEHICLE COMMUNICATIONS

by

CHUAN LI

DISSERTATION

Submitted to the Graduate School

of Wayne State University,

Detroit, Michigan

in partial fulfillment of the requirements

for the degree of

DOCTOR OF PHILOSOPHY

2018

MAJOR: COMPUTER SCIENCE

Approved By:

_____

Advisor Date

_____

_____

_____

_____

DEDICATION

To my wife, my parents, my brother, and my parents in-law.

ACKNOWLEDGMENTS

First, I would like to thank my advisor Dr. Hongwei Zhang for his guidance in my Ph.D journey. His knowledge, advices, methods, attitude, patience impressed me so much. His unyielding belief in research and perseverance have been and will be my top reference in doing things in my life hereafter. Without his help, I would not finish my dissertation. I also want to thank Dr. Le Yi Wang, Dr. George Yin for their valuable feedbacks in my research problems, and Dr. Loren Schwiebert, Dr. Nathan Fisher, and Dr. Pei-Yong Wang for serving as my committee members and their feedbacks.

Second, I would also thank all my lab-mates at Dependable Networking and Computing (DNC) research group at Wayne State University, Dr. Xin Che, Dr. Qiao Xiang, Dr. Xiaohui Liu, Yu Chen, Qing Ai, Ling Wang and Pengfei Ren , for all the collaborations. Working with you is a valuable memory that I will cherish forever.

Last but not least, I want to show my sincere gratitude to wife, my parents and my brother. All difficulties and challenges were fragile when facing with your support and love.

TABLE OF CONTENTS

LIST OF FIGURES

LIST OF TABLES

CHAPTER 1: INTRODUCTION

1.1 Wireless Networked Sensing and Control Systems

Evolving from the traditional centralized wired control systems, wireless networked sensing and control (WSC) systems feature distributed control in wireless networks [1]. In WSC systems, communication network is an indispensable component which is responsible for digital signal transmissions. As the name implies, WSC systems adopt wireless networking technologies to reduce deployment cost and possibly improve system maintenance experience. Due to dynamics in non-deterministic and asymmetric signal propagation in wireless medium, communications in WSC systems suffer from packet loss. As a result, WSC systems may not react immediately to system changes because of communication failures. There has been a lot of research efforts on this topic that try to improve WSC system performance. One of the goals is to ensure reliable communication for each link in communication systems. Reliable communication is a key factor to guarantee predictable system behavior given that control feedback is crucial for close-loop control systems. Interestingly, there exists an inherent trade-off among network throughput, delay, and reliability [2]. Due to the different impacts reliability, delay, and throughput have on WSC systems, a WSC system usually requires fine-grained control over the trade-off to guarantee system performance. As a first step toward predictable system behavior and performance in WSC systems, we focus on predictable and controllable link reliability guarantee. By controlling link reliability, people can tune the trade-off to their needs and move WSC systems to the optimal operation point where their benefits are maximized.

Unlike traditional WSC systems that adopt static wireless sensor to form communication networks, WSC in vehicular networks is more challenging. First, the open environments in which vehicles move are more unpredictable since they may contain trees, buildings, rivers, tunnels , and mountains, etc. Such environmental factors affect wireless signal propagation significantly; Second, the high mobility of vehicles causes inter-vehicle communication network topology (in terms of vehicle distribution) to change constantly . Information exchanged in such network requires frequent update in order to remain valid. Existing solutions for communication networks in tradi-

tional static WSC systems usually cannot perform well in inter-vehicle communication networks. Such unique challenges in inter-vehicle communication networks demands new solutions; Third, solution evaluation for inter-vehicle communication networks usually relies on simulation since real world evaluation platforms have high cost. Although several simulators that can be tuned to evaluate solutions for inter-vehicle communication networks, they all tend to be inaccurate. To improve evaluation accuracy, researchers have implement a PHY layer for the ns-3 simulator [3] that simulates signal processing process [4]. Despite many decent efforts people have made, simulation time of solution evaluation remains a challenge due to high density and the large-scale nature of inter-vehicle communication systems.

One of the fundamental cause to packet reception failures in wireless communication is interference. It is difficult for packet receivers to correctly decode packets when large interference exists simultaneously. Interference modeling in the past literature falls into three categories: *protocol model*, *physical model*, and their *hybrid*. Recently, a hybrid model, the Physical-Ratio-K (PRK) interference model, was proposed in [5] which combines the strengths of the previous two models and is suitable for distributed scheduling. We show in Chapter 2 and Chapter 3 that the PRK model is able to model interference relations between network nodes accurately.

1.2 Contributions

In this section, we present the summary of our contributions and the outline of this dissertation.

- **PRK-based scheduling with predictable reliability guarantee for wireless networked sensing and control [6].** In this work, we solved an issue on reliable *unicast* communication. Network nodes adaptively declare their neighbors as conflicting with themselves based on their link reliability. The intuition is that when a link has low link reliability, the receiver of the link declare more neighbors as conflicting. On the contrary, when a link achieves higher reliability than it needed, the receiver of the link tries to declare fewer neighbors as conflicting in order to allow more neighbors to transmit concurrently and improve network throughput. We formulate the controllable link reliability problem into a regulation control

problem and design a controller to adaptively control the parameter of the PRK model such that the mean reliability of each link is no less than a given value, i.e., the communication reliability required by applications. Furthermore, we design a scheduling algorithm based on the control problem and address issues related to scheduling and protocol signaling.

- **Cyber-physical interference modeling for reliability of inter-vehicle communications [7].** With the previous work that guarantees predictable reliable communication in mostly-static networks, we switch our focus to a more challenging problem that involves high mobility. In this work, we address the one-hop *broadcast* problem in inter-vehicle communication networks. We use the same approach to control per-link reliability. However, a sender can have multiple receivers in broadcast settings. How do these receivers of the same sender cooperate to achieve reliable communication yet guarantee close-to-optimal network throughput is a key goal in this work. One of our major contributions in this work is to solve this problem. To this end, we define an approximated PRK model for inter-vehicle communication to address the problem of large communication overhead. We further propose mechanisms to let receivers *cooperatively* adapt their PRK model parameter K regarding the same sender. We also use unscented Kalman filter to estimate vehicle locations which are then used to estimate interference relationships between vehicles.
- **Enabling short-term reliability in inter-vehicle communication with power control.** In this work, we design a power control scheme and apply it jointly with a distributed scheduling strategy in order to achieve short-term packet successful reception probability guarantee. We extensively use samples from the network and estimate their statistics. We then use the statistics to guide our decision and provide probabilistic interference plus noise bound, power control feedback, etc. We also evaluate our solution in a network with complex yet realistic settings.

1.3 Organization

The rest of this dissertation is organized as follows: Chapter 2 describes the PRKS protocol that guarantees reliable communication in wireless sensor networks; Chapter 3 describes the CPS

protocol that enable reliable one-hop broadcast in inter-vehicle communication networks; Chapter 4 covers our solution for enabling short-term link reliability using power control techniques; Chapter 5 concludes this dissertation.

CHAPTER 2: SCHEDULING WITH PREDICTABLE LINK RELIABILITY FOR WIRELESS NETWORKED CONTROL

2.1 Introduction

Due to difficulties in achieving good control-ability in open-loop control, the embedded wireless networking community are exploring closed-loop sensing and control solutions for various applications such as real-time or environmental sensing [8]. Message passing in wireless networked sensing and control (WSC) is extremely important for network-wide or local coordinations among system components in WSC. Reliable and real-time message passing in mission-critical systems such as industrial process control is a basic requirement [8, 1]. However, various research efforts have revealed that the wireless medium is inherently dynamic and possesses uncertainties. Specific to wireless communications, collisions caused by co-channel interference introduced by concurrent transmissions are major sources of uncertainties [5, 9, 10]. To control interference and improve network throughput as well as reliability, scheduling algorithms become important for message passing in WSC systems.

Combining control and wireless networking together, WSC systems inherit both uncertainties in wireless communications and dynamics in control systems. Thus, WSC systems usually have different requirements on reliability and real-time in message passing [11]. While centralized scheduling algorithms generally yield better results compared to their counterparts, they can be infeasible in practice due to lack of infrastructure support or the large scale of networks themselves. Therefore, distributed scheduling algorithms become desirable for interference control in WSC networks. The state-of-art literature controls interference in scheduling by assuming the underlying interference model among network nodes is either protocol interference model or physical interference model. As [5] shows, neither of them should be used for designing distributed scheduling algorithms as they could be either inaccurate or infeasible, respectively.

The physical interference model considers all concurrent transmitters *network-wide* when deciding SINR values at receivers side, thus rendering high-fidelity results. However, since it requires network-wide information, it is combinatorial and not suitable for distributed scheduling

algorithm design as distributed algorithms should only use local information for decision-making. Scheduling algorithms based on physical interference model have strong assumptions on network-wide knowledge, node locations, as well as wireless channel conditions. All of these factors may not be available in practice. As a result, the physical interference model may not guarantee reliability and real-time in communication [12, 13, 14, 15]. There are also works that do not assume additive interference, such as [16], which is not true in practice. In addition, there are scheduling algorithms that aim at improving throughput and do not control multi-hop interference for reliability-aware scheduling [17, 5].

On the contrary, the protocol interference model is inherently local and suitable for distributed scheduling algorithm design as well as implementation. Yet it is not a perfect choice for practical work due to its flaws in representing real-world facts. For instance, network nodes beyond the region defined by protocol model can still be regarded as interfering nodes. [18]. In a field test, the RTS-CTS based handshake style scheduling algorithm only achieves packet delivery ratio (PDR) of around 50% [9]. [19] also shows that CSMA and RTS-CTS based medium access algorithms may only achieve PDR of 16.9% and 36.8% respectively. As a side note, PDR is defined as the ratio of the number of received packets to the number of transmitted packets of a link. General pairwise interference models have also been considered in theoretical study [20, 21], but the important question of how to identify the set of links that interfere with a link is not addressed, and their implementation usually assumes a model similar to the protocol model [21].

The above discussion has identified a need for a better interference model which should possess high fidelity comparable to that of the physical interference model and be suitable for distributed scheduling in WSC systems. The PRK interference model proposed in [5] integrates merits from both physical interference model and protocol interference model. As [6] shows, the PRK interference model help achieves accurate interference modeling by ensuring predictable packet delivery ratio under realistic assumptions. For a link with sender S and receiver R, a concurrent transmitter C interferes with data transmissions of S to R and thus may cause packet

decode errors at receiver R if and only if

$$P_{C,R} > \frac{P_{S,R}}{K_{S,R,T_{S,R}}}. \tag{2.1}$$

In the above equation, $P_{C,R}$ and $P_{S,R}$ denote signal strength introduced by C's transmission and S's transmission to receiver R, respectively. The parameter $K_{S,R,T_{S,R}}$ is the minimum real number chosen such that with all situations considered, the packet delivery ratio from S to R is at least $T_{S,R}$. $T_{S,R}$ is an application requirement posed by WSC systems.

The PRK interference model is local because its definition only needs $P_{C,R}$ and $P_{S,R}$ which are locally measurable. The application requirement $T_{S,R}$ is application-specific and is irrelevant to scheduling algorithm design regardless of distributed or centralized ones. As shown in [6], scheduling algorithms should tune the parameter $K_{S,R,T_{S,R}}$ in order to adapt network dynamics to meet the application required $T_{S,R}$. The PRK interference model is of high-fidelity because it requires network nodes to directly measure signal strength from close-by neighbors. As a result, it is able to capture different dynamics in wireless communications, for instance, small-scale and large scale fading, cumulative interference, etc. Experiment study and analysis in [5] have shown PRK interference model's potential in achieving required link reliability in scheduling. Scheduling algorithms using the PRK interference model can help reduce data delivery delay by minimizing packet retransmissions. [5] also shows PRK-based scheduling algorithms can enable throughput of 95% of what a physical model based scheduling can achieve. As a result, the PRK interference model is a promising model to achieve accurate interference control and is able provide agile adaptation to network dynamics.

The PRK work focuses on formulating the PRK interference model and its analytical characteristics but has not addressed the actual scheduling problem. Thus, the PRK-based scheduling problem is left open. To design a PRK-based scheduling algorithm, we have to address the following key issues.

- Due to variations in wireless channel, the parameter $K_{S,R,T_{S,R}}$ in Equation 2.1 may not be able to guarantee a minimum PDR of $T_{S,R}$. In such a case, how should a link $\langle S, R\rangle$ change the parameter $K_{S,R,T_{S,R}}$ to achieve $T_{S,R}$?
- For a link $\langle S, R\rangle$ and its PRK model parameter $K_{S,R,T_{S,R}}$, it defines an exclusion region $\mathbb{E}_{S,R,T_{S,R}}$ at the receiver R's side. According to the PRK interference model, only nodes $C \notin \mathbb{E}_{S,R,T_{S,R}}$ are allowed to transmit concurrently with S. However, interference range is generally larger than data communication range of nodes, how would a node ensure nodes in $\mathbb{E}_{S,R,T_{S,R}}$ do not transmit concurrently with itself, especially when wireless channels themselves have uncertainties?

To address the open question of PRK-based scheduling, we have designed a fully distributed, reliability-aware PRK-based MAC layer scheduling algorithm called *PRKS*. We have modeled the PRK interference model parameter $K_{S,R,T_{S,R}}$ instantiation problem as a minimum-variance regulation control problem. We designed such a controller and let it run at each link to allow each link to adapt the parameter $K_{S,R,T_{S,R}}$ independently in order to achieve the application requirement $T_{S,R}$. To prevent nodes in exclusion from transmitting concurrently, we have proposed to record neighbor average signal strength attenuation into a map, called signal map. Later when a link decides if a neighbor is in its exclusion region or not, the link checks if the calculated average signal strength that would be introduced by the same neighbor is greater than the signal strength that defines its exclusion region boundary. If smaller, the neighbor is not considered as in the links exclusion region and can transmit concurrently with the link itself. We propose to use control packets that are sent in a separate frequency domain to share information and build signal map records. One intuition of this decision is that PRKS needs high transmission power to allow nodes beyond normal data transmission range to receive packet correctly in order to decode necessary information piggybacked in control packets to enable signal strength attenuation calculation. Another intuition is that we do not wish transmissions for control packet generate extra deadly interference to normal data receptions.

We have implemented PRKS in ns-3.13 [3]. Through extensive experimental analysis, we observe that 1) the distributed controllers enable network-wide convergence to a state where the desired link reliabilities are ensured, 2) unlike existing scheduling protocols where link reliability can be as low as 2.49%, PRKS enables predictably high link reliability (e.g., 95%) in different network and environmental conditions without a priori knowledge of these conditions, 3) through local, distributed coordinations, PRK achieves a throughput very close to what is enabled by the state-of-the-art centralized scheduler iOrder [22] while ensuring the required link reliability.

The rest of the chapter is organized as follows. We elaborate on the design of PRKS in section 2.2, and we evaluate the performance of PRKS in section 2.3. We discuss related work in Section 2.4 and make concluding remarks in Section 2.5.

2.2 PRKS: PRK-based Scheduling

In this chapter, we focus on a scenario where network nodes do not move or move very slowly in a way such that for two nodes in the WSC network, the *average* signal attenuation between two nodes do not change fast. For instance, the average changes in minutes. This is so that the way we sample signal map records as will be discussed in Section 2.2.2 can achieve high accuracy in capturing average signal attenuations. We focus our scheduling algorithm on links chosen such that without interference, the expected data delivery ratio will be higher than the application requirement $T_{S,R}$. We will discuss achieving predictable link PDR in the next section. In this section, we first present the design of a minimum-variance controller. We then present a signal map sampling method in the NetEye sensor testbed. Finally, we discuss the distributed PRKS scheduling algorithm which is based on the PRK interference model.

2.2.1 A control-theoretic approach to PRK model instantiation

Minimum-variance regulation control. The intuition of designing a minimum-variance regulation controller is such that when network conditions change, a link $\langle S, R\rangle$ should be able to adapt to the changes by changing its PRK model parameter $K_{S,R,T_{S,R}}$ accordingly. Later in this section, we will present the control law. We formulate the problem of instantiating the parameter $K_{S,R,T_{S,R}}$ as a classical *regulation control* problem [23] in order to use the tool set control theory

offers to designing and reasoning. In the formulated control problem, the "reference input" is the application required link reliability $T_{S,R}$, and the "output" is the PRK model parameter $K_{S,R,T_{S,R}}$.

To formulate the control problem completely, we need to identify its "plant model", i.e., how would the PRK model parameter $K_{S,R,T_{S,R}}$ change given a link PDR output $Y_{S,R}$. This is challenging because the relation is complicated, and the decision depends on in-situ network dynamics which can be unpredictable. Intuitively, we notice that a PRK model parameter $K_{S,R,T_{S,R}}$ corresponds to a distribution of the background interference. By changing $K_{S,R,T_{S,R}}$, we are changing the background interference observed at the receiver R's side. To facilitate our discussion, let ΔI_R denote the change of interference at receiver R. We propose to use ΔI_R to be the actual control input for the minimum-variance controller. By doing so, we can employ findings of existing communication theory to drive the relation between $Y_{S,R}$ and ΔI_R as follows.

To ease the discussion, let $I_R(t)$ denote the background interference including a zero-mean white noise at receiver R's side in the unit of dBm at time t. Let $P_{S,R}$ be the received *normal* data reception signal strength in the unit of dBm. For a given modulation and coding scheme, according to communication theory, we have [5]

$$Y_{S,R}(t) = f(P_{S,R}(t) - I_R(t)), \tag{2.2}$$

In the above equation, $P_{S,R} - I_R$ represents the SINR value at receiver R's side in dB. $f(\cdot)$ is an increasing function that maps SINR value to PDR. Existing works have identified that $f(\cdot)$ is non-linear. To address the challenges in non-linear control, we propose to approximate function $f(\cdot)$ by multiple line functions. Depending on the current operating point of the control system, we use self-tuning regulators [23] to adapt controller behaviors. For SINR $\gamma(t) = P_{S,R}(t) - I_R(t)$ at time t, we approximate $f(\cdot)$ with the following linear function formulation:

$$Y_{S,R}(t) = a(t)(P_{S,R}(t) - I_R(t)) + b(t), \tag{2.3}$$

where $a(t)$ is the derivative of function $f(\cdot)$ when the $\gamma(t) = P_{S,R}(t) - I_R(t)$, that is, $a(t) = f'(P_{S,R}(t) - I_R(t))$, and $b(t) = f(P_{S,R}(t) - I_R(t)) - (P_{S,R}(t) - I_R(t))f'(P_{S,R}(t) - I_R)(t)$. Note that time t does not denote time slot. Instead, it denotes the time a link adapts its PRK model parameter $K_{S,R,T_{S,R}}$.

Given that background noise in sensor networks is normally formulated as a zero-mean random variable, we assume the noise keeps the same from time t to $t+1$. The interference experienced at receiver R's side can change due to the following reasons:

- From one controller adaptation happened at time t to the next controller adaptation happened at $t+1$, unless link reliability is exactly the same as $T_{S,R}$, the controller running on link $\langle S, R\rangle$ needs to adapt in order to meet the application requirement. We denote the PRK model parameter at time t as $K_{S,R,T_{S,R}}(t)$ and similarly denote the PRK model parameter at time $t+1$ as $K_{S,R,T_{S,R}}(t+1)$. Then we have $K_{S,R,T_{S,R}}(t+1) \neq K_{S,R,T_{S,R}}(t+1)$ if link reliability $Y_{S,R}(t+1) \neq T_{S,R}$. Due to the change in PRK model parameter K, the exclusion region defined by the parameter K also changes from t to $t+1$. We denote the two exclusion regions as $\mathbb{E}_{S,R,T_{S,R}}(t)$ and $\mathbb{E}_{S,R,T_{S,R}}(t+1)$ respectively. Assume $K_{S,R,T_{S,R}}(t+1) > K_{S,R,T_{S,R}}(t)$, then the link $\langle S, R\rangle$ should increase its exclusion region as compared to that at time t. In this case, nodes that belong to $\mathbb{E}_{S,R,T_{S,R}}(t+1) \setminus \mathbb{E}_{S,R,T_{S,R}}(t)$ and were once able to transmit before controller adaptation at time $t+1$ but can no longer transmit after the controller adaptation at time $t+1$ are the source of difference in background interference. We denote it as $\Delta I_R(t)$. Notice that this $\Delta I_R(t)$ is the control input to the minimum-variance controller. Note that similarly, if $K_{S,R,T_{S,R}}(t+1) < K_{S,R,T_{S,R}}(t)$, the link $\langle S, R\rangle$ should decrease its exclusion. Notice that nodes in $\mathbb{E}_{S,R,T_{S,R}}(t) \setminus \mathbb{E}_{S,R,T_{S,R}}(t+1)$ contributes to the background interference difference as denoted by $\Delta I_R(t)$
- Another source of interference difference comes from concurrent transmissions that happened outside of both $\mathbb{E}_{S,R,T_{S,R}}(t)$ and $\mathbb{E}_{S,R,T_{S,R}}(t+1)$. The concurrent transmitter set between t and $t+1$ can be different. Thus, the interference introduced by these concurrent transmitters also changes. We let $\Delta I_U(t)$ denote the change. Since the minimum-variance

controller only prevents nodes in exclusion region from transmission, $\Delta I_U(t)$ is out of the controller's control. We propose to model $\Delta I_U(t)$ as system disturbance. We use $\mu_U(t)$ to denote the mean of $\Delta I_U(t)$ and use $\sigma_U^2(t)$ to denote its variance.

According to the above discussion, we have

$$I_R(t+1) = I_R(t) + \Delta I_R(t) + \Delta I_U(t),$$

where $\Delta I_R(t)$ and $\Delta I_U(t)$ are in unit of dB. Using the linear approximation of function f as shown by Equation (2.3) at time t, the predicted link reliability for time $t+1$ calculates as follows:

$$Y_{S,R}(t+1) = a(t)(P_{S,R}(t+1) - I_R(t+1)) + b(t).$$

Therefore, the "plant model" for link $\langle S, R\rangle$ at time t is

$$\begin{aligned} I_R(t+1) &= I_R(t) + \Delta I_R(t) + \Delta I_U(t) \\ Y_{S,R}(t+1) &= a(t)(P_{S,R}(t+1) - I_R(t+1)) + b(t) \end{aligned} \tag{2.4}$$

where $I_R(\cdot)$ and $Y_{S,R}(\cdot)$ are the "state" and the "output" of the plant respectively. To deal with the noise in measuring $Y_{S,R}(\cdot)$, we use an exponentially-weighted-moving-average (EWMA) filter with a weight factor c ($0 \leq c < 1$) in the feedback loop [23]. Thus, the system model is as shown in Figure 2.1, where

$$\begin{aligned} y(t) &= cy(t-1) + (1-c)Y_{S,R}(t). \\ &= cy(t-1) + (1-c)[a(t-1)(P_{S,R}(t) - I_R(t)) + b(t-1)] \end{aligned} \tag{2.5}$$

Since dynamics in wireless communication and packet decoding process, the measured link reliability denoted as $y(t)$ in the previous formulation has oscillations. Also note that interference changes from outside of exclusion region of a link as denoted by $\Delta I_U(t)$ is beyond the controller's control, we propose to minimize the perturbations of the measured $y(t)$ on the condition that the

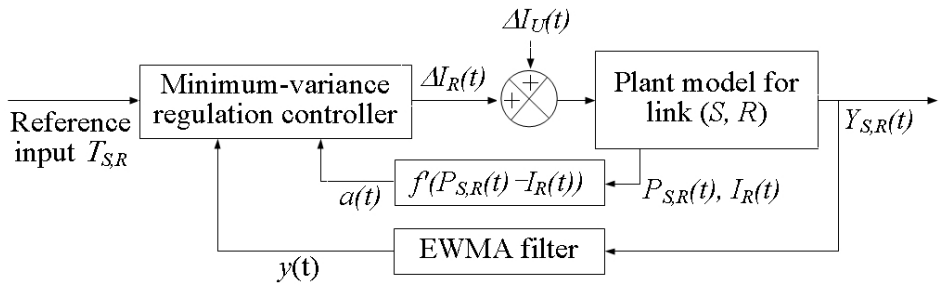

Figure 2.1: PRK model instantiation: minimum-variance regulation control diagram

average link reliability is still guaranteed, i.e., $E[y(t+1)] = T_{S,R} + \delta_Y$. Note that $\delta_Y \geq 0$ is used to control the probability of the measured $y(t)$ when it is smaller than $T_{S,R}$ which will be covered by Theorem 2 shortly. Formally, we have the following theorem for the minimum-variance control problem:

Theorem 1. *The control input that minimizes* $var[y(t+1)]$ *while ensuring* $E[y(t+1)] = T_{S,R} + \delta_Y$ *is*

$$\Delta I_R(t) = \frac{cy(t) + (1-c)Y_{S,R}(t) - T_{S,R} - \delta_Y}{(1-c)a(t)} - \mu_U(t), \tag{2.6}$$

and the minimum value of $var[y[t+1]]$ *is*

$$\sigma^2_{y,min}(t+1) = (1-c)^2 a(t)^2 \sigma^2_U(t). \tag{2.7}$$

(Interested readers can find the proof in [24].)

As we will show later, the scheduling algorithm depends on random numbers to decide transmitting node, thus we assume the concurrent transmitters are randomly distributed in the network. Therefore, we assume $\mu_U(t)$ tends to be zero statistically in our PRK-based scheduling problem settings. We have verified this claim by inspecting a typical link in the evaluation scenario specified in section 2.3. For instance, $\mu_U(t) = 0.00005$dB with a 95% confidence interval of $[-0.0453\text{dB}, 0.0452\text{dB}]$. Moreover, as figure 2.2 shows, $\Delta I_U(t)$ varies around zero dB with high probability. This justifies our claim on $\mu_U(t)$ is statistically zero. Therefore, in our future discussions, we will assume $\mu_U(t)$ is zero.

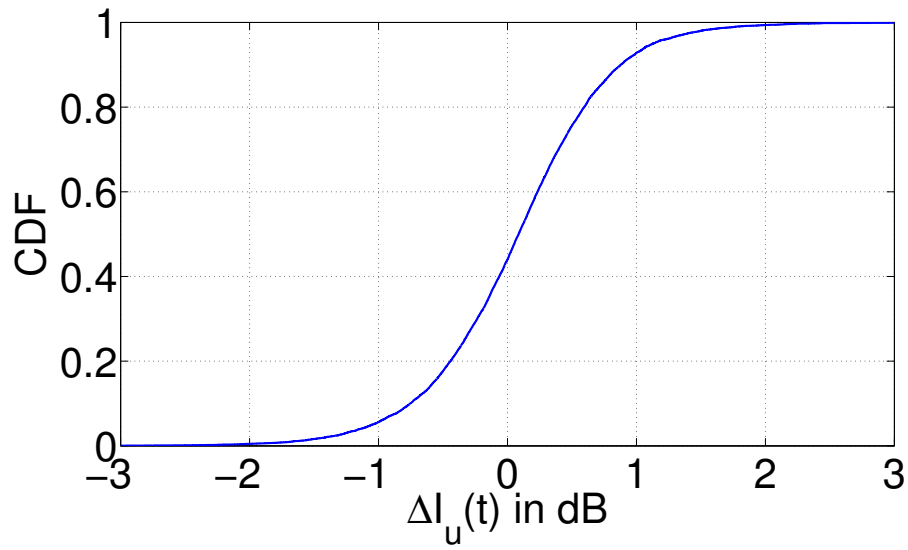

Figure 2.2: Cumulative distribution function (CDF) of $\Delta I_U(t)$ at a typical link

In theory, the design of the controller (2.6) guarantees the link reliability for link $\langle S, R\rangle$ is at least $T_{S,R}$. As mentioned earlier, the probability $Pr\{y(t) < T_{S,R}\}$ can be controlled by adjust $\delta_Y(t)$. For this issue, we have,

Theorem 2. *Pr*$\{y(t+1) \leq T_{S,R}\} \leq \dfrac{(1-c)^2 a(t)^2 \sigma_U^2(t)}{\delta_Y^2}$.

Proof. By Chebyshev Inequality,

$$\Pr\{|y(t+1) - E[y(t+1)]| \geq k\sigma_{y(t+1)}\} \leq \frac{1}{k^2}.$$

Thus,

$$\Pr\{y(t+1) \leq E[y(t+1)] - k\sigma_{y(t+1)}\} \leq \frac{1}{k^2}.$$

With the control design(2.6), $E[y(t+1)] = T_{S,R} + \delta_Y$. Thus,

$$\Pr\{y(t+1) \leq T_{S,R} + \delta_Y - k\sigma_{y(t+1)}\} \leq \frac{1}{k^2}.$$

Letting $\delta_Y - k\sigma_{y(t+1)} = 0$, we have $k = \dfrac{\sigma_y}{\sigma_{y(t+1)}}$. Thus

$$\Pr\{y(t+1) \leq T_{S,R}\} \leq \frac{\sigma^2_{y(t+1)}}{\delta_Y^2}.$$

From (2.7), $\sigma^2_{y(t+1)} = (1-c)^2 a(t)^2 \sigma_U^2(t)$ with the control design (2.6). Thus,

$$\Pr\{y(t+1) \leq T_{S,R}\} \leq \frac{(1-c)^2 a(t)^2 \sigma_U^2(t)}{\delta_Y^2}.$$

□

Theorem 2 shows that the undershoot probability is decided by three factors. c denotes the parameter we have chosen for EWMA filter, δ_Y is a non-negative parameter we used to guarantee the average link reliability to be at least $T_{S,R} + \delta_Y$. Notice that since our minimum-variance controller aims at minimizing the variance of $y(t)$, we can reduce the undershoot probability by increasing δ_Y. σ_U^2 is the interference difference variance from out side of receiver R's exclusion region. As our discussion reflected, we are interested in average link reliability. Short-term or expected per-packet reception probability is relegated as future work. In our evaluation, we let $\delta_Y = 0$ and $c = 15/16$.

From $\Delta I_R(t)$ to $K_{S,R,T_{S,R}}(t+1)$. To instantiate the PRK model parameter $K_{S,R,T_{S,R}}(t+1)$, we need to measure link reliability, signal strength from both S to R and neighbors to R. Since packet reception happens at receivers' side, and much information needed for instantiating PRK model parameter can directly be measured by R, receiver side becomes the perfect place for a link to run the minimum-variance controller with its input defined in Equation 2.6. Based on measured $y(t)$ and $y(t+1)$, and use our proposed controller, a receiver R is able to compute a control input $\Delta I_R(t)$. The actual PRK model parameter instantiation takes $\Delta I_R(t)$ as input and considers increasing $K_{S,R,T_{S,R}}(t+1)$ or decreasing $K_{S,R,T_{S,R}}(t+1)$ depending on the value of $\Delta I_R(t)$. More

specifically, we have:

$$\begin{cases} K_{S,R,T_{S,R}}(t+1) = K_{S,R,T_{S,R}}(t), & \text{if } \Delta I_R(t) = 0 \\ K_{S,R,T_{S,R}}(t+1) > K_{S,R,T_{S,R}}(t), & \text{if } \Delta I_R(t) < 0 \\ K_{S,R,T_{S,R}}(t+1) < K_{S,R,T_{S,R}}(t), & \text{if } \Delta I_R(t) > 0 \end{cases} \tag{2.8}$$

In case of exclusion region increase, $|\Delta I_R(t)|$ denotes the interference introduced by nodes in $\mathbb{E}_{S,R,T_{S,R}}(t+1) \setminus \mathbb{E}_{S,R,T_{S,R}}(t)$. Similarly, in case of exclusion region decrease, $|\Delta I_R(t)|$ denotes the interference introduced by nodes in $\mathbb{E}_{S,R,T_{S,R}}(t) \setminus \mathbb{E}_{S,R,T_{S,R}}(t+1)$. With the help of signal map records reside at receiver R's side, the PRK model parameter instantiation process, also called exclusion region adaptation process, can be achieved by only involving receiver R. We will discuss local signal maps in Section 2.2.2. Interested readers can check the detailed derivation of $K_{S,R,T_{S,R}}(t+1)$ at Section 2.1 of [24].

Stability of self-tuning adaptive control. As aforementioned, the controller design and analysis employ linear approximation (2.3) of a theoretical non-linear curve. The actual control output becomes less accurate as the system operating point digresses from the point of $T_{S,R}$. By inspecting theoretical SINR-PDR curve, we notice that when $y(t)$ is far away from the application required reliability, the slope of linear approximation lines (2.3) introduce either extremely slow convergence rate (when $y(t) \sim 0$) or too drastic changes (when $t(t) \sim 1$). This drastic changes usually cause system to be unstable. Assuming the target operating point is A where the link reliability is $T_{S,R}$ in Figure 2.3, for instance, applying the linear model (2.3) and the control input (2.6) when the operating point is B at time t will lead to $E[y(t+1)] = T_{B'}$, which is significantly lower than $T_{S,R}$ and thus leads to significant undershoot; similarly, applying the linear model (2.3) and the control input (2.6) when the operating point is C at time t will lead to $E[y(t+1)] = T_{C'}$, which is significantly higher than $T_{S,R}$ and thus leads to significant overshoot. Large undershoot and overshoot certainly harm system stability. With wireless communication dynamics causing

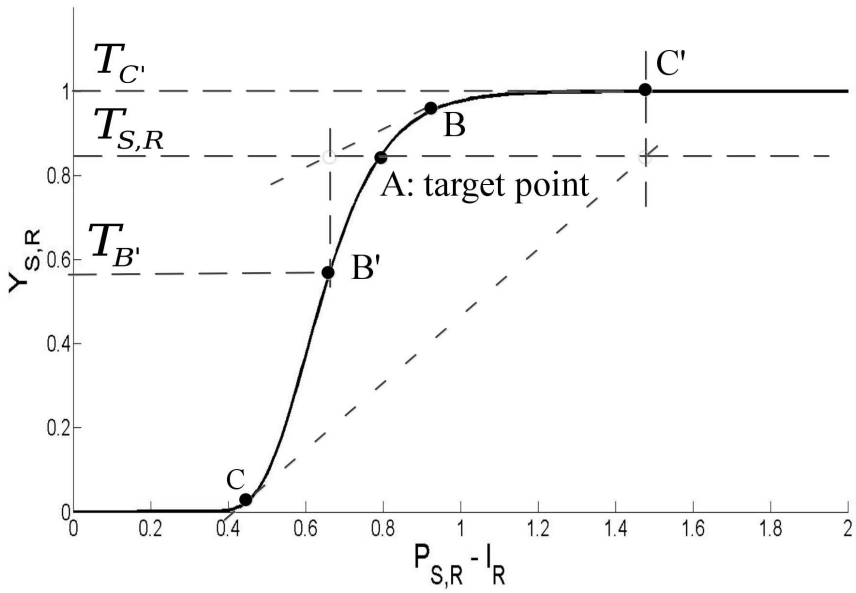

Figure 2.3: Convergence of adaptive control (2.6)

problem worse and the disturbance $\Delta I_U(t)$ which is beyond controller's control ability, we should avoid them.

We therefore propose to use the linear approximation that connects $y(t)$ and $T_{S,R}$ if $y(t)$ is quite different from $T_{S,R}$. Suppose we use $a_r(t)$ to denote the new slope of the linear approximation line, we revise the system and take value of $a_r(t)$ as follows:

$$a_r(t) = \begin{cases} a(t), & \text{if } |y(t) - T_{S,R}| \leq e_0 \\ a_0, & \text{if } |y(t) - T_{S,R}| > e_0 \end{cases} \tag{2.9}$$

where e_0 is a threshold value for the linear model (2.3) to be accurate around the neighborhood of $T_{S,R}$, and $a_0 = \dfrac{T_{S,R} - y(t)}{f^{-1}(T_{S,R}) - f^{-1}(y(t))}$ is the gradient of the line connecting the current operating point $y(t)$ and the target point $T_{S,R}$ on function $f(\cdot)$. Letting $a(t) = a_0$ when $|y(t) - T_{S,R}| > e_0$ avoids overshoot and undershoot in the feedback control of $K_{S,R,T_{S,R}}(\cdot)$ at link $\langle S, R\rangle$, thus preventing $Y_{S,R}(\cdot)$ from oscillating around $T_{S,R}$ for a given mean disturbance $\mu_U(\cdot)$ and helping enable network-wide convergence in the regulation control. Note that, according to Huang et al. [25], the functional form of f in Equation (2.2) and thus its gradient are much more stable than the specific

realization of f (e.g., specific mapping between $Y_{S,R}$ and $P_{S,R} - I_R$) across different network and environmental conditions; hence letting $a_r(t)$ be $a(t)$ instead of a_0 when $|y(t) - T_{S,R}| \leq e_0$ helps address the inaccuracy of the theoretical model (2.2) in practice. In our implementation, we use a value of 5% for e_0 [24].

2.2.2 Protocol signaling for real-world use of the PRK model

One fundamental requirement for the PRK-based scheduling algorithm to work is to prevent nodes lie in the exclusion region defined by the PRK model parameter $K_{S,R,T_{S,R}}(t)$ from transmitting. We use $\mathbb{E}_{S,R,T_{S,R}}(t)$ to denote the nodes defined by the PRK model parameter, i.e., a node $C \in \mathbb{E}_{S,R,T_{S,R}}(t)$ if and only if $P_{C,R}(t) \geq \dfrac{P_{S,R}(t)}{K_{S,R,T_{S,R}}(t)}$. This requirement is challenging due to the following aspects:

- The set $\mathbb{E}_{S,R,T_{S,R}}(t)$ is usually larger than the normal data communication range of receiver R. In this case, R cannot reach all nodes in $\mathbb{E}_{S,R,T_{S,R}}(t)$ using normal data transmission power.
- Wireless communication signal spreads in all directions, and can be anisotropic. It is difficult for receiver R to only inform nodes in its exclusion region $\mathbb{E}_{S,R,T_{S,R}}(t)$, no more and no less.
- Wireless communication channel is asymmetric in real-world settings, and signal attenuation from receiver R to a neighbor C and from the neighbor C to receiver R can be different. This would potentially make R and C see interfering relation differently. That is, R may believe C lies in its exclusion region, but C may not by inspecting $P_{C,R}$.

Local signal maps. To overcome the challenges listed above, we propose nodes in network maintain a *local* signal map themselves. For each node R, each of its signal map records contains the address, serving as ID, of one of its neighbor C and the average signal power attenuations h from R to C and from C to R. Note that the signal power attenuation from R to C is not directly available to R. Thus, C needs to send the average attenuation from R to C back to C as a feedback. When nodes transmit packets for the purpose of establishing signal maps, they also piggyback their packet transmission power in their packets. Receivers of such packets can then check the transmission power of the packets, and also by sampling local RSSI, they are able to infer the

signal attenuations between packet transmitters by themselves. Let P_C denote the piggybacked packet transmission power. As shown in Figure 2.4, $P_{C,R}$ denote the portion of received power introduced by C to R. Since the sampled RSSI as denoted by P_{total} also contains interference and noise, we use P'_I to denote interference plus noise. To infer signal attenuation, we need to remove P'_I from RSSI. To achieve this, we also let node sample RSSI immediately after a successful packet reception. The sampled RSSI as denoted by P_I is believed to be close to the value of P'_I, i.e.,

$$P_{C,R} = P_{total} - P'_I \approx P_{total} - P_I. \tag{2.10}$$

As we will discuss in Section 2.2.3, [24] has verified that P_{total} and P_I can be sampled at very short

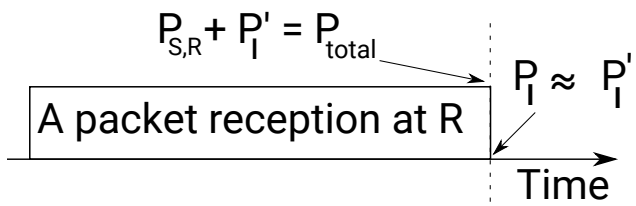

Figure 2.4: Estimation of signal power attenuation

intervals (e.g., less than 0.01 milliseconds for TelosB motes [26]) and that the background noise power as well as the interference power do not change much in such short intervals in CSMA/CA-based wireless networks, the sum of the background noise power and the interference power do not change much immediately before and immediately after a packet reception, i.e., $P'_I \approx P_I$. Once R gets a sample of $P_{C,R}$, it can compute a sample of $P'_{C,R}$ as

$$P'_{C,R} = P_C - P_{C,R}. \tag{2.11}$$

This way, R can get a series of samples of $P'_{C,R}$ and then use these samples to derive the average signal power loss from C to itself.

Notice that the above procedure involves no network-wide coordinations, thus is local. One advantage of this method is that it directly samples RSSI and is able to capture various dynamics in wireless communication, e.g., fading and shadowing. For instance, as mentioned in [24], Figure 2.5

shows the boxplot of the relative errors[1] in estimating power attenuation across links in the NetEye

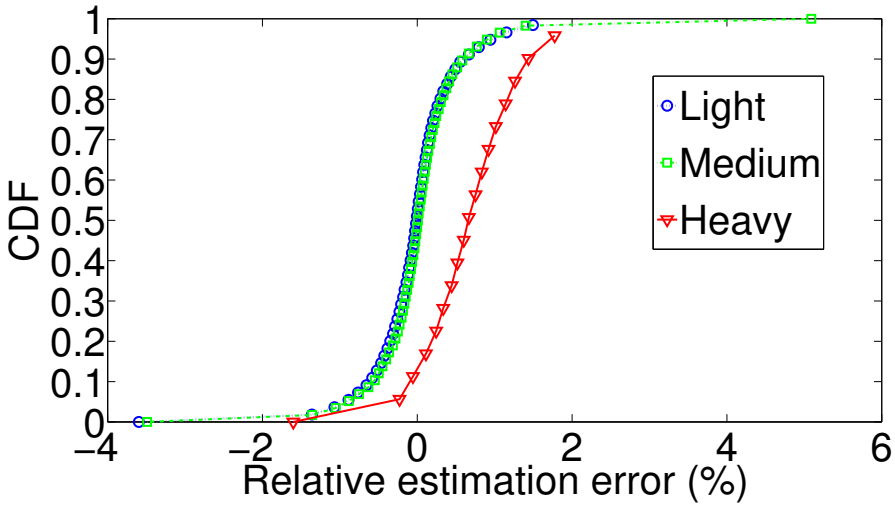

Figure 2.5: Relative errors in estimating link signal power attenuation in NetEye

[27] sensor network testbed when all the 130 TelosB motes transmit packets using the CSMA/CA-based B-MAC [28] and at an average inter-packet interval of 25 seconds, 2.5 seconds, and 0.1 seconds respectively, which we denote as light traffic, medium traffic and heavy traffic respectively. We see that the estimation is quite accurate. For instance, the relative estimation errors are all very close to 0 and almost always less than 2%; in addition, the 95% confidence interval for the median relative error is $[-0.0508\%, 0.0535\%]$, $[-0.0152\%, 0.0280\%]$, and $[-0.0087\%, 0.0245\%]$ for the light, medium, and heavy traffic condition respectively, thus the estimation error is 0 at the 95% confidence level for all traffic conditions. We have also observed similar accuracy for estimating link power attenuation in the Indriya testbed [29], showing the effectiveness of our method of signal power attenuation estimation in different network and traffic conditions; interested readers can find more detailed validation results for our estimation method in [30].

We maintain signal power attenuations in signal map instead of actual received signal strength so that if a node knows the transmission power (possible a different from the power when sampling attenuation) of a neighbor, the node can infer what will be the average reception power

[1]The relative error for a link is defined as the estimated attenuation minus the ground-truth attenuation and then divided by the ground-truth attenuation.

it will have when this neighbor node is transmitting. This is helpful when we do control signalling for our PRK-based scheduling algorithm in Section 2.2.3.

Protocol signaling based on signal maps. In this work, we propose to use a different channel for control signaling and assume communications in different frequency do not interfere with each other. Given that each $C \in \mathbb{E}_{S,R,T_{S,R}}(t)$ might be beyond normal data transmission range of R, we use the power control algorithm proposed by [31] to enable high control signal reception probability for each C. Thus, control signaling may use a transmission power level higher than what normal data transmissions normally use. With such a power control algorithm, we have addressed the challenges of signaling every interfering nodes in exclusion region which may well be much larger than normal data communication range. Considering the larger coverage of the entire network, the control signaling is still local.

For a receiver R, a sender S and a neighbor C, when R shares necessary information to neighbors so that neighbors (in this case C) can figure out if they interfere with R's data reception, C shares signal power attenuation from S to R, *signal power attenuation from C to R* as well as the PRK model parameter $K_{S,R,T_{S,R}}$ of link $\langle S, R\rangle$. Once C receives all the information, C is able to estimate interference it can introduce to R by checking attenuation from C to R and assuming *predefined* data transmission power. C can subtract the attenuation from transmission power. To make the estimation more accurate, C should also consider transmission and reception power gains as well as background noise. Once C figures out its potential interference to R, C can check the ratio of $\frac{P_{S,R}}{P_{C,R}}$ and see if the ratio is smaller than $K_{S,R,T_{S,R}}$. If the ratio is no smaller than $K_{S,R,T_{S,R}}$, C is considered as an interferer to S and should not transmit concurrently with S.

Since every node in the network can achieve this check by overhearing control messages in control channel, nodes in exclusion region will not transmit concurrently with the sender of the link that defines the exclusion region.

With the controller described in Section 2.2.1, our protocol signaling mechanism and the PRK model parameter instantiation method, we are able to develop a solution that has highly accurate interference relation identification. Since all operations are local, the solution is suitable

for distributed data transmission scheduling algorithm without infrastructure support in WSC networks.

2.2.3 Protocol PRKS: putting things together

With what we covered so far, we have a complete solution to identify interfering neighbors with high accuracy. What is left is the actual data transmission scheduling. Only if a sender, say S, transmits, shall all nodes in its corresponding receiver's, say R, exclusion not transmit. In this work, we assume normal data transmissions happen in the same channel. Thus, the major work is to address co-channel interference. For reliable data transmission, we argue traditional RTS-CTS carrier sensing schemes will not work because of the following reasons:

- When each node performs carrier sensing randomly, it is able to figure out when channel is clear. Yet, it cannot eliminate the situation where two close-by neighbors suddenly start transmission *simultaneously*.
- The RTS-CTS scheme is able to improve transmission reliability; however, it suffers from both hidden- and exposed-terminal problem, which jeopardize successful packet delivery.
- These schemes do not have accurate interference modeling method, and are not able to control interference effectively.

The reason we choose to separate normal data transmission from control signaling in frequency is because if control signaling is done in the same channel as normal data transmission, as we have discussed before, because exclusion regions of links usually are larger than normal data communication ranges, we need high transmission power for control signaling. Control signaling with high transmission power will introduce deadly interference to on-going normal data transmissions. This leads to system instability.

Thus, we choose to separate control and data packet transmissions in frequency to address the challenges listed above. As shown in Figure 2.6, in control plane, a link $\langle S, R\rangle$ gets all the data received for itself to figure out the links that lie in its exclusion region. The link also figures out the links whose data reception will be negatively affected if the link itself transmits data packets, please refer to Section 2.2.2 for details. We define these links as the conflict set of link $\langle S, R\rangle$.

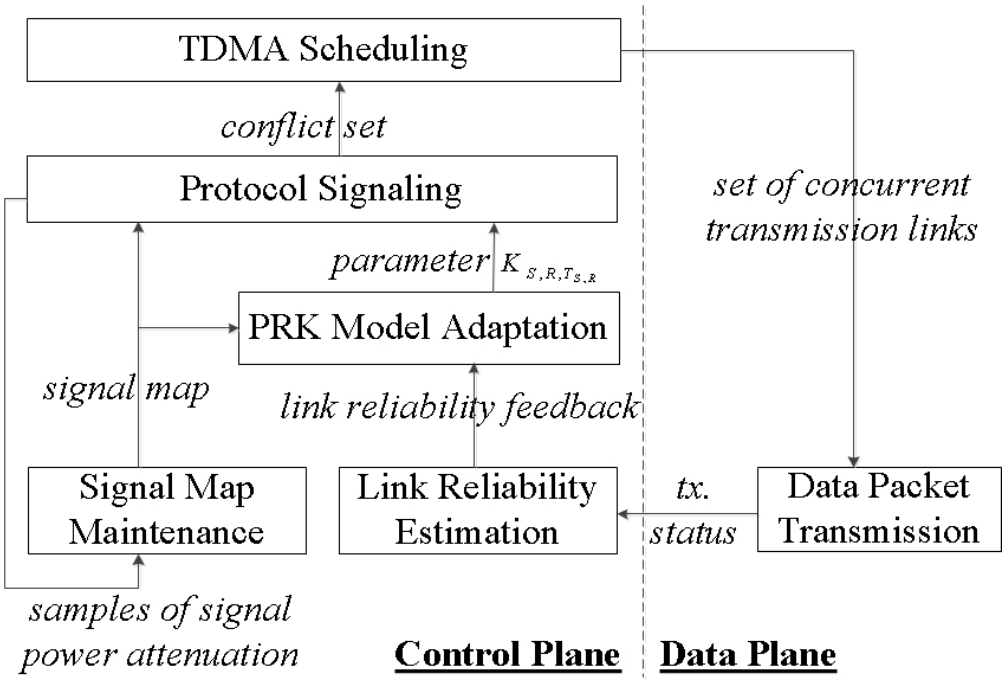

Figure 2.6: Architecture of PRKS

More specifically, a link $\langle C, D\rangle$ is in the conflict set of $\langle S, R\rangle$ and thus conflicting with $\langle S, R\rangle$ at time instant t if $C \in \mathbb{E}_{S,R,T_{S,R}}$ or $S \in \mathbb{E}_{C,D,T_{C,D}}$, where $T_{S,R}$ and $T_{C,D}$ are required packet delivery reliability across $\langle S, R\rangle$ and $\langle C, D\rangle$ respectively. Once we have well-defined conflict set for links, transmission scheduling can follow the random link activation process called Link-Activation-Multiple-Access (LAMA) as proposed in [32] which is a TDMA scheme. In LAMA, a link $\langle S, R\rangle$ contents for medium access with all links in its conflict set. All links use a uniform manner to define random number generator seed. The seeds are different only by link ID and time slot. In our PRK-based scheduling algorithm, we assume every link has an ID, and these IDs are known too all links. Thus, every link knows the random number generator seed of each other. This also makes the outcome of random number generator of one link known to other links without any data transmission. We call the out come of random number generator link priority. By considering all conflicting links of link $\langle S, R\rangle$ and the link $\langle S, R\rangle$ itself, and if the link $\langle S, R\rangle$ has the highest link priority, the link is considered as active for the slot that helped in defining random number generator seeds. The conflicting links, by inspecting their own link priorities and compare with the link priority link $\langle S, R\rangle$ has, automatically realize they are not allowed to transmit because

they do not have the highest link priority value out of all their conflict links. In this way, we achieve single transmission within an exclusion region. By PRK model definition, link reliability is guaranteed. For our scheduling algorithm to work, we need accurately maintained exclusion regions. These exclusion regions are controlled by PRK model parameters. Further more, the controller that runs in each link generates input for PRK model parameter instantiations. As we discussed before, the control design needs $y(t)$ which is data transmission reliability. When $\langle S, R\rangle$ is active, S transmits data to R. The packet delivery status, whether success or failure, is passed to link estimator that estimates data delivery reliability after enough packet transmissions have been observed and results sampled. Notice that one benefit of high power control signaling is to help nodes establish and maintain accurate signal maps as we have discussed in Section 2.2.2.

Our discussions in this chapter focus on ensuring data delivery reliability across links, thus we have focused on the exclusion regions around receivers alone. If it is important to ensure ACK reliability at the link layer (e.g., for avoiding unnecessary retransmissions), similar approaches to protecting data receptions can be applied to protect ACK receptions by maintaining an exclusion region around the transmitter of each link. For conciseness of the presentation, however, we only focus on ensuring data delivery reliability in this chapter.

2.3 Experimental evaluation

2.3.1 Methodology

Protocols. To understand the design decisions of PRKS, we have comparatively studied PRKS with its variants. Interested reader can refer [30] for detailed discussions.

In order to understand the performance of PRKS, we compare different metrics with the following existing protocols in our evaluations:

- *B-MAC*: A representative protocol for CSMA/CA fasion medium access control protocols. B-MAC utilizes carrier sensing mechanisms to tell if medium is busy or ideal. [28]
- *S-MAC*: A representative protocol for RTS-CTS based protocols. S-MAC uses RTS-CTS handshake packets to negotiate packet transmitters and receivers. While this handshake

mechanism helps in improving packet transmisison reliability, its underline interference model is simplified, thus unable to achieve accurate co-channel interference control [33].

- *RID-B*: A representative protocol for TDMA-based medium access control. The underline protocol is similar to LAMA which is used in our PRK-based scheduling. However, even though RID-B uses physical interference model to establish interference relations between nodes, RID-B ignores cumulative interference in networks. As a result, it still cannot achieve accurate interference control. [16]

Network and environmental settings. We experimentally evaluate PRKS and the related protocols in ns-3.13 [3]. In simulations, we assume that nodes use the CC2420 radio which complies with the IEEE 802.15.4 sensor network standard (e.g., in terms of physical layer techniques). In our simulation, we have employed an analytical model proposed by [34] which gives the SINR to PDR curve as Figure 2.7 shows. We consider networks where nodes are uniformly distributed

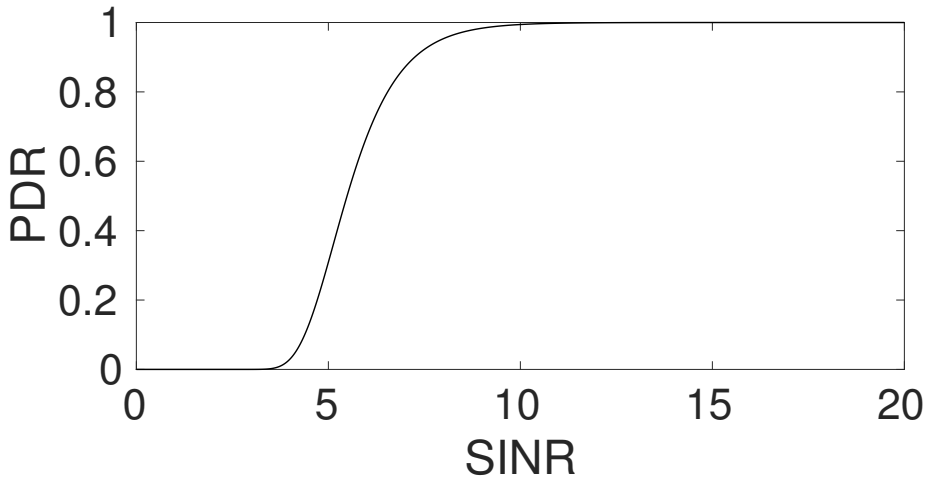

Figure 2.7: SINR v.s. PDR curve in simulation

on a 2D plane, with five nodes in any square area of 100 meters by 100 meters on average. We assume the average wireless path loss exponent is 3.3, and we use the radio-irregularity-model [35] to reflect anisotropy and asymmetry in wireless communication. Each node transmits data packets at the minimum power level that ensures 90% data delivery reliability to nodes 50 meters away in the absence of interference; to enable concurrency in data transmissions, we assume that the

network links are chosen such that each node has a receiver to whom the packet delivery reliability is the closest to 90% in the presence of an interference power that is 2dB compared with the data reception power at the receiver. In this context, we consider two networks in simulations: a small network with 125 nodes distributed in an area of 500 meters by 500 meters, and a large network with 270 nodes distributed in an area of 700 meters by 700 meters.

We assume every node transmits a data packet to its receiver every 50ms (e.g., for a sensor sampling frequency of 200Hz). For reflecting different application scenarios, we consider the cases when the minimum required data delivery reliability (PDR) is 70%, 80%, 90%, or 95% for all the links and the case when the minimum required reliability for each link is randomly chosen as 70%, 80%, 90%, or 95% with equal probability.

We have experimented with other network and traffic conditions, and we have observed similar phenomena as what we will present in Section 2.3.2; our preliminary study in the Net-Eye [27] and Indriya [29] sensor network testbeds have also corroborated the simulation results. Interested readers can find the detailed discussion on this in our technical report [30].

Metrics. For each combination of protocols, network, and application requirement on minimum link reliability, we run it for 10 times and evaluate protocol performance in terms of the following metrics:

- Packet delivery reliability (PDR): probability for a transmission along a link to be successful;
- Concurrency: number of concurrent transmissions at a time instant;
- Packet delivery delay: time taken to successfully deliver (including potential retransmissions) a packet across a link.

2.3.2 Experimental results

The observations (e.g., on the relative performance of different protocols) in the small network and the large network are similar, thus we mainly present data on the small network.

In the discussion below, we refer to te simulation results for the small network unless explicitly specified otherwise.

Behavior of PRKS. For different PDR requirements, Figures2.8 and 2.9 show the boxplots of link packet delivery reliability (PDR) and PRK model parameter in PRKS respectively. We see that PRKS adapts the PRK model parameter according to different PDR requirements, and that the required PDR is always guaranteed in the PRKS through predictable interference control. In particular, the PRK model parameter increases with the PDR requirement so that more close-by nodes are prevented from transmitting concurrently with a link's transmission. To understand the

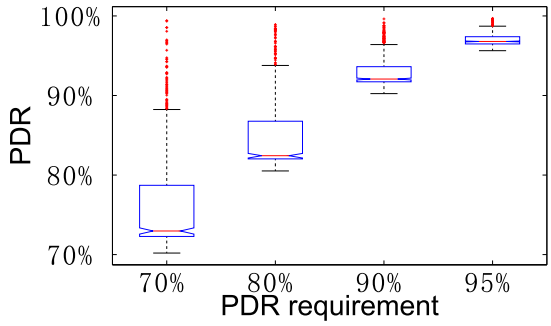

Figure 2.8: Packet delivery reliability in PRKS

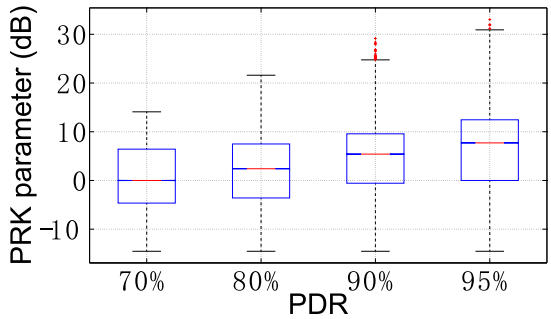

Figure 2.9: PRK model parameter in PRKS

spatial reuse in PRKS, Figure 2.10 shows the mean concurrency and its 95% confidence interval in PRKS as well as in a state-of-the-art, centralized scheduling protocol *iOrder* [22] which maximizes channel spatial reuse in interference-oriented scheduling.[2] We see that, despite its nature of distributed control, PRKS enables a concurrency and spatial reuse close to (e.g., up to 88.92%)

[2]In tmers of maximizing spatial reuse, iOrder has been shown to outperform well-known existing scheduling protocols such as Longest-Queue-First [14], GreedyPhysical [36], and LengthDiversity [37]

what is enabled by the centralized algorithm iOrder while ensuring the required PDR at the same time.

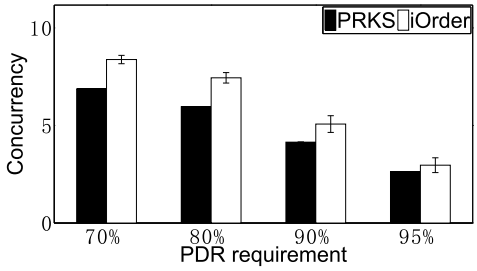

Figure 2.10: Mean concurrency and its 95% confidence interval in PRKS and iOrder

For the "mixed PDR requirement" scenario where different links of the same network have different PDR requirements, Figure 2.11 and 2.12 show the boxplots of link PDR and PRK model parameter for the links grouped by their PDR requirements. We see that PRKS adaptively ensures the required PDR in a predictable manner even when different links of the same network have different PDR requirements.

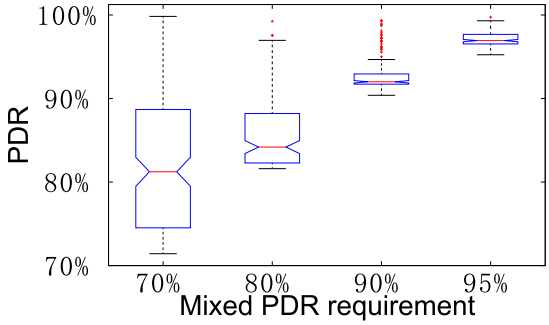

Figure 2.11: Packet delivery reliability in PRKS: mixed PDR requirement

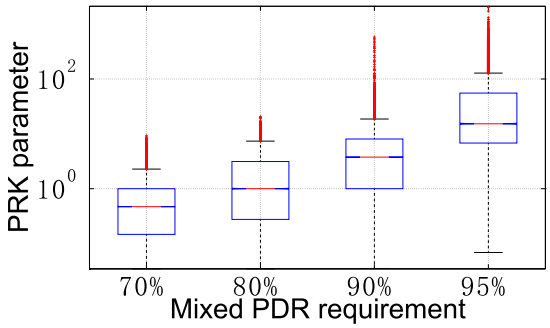

Figure 2.12: PRK model parameter in PRKS: mixed PDR requirement

Despite the distributed nature of the minimum-variance regulation controller in PRKS, the individual controllers converge to a state where the required PDR is satisfied. For a typical link in the network, for instance, Figure 2.13 shows the temporal behavior of link PDR when the minimum application PDR requirement is 90%. We see that the link PDR converges to its steady state after around 20 control steps. As a way of reflecting the network-wide convergence, Figure 2.14 shows the temporal convergence behavior of

$$\frac{\sum_{\text{Every link } \langle S,R \rangle} |Y_{S,R}(t) - T_{S,R}|}{\text{Total number of links}}.$$

In general, link PDRs converge quickly, as shown by Figure 2.15 where the settling time is defined

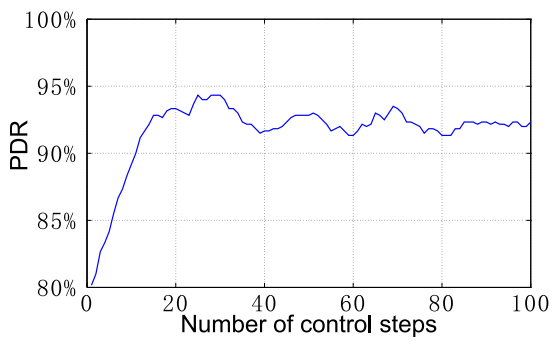

Figure 2.13: Temporal behavior of link PDR

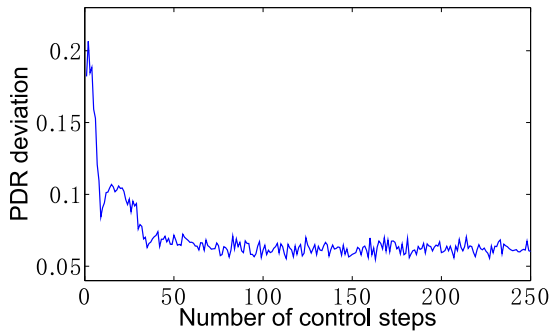

Figure 2.14: Network-wide convergence in PRKS

as the number of control steps taken for a link to reach its steady state PDR distribution. In addition to convergence to a state where the required PDRs are satisfied, the collective behavior of

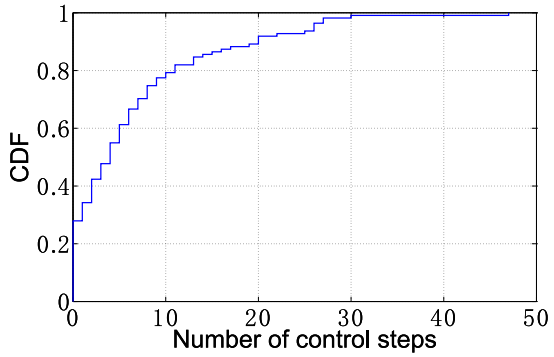

Figure 2.15: Cumulative distribution function (CDF) for the settling time of link PDR

the distributed controllers in PRKS also enables a spatial reuse close to what is feasible with the state-of-the-art, centralized scheduler iOrder as we have shown in Figure 2.10.

Comparison of different protocols. Figures 2.16, 2.17, 2.18 show the mean PDR, mean concurrency, and mean delay as well as their 95% confidence intervals for PRKS and other existing protocols. We see that, unlike PRKS that always ensures application required PDRs, existing protocols do not ensure the required PDRs due to co-channel interference that is not well controlled.

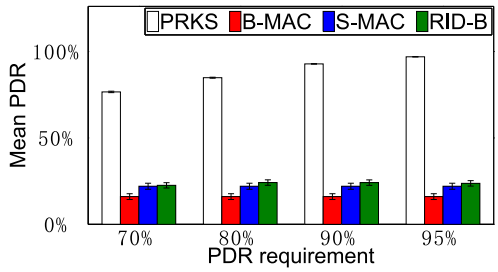

Figure 2.16: Mean PDR and its 95% confidence interval in different protocols

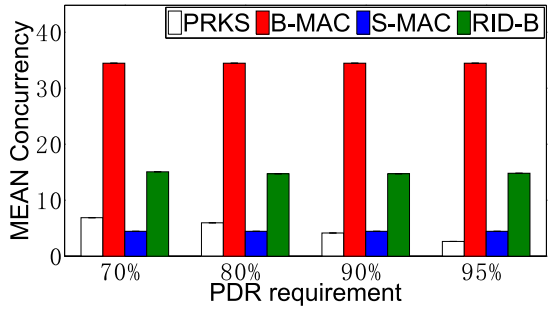

Figure 2.17: Mean concurrency and its 95% confidence interval in different protocols

Among existing protocols, RID-B enables higher PDRs than S-MAC and B-MAC do because RID-

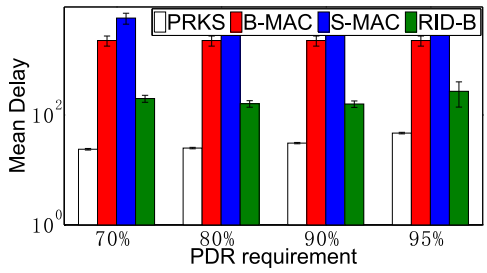

Figure 2.18: Mean delay and its 95% confidence interval in different protocols

B considers the physical interference model and application PDR requirements in defining pairwise interference relations between nodes; nonetheless, due to its lack of consideration of cumulative interference from multiple concurrent interferers, RID-B does not ensure predictable interference control and thus does not ensure predictable link PDR. When the application PDR requirement is 95%, for instance, RID-B can only enable a mean PDR of 15.35%. S-MAC ensures higher PDRs than B-MAC does due to its use of RTS-CTS handshake, but the PDRs are quite low (e.g., less than 8.7%) in both protocols since neither protocols consider physical interference model. Due to the low PDRs in existing protocols, the packet delivery delays are significantly larger in existing protocols than in PRKS, even though the concurrency may be higher in existing protocols than in PRKS.

For the large network, Figure 2.19 shows the mean PDR and its 95% confidence interval in different protocols. We see that, same as the small network, PRKS ensures that the required PDR is satisfied in all the cases. For B-MAC, S-MAC, and RID-B, the link PDRs are even lower in the large network than in the smaller network, because these protocols do not deal with cumulative interference well and there is more cumulative interference in the large network. Figure 2.20 shows the mean concurrency in PRKS. We see that PRKS also enables a concurrency close to what is feasible with the centralized scheduler iOrder.

2.4 Related work

Besides scheduling based on the physical, protocol, and general pairwise interference models as discussed in Section 2.1, the concepts of guard-zone or exclusion-region around receivers have also been adopted in distributed scheduling [38, 39]. But these scheduling algorithms as-

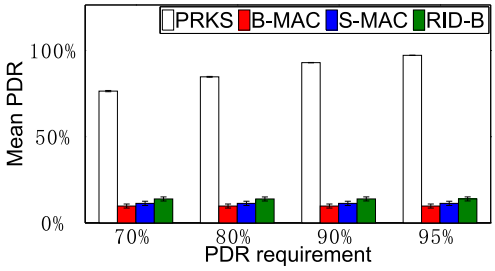

Figure 2.19: Mean PDR and its 95% confidence interval in different protocols: large network

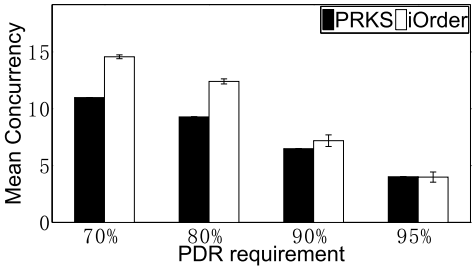

Figure 2.20: Mean concurrency in different protocols: large network

sumed uniform traffic load or uniform wireless signal power attenuation across the whole network, which are unrealistic in general. They did not address the challenge of designing scheduling protocols when interfering links are beyond the communication range of one another either.

Adaptive physical carrier sensing has been proposed to enhance network throughput [40, 41], but cumulative interference is not considered. As observed by Che et al. [5], moreover, throughput-optimal scheduling usually leads to low link reliability, which is not desirable in WSC networks. Park et al. [42] considered link reliability when adapting carrier sensing range, but their solution did not guarantee link reliability and converged slowly (e.g., taking up to 2 minutes). Fu et al. [43] proposed to control carrier sensing range to ensure a certain SINR at receivers. Nonetheless, the derivation of safe-carrier-sensing-range was based on the unrealistic assumption of homogeneous signal power attenuation across the whole network.

Focusing on distributed control of co-channel interference based on the PRK interference model, this work does not consider other interference management techniques such as interference cancellation and multi-channel scheduling, and we do not consider other link-reliability control techniques such as rate adaptation and power control. Nonetheless, we expect this work to be

relevant in the context of these techniques too, since co-channel interference still needs to be managed even with interference cancellation [44], multi-channel scheduling [45], rate control [46], and power control [47]. We will explore this synergy in our future work. Having nodes transmit busy tones in control channels to share their transmission or reception status has also been explored for channel access control [48], but these work did not study the fundamental problem of identifying interference relations between links, thus they could not ensure predictable interference control.

2.5 Concluding remarks

In this chapter, we have proposed PRKS as a scheduling algorithm to solve a reliable wireless communication problem in WSC systems with environmental uncertainties. Our solution has leveraged control theory to design a minimum-variance controller to provide input for PRK model parameter instantiation. The PRK model instantiation process itself requires every node to establish and maintain a signal map such average signal attenuations from and to neighbors are known prior to PRK model parameter instantiation. We have implement PRKS with its comparison protocols in ns-3.13 with radio model changed to be compliant with CC2420. Extensive simulation evaluations have shown that PRKS enables predictable link reliability and achieves high network concurrency in normal data transmission. Besides being important by itself, the predictable link reliability enabled by PRKS also serves as a foundation for real-time data delivery in wireless networked sensing and control; it will be worthwhile to explore this direction of research, since predictable reliability and real-time in data delivery are the basis of many networked cyber-physical systems such as those in smart electric grid and smart transportation.

CHAPTER 3: CYBER-PHYSICAL INTERFERENCE MODELING FOR RELIABILITY OF INTER-VEHICLE COMMUNICATIONS

3.1 Introduction

Transcending the traditional paradigm of single-vehicle-oriented safety and efficiency control, next-generation vehicles are expected to cooperate with one another and with transportation infrastructures to ensure safety, maximize fuel economy, and minimize emission as well as congestion [49, 50]. One basis for this vision of networked vehicle control (e.g., active safety and fuel economy control [50]) is wireless communication between close-by vehicles. Critical to the optimality and safety of networked vehicle control, inter-vehicle communication is required to be predictably reliable. Given the different impact that communication reliability, delay, and throughput have on networked vehicle control [51, 52] and the inherent tradeoff between communication reliability, delay, and throughput [2, 5], the optimal operation of networked vehicle systems also requires controlling the tradeoffs between communication reliability, delay, and throughput, for which controlling communication reliability in a predictable manner is a basis [1, 5].

Inheriting the basic design principles of WiFi such as CSMA-based channel access control, existing IEEE 802.11p-based solutions cannot ensure predictable inter-vehicle communication reliability. When the load of information exchange is high, for instance, they may not even be able to ensure a communication reliability of 30% [53, 6]. One major reason for the unpredictability and low reliability is the lack of predictable interference control among inter-vehicle wireless communications. Thus data transmission scheduling is a basic element of inter-vehicle networking. In networked vehicle systems, dynamic control strategies introduce dynamic network traffic patterns and pose different requirements on communication reliability [1, 51]. Vehicle mobility also introduces dynamics in network topology which, together with uncertainties in wireless communication, introduces complex dynamics and uncertainties in inter-vehicle communication. For agile adaptation to uncertainties and for avoiding information inconsistency in centralized scheduling, distributed scheduling becomes desirable for interference control in inter-vehicle communications.

Despite decades of research on interference-oriented channel access scheduling, most existing literature are either based on the protocol interference model or the physical interference model, neither of which is a good foundation for distributed interference control in the presence of uncertainties [5, 6]. The protocol model is local and suitable for distributed protocol design, but it is inaccurate and does not ensure reliable data delivery in general [18]. The physical model has high-fidelity, but it is non-local and combinatorial and thus not suitable for distributed protocol design in dynamic, uncertain settings such as those in inter-vehicle communications [5, 6]. To bridge the gap between the existing interference models and the design of distributed, field-deployable scheduling protocols with predictable communication reliability, Zhang et. al [5] have identified the physical-ratio-K (PRK) interference model that integrates the protocol model's locality with the physical model's high-fidelity. Based on the PRK model, Zhang et. al [6] have proposed the PRK-based scheduling protocol PRKS which ensures predictable communication reliability in networks of no or low node mobility. Designed for networks of no or low mobility, however, PRKS does not address the challenges that vehicle mobility poses to transmission scheduling. In particular, vehicle mobility makes network topology and inter-vehicle channel properties highly dynamic, which in turn makes interference relations between vehicles highly dynamic, especially for vehicles on different roads or in opposite driving directions of a same road. The highly dynamic nature of inter-vehicle interference relations challenges the precise identification of interference relations in terms of both control signaling and interference relation estimation. In addition, PRKS focuses on predictable unicast reliability without considering predictable reliability in broadcast which is a fundamental primitive in inter-vehicle communications [50].

For predictable reliability of inter-vehicle communications, we leverage cyber-physical structures of V2V networks to address the challenges of vehicle mobility and broadcast, and make the following contributions:

- For effective control signaling of fast-varying interference relations and leveraging the physical locations of vehicles, we propose a geometric approximation of the PRK interference model, denoted as the gPRK model. The gPRK model enables vehicles to learn their mutual

interference relations in the presence of vehicle mobility and without requiring significant signaling bandwidth.

- For accurate identification of interference relations in the presence of vehicle mobility, we propose to leverage spatial correlations of interference, temporal link reliability bounds, and microscopic vehicle dynamics models for the accurate instantiation, agile adaptation, and effective use of the gPRK model in the presence of vehicle mobility respectively.
- For ensuring predictable broadcast reliability, we address the impact of broadcast on gPRK model adaptation, and we propose a set-cover-based approach to minimizing the overhead of control signaling.
- We propose the Cyber-Physical Scheduling (CPS) framework that integrates the above cyber-physical interference modeling mechanisms in scheduling inter-vehicle communications. We implement CPS in ns-3, and we evaluate CPS through integrated, high-fidelity wireless network simulation (via ns-3) and vehicle dynamics simulation (via SUMO). We observe that CPS ensures predictable inter-vehicle communication reliability while achieving high throughput and low delay in communication.

The rest of the chapter is organized as follows. In Section 3.2, we present the system model and problem specification. We present the CPS scheduling framework in Section 3.3, and we evaluate it in Section 3.4. We discuss the related work in Section 3.5, and we make concluding remarks in Section 3.6.

3.2 Preliminaries

The CPS framework heavily use the PRKS protocol discussed in Chapter 2. For descriptions of the PRK model and details of the PRKS protocol, please refer to Chapter 2. In this section, we focus on the system model and the problem specification of the CPS framework.

System model & problem specification. In inter-vehicle wireless communication networks, referred to as *V2V networks* hereafter, a fundamental communication primitive is single-hop broadcast via which a vehicle shares its states (e.g., location and speed) with close-by vehicles within a certain distance (e.g., 150 meters) [50]. Given the significance of single-hop broadcast (e.g.,

for real-time networked vehicle control [50]) and for conciseness of presentation, our discussion in this chapter focuses on single-hop broadcast, but the proposed methodology for scheduling inter-vehicle broadcasts applies to the scheduling of inter-vehicle single-hop unicast. Even though we only consider single-hop broadcasts by individual vehicles, we do consider real-world settings where the individual vehicles are widely distributed in space and may well be beyond the broadcast range of many other vehicles.

With the above V2V network setup, we study the online slot-scheduling problem [22] where, given a set of vehicles on the road at any time instant, a maximal subset of the vehicles need to be scheduled in a distributed manner to transmit concurrently while ensuring that the mean packet delivery reliability (PDR) from every transmitting vehicle S to each of its broadcast receivers R is no less than an application-required PDR $T_{S,R}$. Note that a vehicle R is a broadcast receiver of a transmitting vehicle S if the Euclidean distance between S and R, denoted by $D(S, R)$, is no more than the communication range of S, denoted by D_S. Focusing on predictable co-channel interference control in broadcast scheduling, we assume that all vehicles share a single communication channel (e.g., the DSRC control channel [54]) and that the broadcast transmission power is fixed for each vehicle even though different vehicle may use different transmission powers; multi-channel scheduling and broadcast power control are relegated as future research.

3.3 Cyber-Physical Interference Modeling of Inter-Vehicle Communications

In what follows, we present our mechanisms that leverage the cyber-physical structures of V2V networks for interference modeling and predictable interference control. For conciseness of presentation, our discussion focuses on a sender S and its receiver set $\mathbf{R} = \{R : R \neq S \wedge D(S, R) < D_S\}$ unless mentioned otherwise.

3.3.1 gPRK: Geometric Approximation of the PRK Model

Challenge of using PRK model in V2V networks. As discussed in Section 2.1, the definition of the PRK interference model is based on signal power between close-by nodes. To use the PRK model in data transmission scheduling, nodes need to maintain local signal maps so that interfering nodes and links can be aware of their mutual interference relations. For networks of no or low node

mobility which Zhang et al. [6] have considered, the average signal power between nodes does not change at timescales such as seconds, minutes, or even hours. Accordingly, the frequency of signal map update and thus the overhead of signal map maintenance tends to be low for networks of no or low mobility [6]. For V2V networks, however, vehicle mobility makes average signal power between close-by vehicles fast-varying in nature, for instance, at the timescales of seconds or less. If we were to apply the PRK interference model to V2V networks, the local signal maps between close-by vehicles[1] need to be updated frequently to ensure that vehicles are aware of their mutual interference relations, which would introduce significant overhead. Assuming there are N close-by vehicles that may interfere with one another, for instance, the signal map would contain, for every vehicle $v_i (i = 1 \ldots N)$, the average signal power from every other vehicle to v_i. Since every vehicle v_i can only estimate the average signal power from every other vehicle to itself through received-signal-strength-indicator (RSSI) sampling [6], it is necessary for every vehicle v_i to share its estimates with every other vehicle in order for every vehicle to establish and maintain its own local signal map about the signal power between close-by vehicles. For instance, a receiver vehicle R can sample and estimate the signal power $P_{C,R}$ from another vehicle C to itself, but R has to shared its estimate of $P_{C,R}$ with C in order for C to know $P_{C,R}$ and thus decide whether itself can interfere with the transmission from a sender vehicle S to R based on the PRK model. Assuming it takes two bytes to encode the signal power from one vehicle to another and it takes six bytes to encode the ID (e.g., MAC address) of each vehicle, it takes $(6 + 8(N - 1))$ bytes for a vehicle v_i to encode the signal power from every other vehicle to itself. Therefore, each update of the signal map takes $N(6+8(N-1))$ bytes of information exchange between vehicles. Assuming the signal map is updated every t_0 seconds, the signal map maintenance will consume $\frac{8N(6+8(N-1))}{t_0}$bps network bandwidth. For typical values of N in V2V networks and different update intervals t_0, Figure 3.1 shows the overhead of signal map maintenance in V2V networks. Considering that the current physical layer of the V2V communication standard IEEE 802.11p can only support a maximum transmission rate of 6Mbps - 27Mbps, that the total bandwidth available to a set of

[1]More precisely, between close-by vehicles that may interfere with one another.

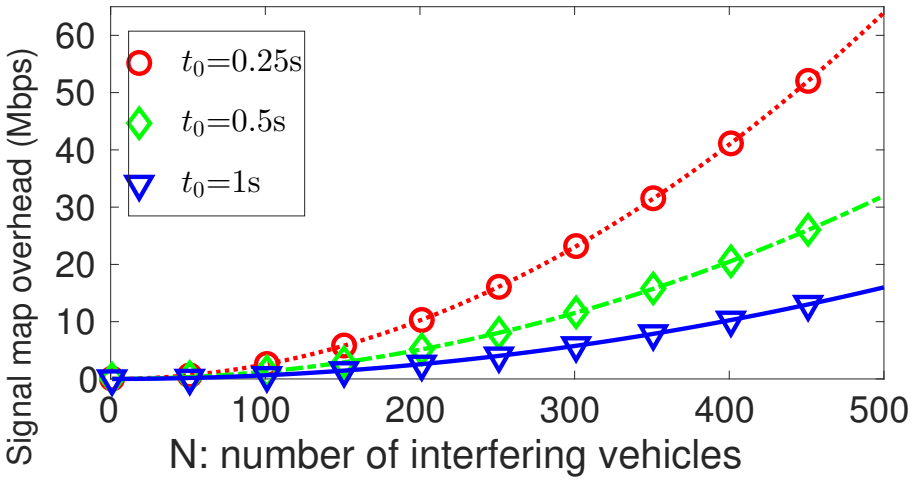

Figure 3.1: Overhead of signal map maintenance

mutually interfering vehicles is no more than the maximum transmission rate, and that N may well be in the range of hundreds (e.g., in urban settings), Figure 3.1 shows that the signal map maintenance overhead accounts for a significant portion or even exceed the total communication bandwidth of V2V networks. This implies that it is too costly or even infeasible to maintain accurate signal maps for PRK-based scheduling in V2V networks. Thus, it is difficult, if not impossible, to directly apply the PRK interference model to data transmission scheduling in V2V networks.

Geometric approximation of PRK model. In V2V network systems, vehicle locations are important factors for networked vehicle control, and thus they are readily available through GPS and/or other mechanisms such as simultaneous-localization-and-mapping (SLAM). Using vehicle locations, it is easy for vehicles to know the distances among themselves. To avoid the significant overhead (and sometimes infeasibility) of maintaining accurate signal maps in V2V networks and considering the fact that, on average, closer-by vehicles tend to introduce higher interference signal power to one another than farther away vehicles, we propose to leverage the availability of vehicle location information to define a geometric approximation of the PRK interference model, denoted as the *gPRK interference model*. In the gPRK model, interference relations among vehicles are defined based on inter-vehicle distance instead of inter-vehicle signal power, and a vehicle C' is

regarded as not interfering and thus can transmit concurrently with the transmission from another vehicle S to its receiver R if and only if

$$D(C', R) > D(S, R)K_{S,R,T_{S,R}}, \tag{3.1}$$

where $D(C', R)$ and $D(S, R)$ is the geometric distance between C' and R and that between S and R respectively, $K_{S,R,T_{S,R}}$ is the minimum real number (i.e., can be non-integer) chosen such that, in the presence of cumulative interference from all concurrent transmitters, the probability for R to successfully receive packets from S is no less than the minimum link reliability $T_{S,R}$ required by applications. As shown in Figure 3.2, the gPRK model defines, for each link $\langle S, R\rangle$,

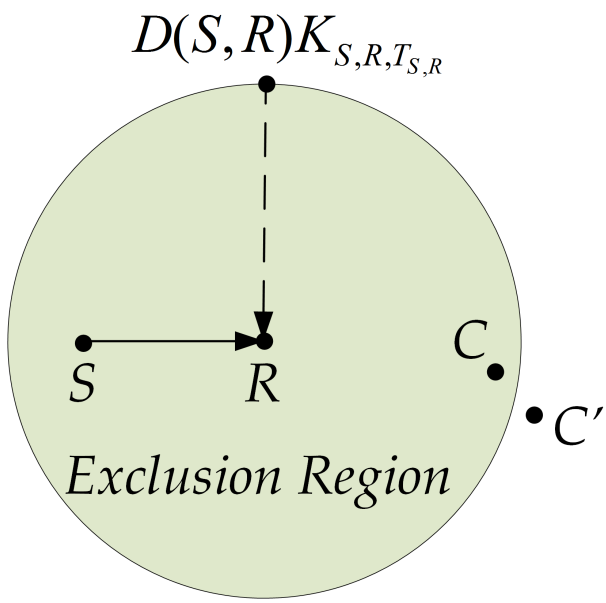

Figure 3.2: gPRK interference model

an exclusion region (ER) $\mathbb{E}_{S,R,T_{S,R}}$ around the receiver R such that a node C is in the region (i.e., $C \in \mathbb{E}_{S,R,T_{S,R}}$) if and only if $D(C, R) \leq D(S, R)K_{S,R,T_{S,R}}$. Similar to the PRK model, the gPRK model is *local* since only local, pairwise interference relations are defined between close-by vehicles, and the gPRK model is suitable for *reliable inter-vehicle communication* since it ensures the application-required link reliability by considering wireless communication properties such as cumulative interference. Unlike the PRK model where the ER around a link may be of an irregular

shape due to anisotropic wireless signal propagation, the ER around a link in the gPRK model is of the regular shape of a disk.

With the gPRK model, a vehicle only needs to share its location with potentially interfering vehicles in order for an interfering vehicle to detect their mutual interference relation using the gPRK model parameter K, and a vehicle does not need to share with other vehicles the signal power from every other potentially interfering vehicle to itself. With seven bytes, a vehicle can encode its longitude and latitude information such that the location information accuracy is 1.11meters. Then, for the case of N mutually-interfering vehicles as discussed earlier and assuming it takes six bytes to encode the ID (e.g., MAC address) of a vehicle, it takes $13N$ bytes of information exchange between vehicles in order for the N vehicles to be mutually aware of one another's location. Assuming that the location update frequency is the same as that of signal map update in PRK-based scheduling, using the gPRK model instead of the PRK model would reduce the control signaling overhead by a factor of $\frac{8N(6+8(N-1))}{13N} = \frac{48}{13} + \frac{64}{13}(N-1)$. Using location prediction via microscopic vehicle dynamics models as we will discuss in Section 3.3.2, the update frequency of vehicle locations can be lower than that of signal map, thus enabling more reduction in control overhead. For highly reliable inter-vehicle communication in large scale V2V networks, N tends to be large and in the range of hundreds. Thus the use of the gPRK model instead of the PRK model enables orders of magnitude reduction in control signaling overhead, which in turn makes it feasible and efficient to use the gPRK model in real-world V2V networks.

Since the ER around a receiver R_i in the gPRK model assumes a disk shape instead of a potentially irregular geometric shape in the PRK model, as shown in Figure 3.3.

Accordingly, the set of vehicles inside the ER of R_i may be different in the gPRK and PRK models. For links with high communication reliability requirements in large scale networks such as V2V networks, the receiver ERs tend to be large (e.g., with a geometric radius twice the sender-receiver distance in many scenarios [5]), and thus the number of differing vehicles in the gPRK- and PRK-based ERs tends to be relatively small as compared to the total number of vehicles in the ERs. For inter-vehicle broadcast, since the sender ER of a vehicle S is the union of the ERs

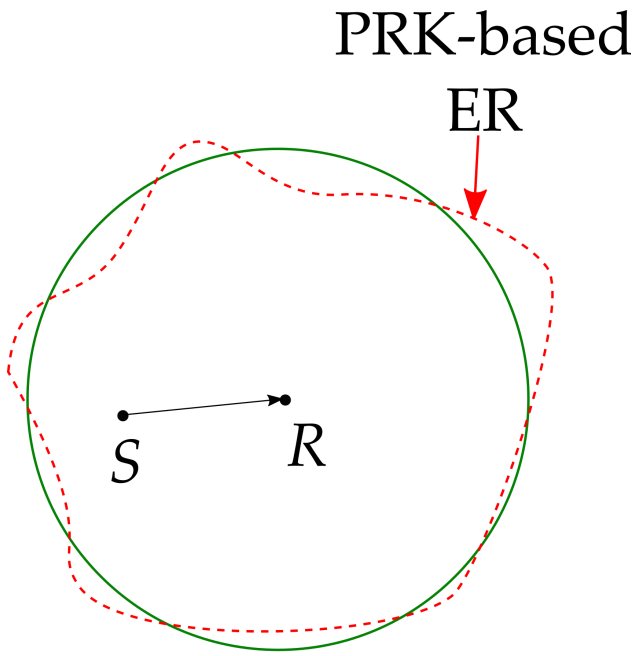

Figure 3.3: gPRK- vs. PRK-based receiver ER

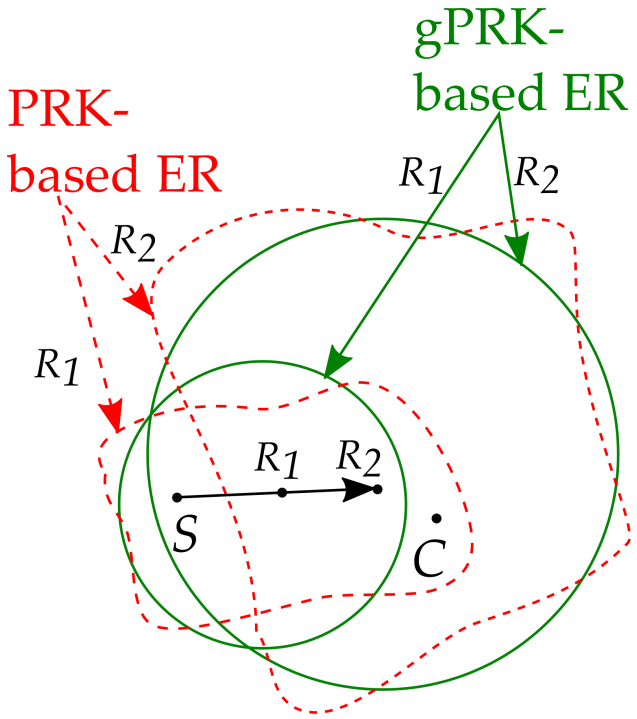

Figure 3.4: gPRK- vs. PRK-based sender ER

around all of its receivers, the size of the sender ER is even larger than the size of individual receiver ERs, and a vehicle in the interior of the sender ER that is in the PRK-based but not in the gPRK-based ER (or in the gPRK-based but not in the PRK-based ER) of a receiver R_i may well be in the gPRK-based ER (or the PRK-based ER) of another receiver $R_j (j \neq i)$. Therefore, the differences between gPRK- and PRK-based sender ERs tend to be even less significant. As shown in Figure 3.4, for instance, vehicle C is in the PRK-based ER but not in the gPRK-based ER of receiver R_1, but C is in the gPRK-based ER of R_2, thus C is in both the PRK- and gPRK-based sender ER of S.

gPRK model adaptation. Similar to the PRK model, the parameter $K_{S,R,T_{S,R}}$ of the gPRK model needs to be instantiated for every link $\langle S, R\rangle$ according to in-situ, potentially unpredictable network and environmental conditions such as vehicle spatial distribution and wireless signal power attenuation. To this end, we use the control-theoretic approach of Zhang et al. [6] that, upon a feedback on the link reliability of $\langle S, R\rangle$ at time t, denoted by $Y_{S,R}(t)$, computes the change of cumulative interference power at the receiver R, denoted by $\Delta I_R(t)$, that the change of $K_{S,R,T_{S,R}}$ at time t needs to introduce to make $Y_{S,R}(t+1) = T_{S,R}$ at time $t+1$. In particular, letting $y(t) = cy(t-1) + (1-c)Y_{S,R}(t)$ $(0 \leq c < 1)$, $\Delta I_R(t)$ is computed as follows [6]:

$$\Delta I_R(t) = \frac{(1+c)y(t) - cy(t-1) - T_{S,R}}{(1-c)a(t)} - \mu_U(t), \tag{3.2}$$

where $a(t) = f'(f^{-1}(Y_{S,R}(t)))$, $f(.)$ is the radio model function that defines the relation between link reliability $Y_{S,R}(t)$ and the signal-to-interference-plus-noise-ratio (SINR) at the receiver R at time t, and $\mu_U(t)$ denotes the mean change of the cumulative interference power that vehicles not in $\mathbb{E}_{S,R,T_{S,R}}(t) \cup \mathbb{E}_{S,R,T_{S,R}}(t+1)$ introduce to the receiver R from time t to $t+1$. Since the receiver R can locally measure or estimate $y(t), y(t-1), a(t)$, and $\mu_U(t)$ [6], R can locally compute $\Delta I_R(t)$.

After computing $\Delta I_R(t)$ at time t, R needs to compute $K_{S,R,T_{S,R}}(t+1)$ so that

$$\begin{cases} K_{S,R,T_{S,R}}(t+1) = K_{S,R,T_{S,R}}(t), & \text{if } \Delta I_R(t) = 0 \\ K_{S,R,T_{S,R}}(t+1) > K_{S,R,T_{S,R}}(t), & \text{if } \Delta I_R(t) < 0 \\ K_{S,R,T_{S,R}}(t+1) < K_{S,R,T_{S,R}}(t), & \text{if } \Delta I_R(t) > 0 \end{cases} \tag{3.3}$$

and that, when the PRK model parameter is $\min\{K_{S,R,T_{S,R}}(t), K_{S,R,T_{S,R}}(t+1)\}$, the expected interference introduced to R by the nodes in either $\mathbb{E}_{S,R,T_{S,R}}(t)$ or $\mathbb{E}_{S,R,T_{S,R}}(t+1)$ but not in both is as close to $|\Delta I_R(t)|$ as possible while ensuring that the expected link reliability is no less than $T_{S,R}$ when the PRK model parameter is $K_{S,R,T_{S,R}}(t+1)$.[2] To realize this, we define, for each node C that may be included in the exclusion region of R during network operation, the expected interference $I_{C,R}(t)$ that C introduces to R when C is not in the exclusion region of R. Then $I_{C,R}(t) = \beta_C(t)P_{C,R}(t)$, where $\beta_C(t)$ is the probability for C to transmit data packets at time t and $P_{C,R}(t)$ is the power strength of the data signals reaching R from C.[3] Considering the discrete nature of node distribution in space and the requirement on satisfying the minimum link reliability $T_{S,R}$, we propose the following rules for computing $K_{S,R,T_{S,R}}(t+1)$:

- <u>Rule-ER0:</u> If $\Delta I_R(t) = 0$, let $K_{S,R,T_{S,R}}(t+1) = K_{S,R,T_{S,R}}(t)$.
- <u>Rule-ER1:</u> If $\Delta I_R(t) < 0$ (i.e., need to expand the exclusion region), let $\mathbb{E}_{S,R,T_{S,R}}(t+1) = \mathbb{E}_{S,R,T_{S,R}}(t)$, then keep adding nodes not already in $\mathbb{E}_{S,R,T_{S,R}}(t+1)$, in the non-decreasing order of their distance to R, into $\mathbb{E}_{S,R,T_{S,R}}(t+1)$ until the node B such that adding B into $\mathbb{E}_{S,R,T_{S,R}}(t+1)$ makes $\sum_{C \in \mathbb{E}_{S,R,T_{S,R}}(t+1) \setminus \mathbb{E}_{S,R,T_{S,R}}(t)} I_{C,R}(t) \geq |\Delta I_R(t)|$ for the first time. Then let $K_{S,R,T_{S,R}}(t+1) = \dfrac{D(B,R,t)}{D(S,R,t)}$, where $D(B,R,t)$ and $D(S,R,t)$ denote the distance from B and S to R at time t respectively.
- <u>Rule-ER2:</u> If $\Delta I_R(t) > 0$ (i.e., need to shrink the exclusion region), let $\mathbb{E}_{S,R,T_{S,R}}(t+1) = \mathbb{E}_{S,R,T_{S,R}}(t)$, then keep removing nodes out of $\mathbb{E}_{S,R,T_{S,R}}(t+1)$, in the non-increasing order

[2] Due to the discrete nature of node distribution, the resulting link reliability may be slightly higher than the required reliability $T_{S,R}$ instead of being exactly equal to $T_{S,R}$.

[3] $P_{C,R}(t)$ and $\beta_C(t)$ can be estimated through purely local coordination between R and C [6].

of their distance to R, until the node B such that removing any more node after removing B makes $\sum_{C \in \mathbb{E}_{S,R,T_{S,R}}(t) \setminus \mathbb{E}_{S,R,T_{S,R}}(t+1)} I_{C,R}(t) > \Delta I_R(t)$ for the first time. Then let $K_{S,R,T_{S,R}}(t+1) = \frac{D(B,R,t)}{D(S,R,t)}$.

(An example of gPRK model adaptation can be found at [55].) For convenience, we call the above rule the *gPRK-model-adaptation* rule.

3.3.2 gPRK Modeling in the Presence of Vehicle Mobility

Vehicle mobility makes network topology and interference relations highly dynamic (especially for vehicles on different roads or in opposite driving directions of a same road), and this challenges the initialization, adaptation, and use of the gPRK model in V2V networks. In what follows, we elaborate on our design that addresses the challenges by effectively leveraging cyber-physical structures of V2V networks such as the spatial interference correlation, temporal link reliability bounds, and microscopic vehicle dynamics models.

Accurate initialization of gPRK model. Due to vehicle mobility and starting of vehicles, new links may form when vehicles come within one another's communication ranges. Considering the potentially short lifetime of links (e.g., those between vehicles along opposite driving directions of a same road), time-varying link properties, and the need for reliable inter-vehicle communication, it is desirable for the gPRK model parameters of the newly-formed links to quickly converge to their steady-state where application-required link reliabilities are ensured. To this end, it is desirable to initialize the gPRK model parameters of newly formed links close to where their steady-state may be, and we propose to leverage spatial interference correlation to accomplish this. More specifically, in large scale wireless networks such as V2V networks, close-by links whose senders and receivers are close to one another respectively tend to experience similar interference power and similar set of close-by, strong interferers [56]. This spatial correlation of interference enables us to develop mechanisms for accurate gPRK model initialization as we explain next.

When a new link from S_i to R_i, denoted by $\langle S_i, R_i \rangle$, is formed at time t, R_i first checks whether there exists another sender vehicle $S_j (j \neq i)$ for which the gPRK model parameter

$K_{S_j,R_i,T_{S_j,R_i}}(t)$ has converged to a steady state for link $\langle S_j, R_i\rangle$ (i.e., the communication reliability from S_j to R_i has met the requirement T_{S_j,R_i}). For convenience, we call the link $\langle S_j, R_i\rangle$ a *self-reference link* for $\langle S_i, R_i\rangle$. Let $\mathbb{S} = \{S_j : \langle S_j, R_i\rangle$ is a self-reference link for $\langle S_i, R_i\rangle\}$, and let S^* be the vehicle that is closest to S_i out of all the vehicles in $\mathbb{S}$. R_i then uses $\langle S^*, R_i\rangle$ to initialize the gPRK model for $\langle S_i, R_i\rangle$. More specifically, denoting the data signal power from S^* and S_i to R_i at time t by $P_{S^*,R_i}(t)$ and $P_{S_i,R_i}(t)$ respectively and assuming that R_i experiences similar interference power when senders S^* and S_i transmit with similar communication reliability requirements, R_i sets $K_{S_i,R_i,T_{S_i,R_i}}(t) = K_{S^*,R_i,T_{S^*,R_i}}(t)$ and computes $\Delta I_{R_i}(t) = P_{S_i,R_i}(t) - P_{S^*,R_i}(t) + P_{S_i,R_i}(t)(\frac{1}{f^{-1}(T_{S_i,R_i})} - \frac{1}{f^{-1}(T_{S^*,R_i})})$, where the term $P_{S_i,R_i}(t) - P_{S^*,R_i}(t)$ accounts for the difference in tolerable interference due to different signal power from S^* and S_i, and the term $P_{S_i,R_i}(t)(\frac{1}{f^{-1}(T_{S_i,R_i})} - \frac{1}{f^{-1}(T_{S^*,R_i})})$ accounts for the change in tolerable interference when the communication reliability requirement by $\langle S_i, R_i\rangle$ changes from T_{S^*,R_i} to T_{S_i,R_i}; then R_i applies the gPRK model adaptation rule Rule-ER0, Rule-ER1, or Rule-ER2 (as discussed in Section 3.3.1) to adjust the value of $K_{S_i,R_i,T_{S_i,R_i}}(t)$, and the final value of $K_{S_i,R_i,T_{S_i,R_i}}(t)$ is set as the initial gPRK model parameter for the newly formed link $\langle S_i, R_i\rangle$.

If there exists no self-reference link for $\langle S_i, R_i\rangle$ when it newly forms (e.g., when vehicle R_i just got started), R_i tries to identify a *neighbor-reference link* $\langle S_j, R_j\rangle (j \neq i)$ such that the gPRK model parameter $K_{S_j,R_j,T_{S_j,R_j}}(t)$ has converged to a steady state, and $D(S_j, S_i, t)$ as well as $D(R_j, R_i, t)$ are less than a threshold D_0, where D_0 is chosen such that links $\langle S_j, R_j\rangle$ and $\langle S_i, R_i\rangle$ experience similar interference power and close-by, strong interferers, and $D(V_j, V_i, t)$ denotes the geometric distance between two vehicles V_j and V_i at time t. Let $\mathbb{L} = \{\langle S_j, R_j\rangle : \langle S_j, R_j\rangle$ is a neighbor-reference link for $\langle S_i, R_i\rangle\}$, define the distance between two links $\langle S_j, R_j\rangle$ and $\langle S_i, R_i\rangle$ at time t as $\max\{D(S_j, S_i, t), D(R_j, R_i, t)\}$, and let $\langle S^*, R^*\rangle$ be the link closest to $\langle S_i, R_i\rangle$ among all the links in $\mathbb{L}$. R_i then uses $\langle S^*, R^*\rangle$ to initialize the gPRK model for $\langle S_i, R_i\rangle$ as in the case of estimation via self-reference links as discussed above.

Leveraging the spatial correlation between $\langle S_i, R_i\rangle$ and its self-reference and neighbor-reference links, the above gPRK model initialization mechanism enables good approximation of

the steady-state gPRK model parameter of $\langle S_i, R_i \rangle$ in normal and heavy vehicle traffic settings where there are usually enough number of surrounding vehicles/links around $\langle S_i, R_i \rangle$. In the case of very light vehicle traffic settings (e.g., at 3 a.m.), there may exist no self-reference link nor neighbor-reference link for a newly formed link $\langle S_i, R_i \rangle$. In this case, vehicles are sparsely distributed, cumulative interference from far-away vehicles tends to be small, and the exclusion region (ER) tends to be smaller than in the case of normal and heavy vehicle traffic settings. Accordingly, R_i can approximate its steady-state gPRK model parameter by only considering pairwise interference among close-by vehicles. More precisely, R_i sets the initial value of the gPRK model parameter such that the initial ER around itself includes every vehicle whose transmission alone, concurrent with the transmission from S_i to R_i, can make the communication reliability drop below T_{S_i,R_i}.

Agile adaptation of gPRK model. As network topology and link properties vary over time (e.g., due to vehicle mobility), the gPRK model parameters need to be adapted accordingly. As we have discussed in Section 3.3.1, the gPRK model adaptation for a link $\langle S, R \rangle$ is triggered by each new feedback of the latest link reliability $Y_{S,R}(t)$. For accurate feedback of in-situ link reliability and to circumvent uncertainties in the radio model function $f(.)$ [57], it is desirable to measure the delivery status (i.e., success or failure) of a sequence of W data packet transmissions from S to R to get one link reliability feedback. In a measurement window of W packet transmissions, if there are U number of successful packet deliveries, the feedback $Y_{S,R}(t)$ is computed as $\frac{U}{W}$. Given a link reliability requirement $T_{S,R}$, W needs to be no less than $W_0 = \lceil \frac{1}{1 - T_{S,R}} \rceil$ in order for R to decide whether the actual link reliability exceeds $T_{S,R}$. To ensure a feedback accuracy of $\pm r\%$ at a confidence level of $100(1-\alpha)\%$ when the expected link reliability is p, W needs to be no less than $W_1 = z^2_{1-\alpha/2} \frac{p(1-p)}{r^2}$ [58], where $z_{1-\alpha/2}$ is the $(1-\alpha/2)$-quantile of a unit Gaussian variate. Therefore, $W = \max\{W_0, W_1\}$. For V2V networks requiring high communication reliability (e.g., $T_{S,R} = 95\%$), W tends to be in the range of tens of packet transmissions (e.g., no less than 20). For V2V networks with potentially fast-varying link properties (e.g., between vehicles moving in opposite directions of a same road), the gPRK model adaptation might well be too slow if a link

had to always wait for W packet transmissions to get a link reliability feedback, and the slow adaptation may well lead to low communication reliability in fast-varying network settings. To ensure communication reliability, we propose mechanisms that leverage temporal link reliability bounds to enable early detection of low link reliability and thus agile adaptation of gPRK model parameters as we explain next.

While it takes at least W_0 number of packet transmissions to detect the case of actual link reliability exceeding the required one $T_{S,R}$, it usually takes significantly fewer number of packet transmissions to detect the case of actual link reliability being lower than $T_{S,R}$. More specifically, at a time instant t_f when there already have $F_0 = \lfloor (1-T_{S,R})W \rfloor + 1$ number of packet delivery failures since the last link reliability feedback, the receiver R knows already that the link reliability sample in this feedback window will be less than $T_{S,R}$. Since the number of successful transmissions in this feedback window will be no more than $W - F_0$, the link reliability sample will be no more than $\frac{W - F_0}{W}$. At time t_f, R could treat $\frac{W - F_0}{W}$ as an upper bound of $Y_{S,R}(t_f)$ and apply Formula (3.2) to compute $\Delta I_R(t_f)$ and expand its exclusion region. Considering temporal link correlation and the packet delivery failure at t_f, however, R may expect a few more packet delivery failures immediately after time t_f, and R could get a tighter upper bound on the in-situ link reliability if it waits to collect a few more samples of packet delivery status. In order not to slow down necessary gPRK model adaptations while trying to get tight upper bound on in-situ link reliability, R continues, after time t_f, sampling packet delivery status until a time instant t'_f when the packet delivery is a success, $|\Delta I_R(t'_f)|$ is large enough so that additional transmission failures in this feedback window will only lead to negligible additional expansion of the exclusion region, or R has already collected W number of transmission status samples, where $|\Delta I_R(t'_f)|$ is computed by conservatively assuming that $Y_{S,R}(t'_f) = \frac{W - F_1}{W}$ with F_1 being the number of transmission failures since the last link reliability feedback. With the above approach to early

detection of low link reliability, $\langle S, R\rangle$ adapts its gPRK model parameter in an agile manner to ensure application-required communication reliability in the presence of vehicle mobility.

Effective use of gPRK model. In order for vehicles to use the gPRK model to detect their mutual interference relations in a distributed manner, close-by, potentially interfering vehicles need to be aware of one another's locations. A vehicle can update and share its location with close-by vehicles by broadcasting its location periodically. In the presence of high vehicle mobility, however, the relative positions of two vehicle may change in an non-negligible manner during the broadcast intervals. For instance, even if the location information is updated every half a second, the distance between two vehicles driving at a speed of 80km/h (i.e., 50mph) along the opposite directions of a road may change 22.22 meters during the update interval. In order for vehicles to have accurate information about one another's locations during update intervals and with limited location update frequencies, we propose to have vehicles estimate one another's locations during update intervals. For accurate estimation of vehicle locations, it is important to have a good model for vehicle location dynamics.

Fortunately, vehicle dynamics have been studied extensively in traffic flow theory, and the intelligent-driver-model (IDM) as well as its extensions have been shown to be able to accurately model microscopic vehicle traffic flow dynamics [59]. A key part of the models is the model on vehicle acceleration behavior according to the speed and locations of a vehicle and its surrounding vehicles. In this study, we use an enhanced version of IDM which captures precisely the behavior of adaptive cruise control (ACC). In the model, the vehicle acceleration function a_{ACC} is defined by (3.4) below [59]:

$$a_{ACC}(s, v, v_l, \dot{v}_l) = \begin{cases} a_{IIDM}, & \text{if } a_{IIDM} \geq a_{CAH} \\ (1-c)a_{IIDM} + c[a_{CAH} + & \text{otherwise} \\ b\text{tanh}(\frac{a_{IIDM} - a_{CAH}}{b})], & \end{cases} \tag{3.4}$$

where $c \in [0, 1]$ and is usually set as 0.99,

$$a_{CAH}(s, v, v_l, \dot{v}_l) = \begin{cases} \dfrac{v^2 \tilde{a}_l}{v_l^2 - 2s\tilde{a}_l}, & \text{if } v_l(v - v_l) \leq -2s\tilde{a}_l \\ \tilde{a}_l - \dfrac{(v - v_l)^2 I_{v - v_l \geq 0}}{2s}, & \text{otherwise} \end{cases} \tag{3.5}$$

$$a_{IIDM} = \begin{cases} a(1 - z^2), & \text{if } v \leq v_0, z = \dfrac{s^*(v, v - v_0)}{s} \geq 1 \\ a_{free}(1 - z^{(2a)/a_{free}}), & \text{if } v \leq v_0, z < 1 \\ a_{free} + a(1 - z^2), & \text{if } v > v_0, z \geq 1 \\ a_{free}, & \text{if } v > v_0, z < 1 \end{cases} \tag{3.6}$$

$$a_{free}(v) = \begin{cases} a[1 - (\dfrac{v}{v_0})^{\delta}], & \text{if } v \leq v_0 \\ -b[1 - (\dfrac{v}{v_0})^{a\delta/b}], & \text{otherwise} \end{cases} \tag{3.7}$$

$$s^*(v, v - v_0) = s_0 + \max(0, vT + \frac{v(v - v_l)}{2\sqrt{ab}}). \tag{3.8}$$

In the above equations, v and v_l represent the speed of the modeled vehicle and its lead vehicle (i.e., the vehicle immediately preceding the vehicle considered) respectively, s is the rear-bumper-to-front-bumper distance from the lead vehicle to the vehicle, $\dot{v}_l$ is the acceleration of the lead vehicle, and the effective acceleration of the lead vehicle used in modeling is $\tilde{a}_l = \min(\dot{v}_l, a)$. In the above model, the parameters v_0, T, s_0, δ, a, and b represent the desired speed, time gap between the vehicle and its lead vehicle, minimum space gap between the vehicle and its lead vehicle, acceleration exponent, maximum acceleration, and comfortable deceleration respectively [59].

Using the above model and by treating the speed, location, and bumper-to-bumper distance to its lead vehicle as the "state" of a vehicle, we can derive the dynamic model of the vehicle. Given that the model is nonlinear, we use the Unscented Kalman Filter (UKF) [60] to estimate vehicle locations. By treating the model parameters as a part of the system state and introducing random walks to the parameter evolution [60], the microscopic model can also be adapted according to the individual driving behavior of vehicles. Besides vehicle location estimation, the above approach to

vehicle location estimation can be applied to a vehicle itself to filter out GPS location measurement errors for improved GPS localization accuracy.

The IDM model focuses on the longitudinal movement of a vehicle along a specific lane, and it does not directly model behavior such as lane change and turn. Since it is more difficult to model those behavior accurately [59], we propose, for effectiveness of real-world deployment, not to explicitly model those behavior and resort to event-based quick diffusion of vehicle state to address the impact of lane change and turn; that is, a vehicle immediately shares its new location right after it changes lane or turns. Together, these mechanisms enable vehicles to be aware of one another's locations, thus enabling the effective use of the gPRK model in V2V networks.

3.3.3 gPRK Modeling of Broadcast Interference Relations

Sender ER for reliable broadcast. A fundamental communication primitive in V2V networks is single-hop broadcast via which a vehicle shares its state (e.g., location and speed) with close-by vehicles within a certain distance [50]. Reliable broadcast is a well-known challenge because, even though acknowledgments from receivers are required for many reliability-enhancement mechanisms such as ACK-/negative-ACK-based retransmission of lost packets and RTS-CTS-based collision avoidance in medium access control, it is difficult for a sender to reliably and efficiently get an acknowledgment from every receiver, especially when the number of receivers is large in V2V networks (e.g., up to hundreds).

To address the challenge, we observe that, to ensure a minimum broadcast reliability T_S for a sender S, we need to make sure that the communication reliability along the link from S to every one of its receiver $R_i \in \mathbf{R}$ is at least T_S. This fact enables us to define, for a broadcast sender S, a *receiver exclusion region (ER)* $\mathbb{E}_{S,R_i,T_S}$ for every receiver $R_i \in \mathbf{R}$ based on the gPRK model. Accordingly, we define the *sender ER* for S, denoted by $\mathbb{E}_{S,T_S}$, as the union of the its corresponding receiver ERs; that is, $\mathbb{E}_{S,T_S} = \cup_{R_i \in \mathbf{R}} \mathbb{E}_{S,R_i,T_S}$. For instance, Figure 3.5 shows an example of the sender ER when the sender S has four receivers R_1, R_2, R_3 and R_4. Based on the

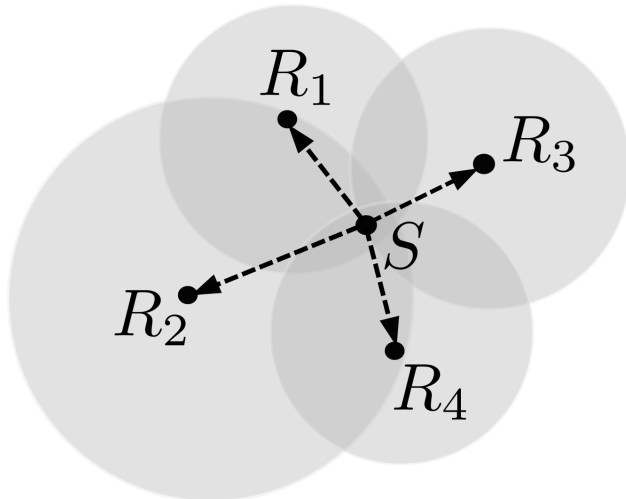

Figure 3.5: Sender ER

definition of the sender ER, the broadcast reliability of T_S is ensured as long as no node in $\mathbb{E}_{S,T_S}$ transmit concurrently with sender S.

Broadcast receiver ER adaptation. For reliable inter-vehicle broadcast, a vehicle C in the sender ER of another vehicle S shall not transmit concurrently with S. Given that the sender ER of a vehicle S is the union of the receiver ERs of S's receivers, a vehicle C may lie in the receiver ER of multiple receivers; that is, the receiver ERs of two receivers R_i and R_j ($i \neq j$) may overlap and share some common vehicles. The overlap of receiver ERs and the fact that the sender ER is the union of all receiver ERs makes the unicast-oriented receiver ER instantiation rule presented in Section 3.3.1 not directly applicable to broadcast. In particular, after a receiver R_i computes $\Delta I_{R_i}(t)$ at time t and if $\Delta I_{R_i}(t) \neq 0$, R_i needs to consider whether a vehicle C lies in the receiver ER of another receiver $R_j (j \neq i)$ when deciding to add or remove C from the receiver ER of R_i itself.

When $\Delta I_{R_i}(t) < 0$ (i.e., R_i needs to expand its receiver ER), the receiver ER expansion rule Rule-ER1 needs to be amended with the following rule:

> <u>Rule-BC1:</u> If a vehicle C is not in the receiver ER of R_i but is in the receiver ER of another receiver $R_j (j \neq i)$ at time t (i.e., $C \in \mathbb{E}_{S,R_j,T_S}(t) \setminus \mathbb{E}_{S,R_i,T_S}(t)$), R_i treats $I_{C,R_i}(t)$ as zero.

The rationale for Rule-BC1 is that, if C is already in the receiver ER of another receiver R_j, C is already in the sender ER of S and does not transmit concurrently with the broadcast transmission by S, and thus C does not introduce any interference to the receiver R_i and its effective interference power to R_i (i.e., $I_{C,R_i}(t)$ is zero.

When $\Delta I_{R_i}(t) > 0$ (i.e., R_i needs to shrink its receiver ER), the receiver ER shrinking rule Rule-ER2 needs to be amended with Rule-BC1 for the same rationale as discussed above. However, if the receiver ER of R_i is completely covered by other receivers' ERs at time t (i.e., $\mathbb{E}_{S,T_S}(t) = \mathbb{E}_{S,T_S}(t) \setminus \mathbb{E}_{S,R_i,T_S}(t)$) or if applying Rule-ER2 and Rule-BC1 at time t would make the receiver ER of R_i completely covered by other receivers' ERs, Rule-ER2 and Rule-BC1 cannot be directly applied since applying these rules will lead to an empty receiver ER for R_i. In this case, we regard R_i as an *unconstrained receiver of* S at time t since the sender ER of S will only depend on the receiver ERs of those receivers other than R_i. Accordingly, we regard a receiver R_j as a constrained receiver of S at time t if R_j is not an unconstrained receiver. For an unconstrained receiver R_i at time t, its receiver ER does not impact the sender ER $\mathbb{E}_{S,T_S}(t)$ at time t, thus we could arbitrarily set its ER if we do not consider network dynamics such as vehicle mobility. Due to network dynamics such as vehicle mobility, however, a vehicle R_j whose receiver ER covers that of R_i at time t may move such that R_j's receiver ER does not cover that of R_i at time $t + k$ $(k \geq 1)$. To address the impact of network dynamics, we propose the following rule of adapting the receiver ER of an unconstrained receiver R_i so that the communication reliability from S to R_i is still ensured at time $t + 1$ even if network dynamics (e.g., vehicle mobility) makes none of other receiver's ERs cover R_i's receiver ER at time $t + 1$. (Note that, for a constrained receiver R_j with $\Delta I_{R_j}(t) > 0$, Rule-ER2 and Rule-BC1 apply.)

<u>Rule-BC2:</u>

(A) If $\Delta I_{R_i}(t) > 0$, R_i is an unconstrained receiver of S, and the receiver ER of R_i is completely covered by other receivers' ERs at time t (i.e., $\mathbb{E}_{S,T_S}(t) = \mathbb{E}_{S,T_S}(t) \setminus \mathbb{E}_{S,R_i,T_S}(t)$), R_i expands its receiver ER to the largest possible that is still completely covered by other re-

ceivers' ERs (i.e., sets $K_{S,R_i,T_S}(t)$ to the largest value that still ensures $\mathbb{E}_{S,T_S}(t) = \mathbb{E}_{S,T_S}(t) \setminus \mathbb{E}_{S,R_i,T_S}(t)$), and then R_i applies Rule-ER2 (but not Rule-BC1) to shrink its receiver ER.

(B) If $\Delta I_{R_i}(t) > 0$, R_i is an unconstrained receiver of S, and $\mathbb{E}_{S,T_S}(t) \neq \mathbb{E}_{S,T_S}(t) \setminus \mathbb{E}_{S,R_i,T_S}(t)$, R_i first lets $\mathbb{E}_0 = \mathbb{E}_{S,R_i,T_{S,R}}(t)$, then keeps removing nodes out of $\mathbb{E}_{S,R_i,T_{S,R}}(t)$, in the non-increasing order of their distance to R, until the condition $\mathbb{E}_{S,T_S}(t) = \mathbb{E}_{S,T_S}(t) \setminus \mathbb{E}_{S,R_i,T_S}(t)$ holds for the first time. Then R_i sets $\Delta I_{R_i}(t)$ as $\Delta I_{R_i}(t) - \sum_{C \in \mathbb{E}_0 \setminus \mathbb{E}_{S,R_i,T_{S,R}}(t)} I_{C,R}(t)$, where $I_{C,R}(t)$ is computed in conformance with Rule-BC1. Then R_i applies Rule-ER2 (but not Rule-BC1) to shrink its receiver ER.

In Rule-BC2(A), the reason why R_i first expands its receiver ER to the largest possible that is still completely covered by other receivers' ERs is to make sure that, before applying Rule-ER2, the value of $\mathbb{E}_{S,R,T_{S,R}}(t)$ corresponds to the network setting from which the value of $\Delta I_{R_i}(t)$ is derived while assuming that no other receiver ER covered the receiver ER of R_i. With Rule-BC2, the communication reliability from S to R_i is ensured even if no other receiver's ER covers the receiver ER of R_i at time $t+1$. This property is important for V2V networks with high vehicle mobility. A special case is when a vehicle $R_j (j \neq i)$ at the boundary of the broadcast communication range of S moves outside the communication range of S while R_i is the the next vehicle closest to the boundary of S's communication range, as shown in Figure 3.6. In this case, R_i's receiver ER is covered by that of R_j, and a significant portion of S's sender ER is also covered by R_j's receiver ER.[4] By having R_i set its receiver ER assuming that it is not covered by that of R_j, the communication reliability from S to R_i and the fast convergence of the sender ER of S are ensured when R_j moves outside the communication range of S.

Lightweight signaling of sender ER. Two vehicles S_i and S_j $(i \neq j)$ interfere with each other and thus cannot transmit concurrently if $S_i \in \mathbb{E}_{S_j,T_{S_j}}$ and/or $S_j \in \mathbb{E}_{S_i,T_{S_i}}$, where T_{S_i} and T_{S_j} are the broadcast reliability requirements by S_i and S_j respectively. In order for vehicles to know the mutual interference relations among themselves, each vehicle S needs to share its sender ER $\mathbb{E}_{S,T_S}$ with potentially interfering vehicles. Since the sender ER is the union of all receiver ERs and the

[4]For clarity of Figure 3.6, the figure does not show other receivers of S nor their ERs.

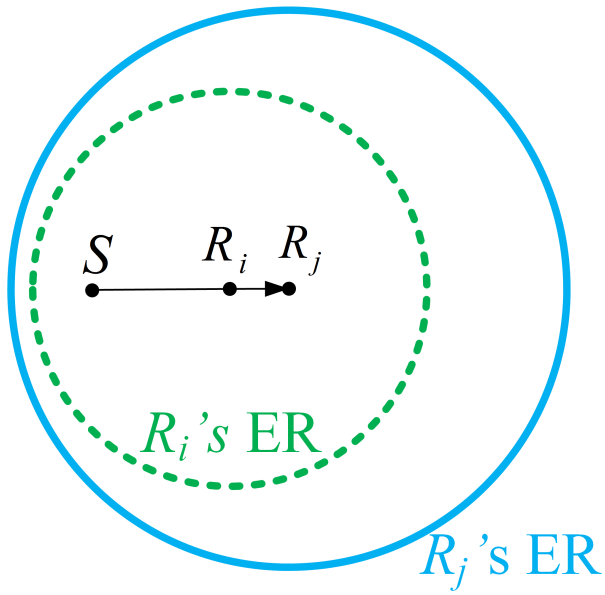

Figure 3.6: Benefit of Rule-BC2

number of broadcast receivers may be large (e.g., up to hundreds), the overhead for a sender to signal its sender ER with potentially interfering vehicles will be high if we represent the sender ER by listing all the receiver ERs individually. High signaling overhead not only reduces effective network capacity, it also makes it difficult for vehicles to share their sender ERs in a timely manner and to be accurately aware of their mutual interference relations. To address the challenge, we observe that, for a given sender S, its receiver ERs tend to overlap with one another, especially in heavy vehicle traffic settings. To minimize signaling overhead, S needs to minimize the number of receiver ERs it signals. By treating each receiver ER as the set of vehicles inside the ER, the minimum signaling overhead problem can be formulated as a *minimum-set-cover (MSC)* problem where the sender S needs to select a minimum number of receiver ERs such that the selected receiver ERs cover all the vehicles that are in the sender ER. More formally, given a sender S and

its receivers $\mathbf{R}(t)$ at time t, the problem can be formulated as follows:

$$\begin{array}{ll} \underline{\text{Problem}} & \mathbf{P}_{\text{MSC}} \\ \text{minimize} & |\mathbf{R}'(t)| \\ \text{subject to} & \mathbf{R}'(t) \subseteq \mathbf{R}(t) \\ & \cup_{R_i \in \mathbf{R}'(t)} \mathbb{E}_{S,R_i,T_S}(t) = \cup_{R_i \in \mathbf{R}(t)} \mathbb{E}_{S,R_i,T_S}(t) \end{array} \tag{3.9}$$

It is well-known that the MSC problem is NP-hard [61], thus we use the following simple, greedy algorithm to solve problem $\mathbf{P}_{\text{MSC}}$:

- Denote the optimal solution to be $\mathbf{R}^*(t)$, and initialize $\mathbf{R}^*(t)$ to be $\emptyset$;
- Iteratively add receivers to $\mathbf{R}^*(t)$ until $\cup_{R_i \in \mathbf{R}^*(t)} \mathbb{E}_{S,R_i,T_S}(t) = \cup_{R_i \in \mathbf{R}(t)} \mathbb{E}_{S,R_i,T_S}(t)$; at each step of the iterative process, choose the receiver whose receiver ER contains the largest number of uncovered vehicles.

The time complexity of the above algorithm is $O(|\mathbf{R}(t)|| \cup_{R_i \in \mathbf{R}(t)} \mathbb{E}_{S,R_i,T_S}(t)|)$. According to Chvatal [61], the above greedy algorithm achieves an approximation ratio no larger than $\ln(|\cup_{R_i \in \mathbf{R}(t)} \mathbb{E}_{S,R_i,T_S}(t)|)+1$, which tends to be small. Our experimental results in Section 3.4 show that the median and maximum reduction in signaling overhead as a result of the set-cover-based approach is up to 75% and 97.37% respectively. Therefore, the above set-cover-based approach enables lightweight signaling of sender ER in a timely manner.

3.3.4 CPS: Putting Things Together

Using the mechanisms presented in Sections 3.3.1, 3.3.2, and 3.3.3, vehicles identify the mutual interference relations among themselves in an agile, distributed manner. Based on the mutual interference relations among vehicles, inter-vehicle communications are scheduled in a TDMA manner as in PRKS [6]. In particular, time is divided into time slots, and, at each time slot, a maximal set of mutually non-interfering vehicles are scheduled to transmit according to the optimal-node-activation-multiple-access (ONAMA) algorithm [62]. To enable the TDMA scheduling via the ONAMA algorithm, control signaling packets (e.g., those containing gPRK model parameters, vehicle locations, and/or sender ERs) and data packets are transmitted in the control channel and

data channel respectively, where the control channel and data channel can be separated in frequency or in time and the transmissions of control signaling packets in the control channel are coordinated in a CSMA/CA manner [6]. Data packets can also be used to piggyback certain control information such as gPRK model parameters and vehicle locations. From each vehicle's perspective, it quickly identifies close-by vehicles, initializes related gPRK model parameters, and identifies mutual interference relations with close-by vehicles immediately after it starts; then, in parallel with data transmissions, the vehicle adapts its gPRK model parameters and thus data transmission schedules accordingly. Figure 3.7 shows the interactions and timescales of the major functional components

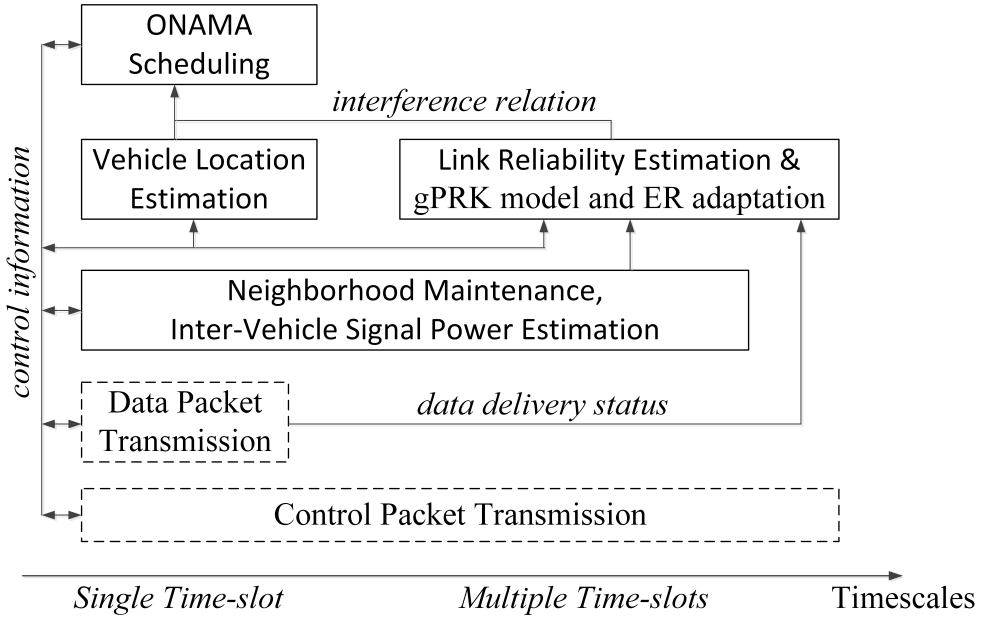

Figure 3.7: A vehicle's perspective of the cyber-physical-scheduling (CPS) framework

at each vehicle. For convenience, we call the above framework of scheduling inter-vehicle communications *cyber-physical scheduling (CPS)* since at its core lies our cyber-physical approach to identifying inter-vehicle interference relations for predictable communication reliability.

3.4 Experimental Evaluation

Due to the lack of large-scale field-deployed public V2V network testbeds for evaluating link layer scheduling algorithms, we implement our CPS scheduling framework in the ns-3 [3] network simulator, and we evaluate the behavior of CPS by integrating ns-3-based wireless network simulation with SUMO-based vehicle dynamics simulation [63].

3.4.1 Methodology

Multi-dimensional high-fidelity simulation and its implementation. High-fidelity simulation of V2V networks requires high-fidelity simulation of V2V wireless channels and vehicle mobility dynamics. For V2V wireless channels, we implement in ns-3 a channel model based on real-world measurement data that capture both large-scale path loss and small-scale fading [64]. For vehicle mobility dynamics, we use the SUMO simulator that simulates microscopic vehicle traffic flow dynamics at high-fidelity [63]. For integrated, high-fidelity simulation of V2V wireless channels and vehicle mobility, we integrate SUMO simulation with ns-3 simulation through the traffic control interface (TraCI) of SUMO, as shown in Figure 3.8. With the TraCI interface, ns-3 can query any desired information (e.g., locations of individual vehicles) from SUMO anytime. When a simulation starts, ns-3 first invokes SUMO with its local configuration files, as shown via link *a* of Figure 3.8; during a ns-3 simulation, ns-3 continuously queries vehicle state information (e.g., lo-

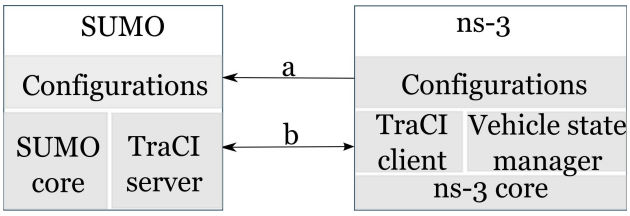

Figure 3.8: Integration of SUMO with ns-3

cations) from SUMO, as shown via link *b* of Figure 3.8). (Via TraCI, ns-3 can also send commands to SUMO to control vehicle movement, but we do not use this feature in this study.)

To make our simulation of high-fidelity, the first step is to replace the default SINR-PDR curve ns-3 has for its wifi module. We use ns-3.13 to implement our protocols and revise its wifi module for vehicular networks. In ns-3.13, whether packet receptions are successful or not is decided in file *src/wifi/model/interference-helper.cc* which defines a class called 'InterferenceHelper'. This class is responsible to calculate SINR at any given instant while a network node is receiving a packet. The first change is to extract SINR values during a packet reception and apply a different packet error rate (PER) that represents settings in vehicular networks. We borrow the measurement

results from [65] and Figure 3.9 shows the resulting SINR-PDR curve we use for packet decoding. In our experiments, we use a packet length of 1500 Byte.

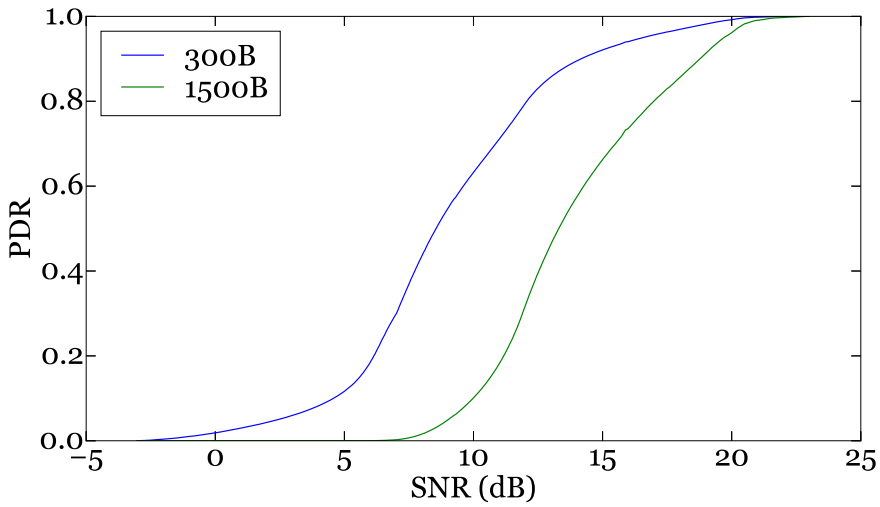

Figure 3.9: Urban network

With SINR-PDR curve revised, we then change the default signal propagation model in ns-3.13. The channel model we use is proposed in [64], and Figure 3.10 shows the channel model we use. As we can see from the figure, the default channel model used in ns-3.13 is quite different from the curve deduced from measurement results. Signal propagation loss is calculated in *src/propagation/model/propagation-loss-model.cc*. We modify signal propagation loss algorithm for 'LogDistancePropagationLossModel' which we then configure for signal propagation loss calculation.

Since the 802.11 Wi-Fi stack by default uses CSMA. Our CPS uses TDMA instead. Thus, we also disable ns-3.13's default CSMA procedure. The crucial method we need to disable is a method called 'StartAccessIfNeeded' defined in *src/wifi/model/dca-txop.cc*. Without this method, the entire CSMA process is disabled. For TDMA implementation, we can use the schedule utility functions to schedule time sensitive events, for instance, packet transmission or reception.

Protocols. To demonstrate the benefits of CPS in scheduling inter-vehicle communications, we comparatively study the following representative V2V network protocols:

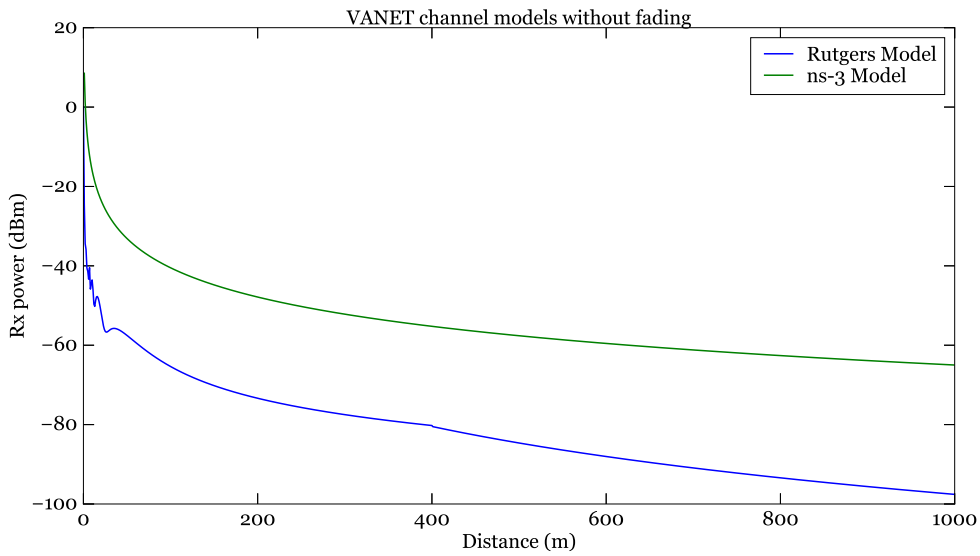

Figure 3.10: Urban network

- *802.11p*: the MAC protocol of the IEEE 802.11p standard which uses CSMA/CA to coordinate channel access and interference control [53]. This is the MAC protocol used in existing field deployments of DSRC implementations (e.g., those by the USDOT).
- *DCC*: an ETSI standard that uses congestion, power, and rate control on top of the IEEE 802.11p protocol to mitigate inter-vehicle interference and improve communication reliability [66].
- *AMAC*: the ADHOC MAC protocol [67] which is a slot-reservation-based TDMA protocol based on the protocol interference model. In the protocol, vehicles transmit in their reserved slots without carrier sensing. If collisions are detected in a certain time slot of the TDMA frame, vehicles will release the slot and reserve another slot .
- *VDDCP*: a TDMA-based MAC protocol [68] that, based on the protocol interference model, first allocates non-overlapping sets of time slots to different roads and then let vehicles on each road compete for channel access in a slot-reservation-based TDMA manner as in AMAC.

To understand the effectiveness of the geometric approximation of the PRK model by the gPRK model, we also study a variant of CPS, denoted as OCPS (for Oracle CPS), that is the same

as CPS except for its use of the PRK model. In OCPS, we assume that after a vehicle R has a new estimation for the signal power $P_{C,R}$ from another vehicle C to itself, the newly estimated $P_{C,R}$ is known to every other potentially interfering vehicle through some oracle without requiring any control signaling packet exchange as we have discussed in Section 3.3.1; this way, the costly and sometimes infeasible signal-map-related control signaling overhead is gone, and OCPS can be executed in our simulation environment.

Network and traffic settings. For understanding protocol behavior in different V2V network settings, we consider two networks: an *urban* network consisting of vehicles in midtown Detroit, and a *freeway* network consisting of vehicles on I-75 north to midtown Detroit.

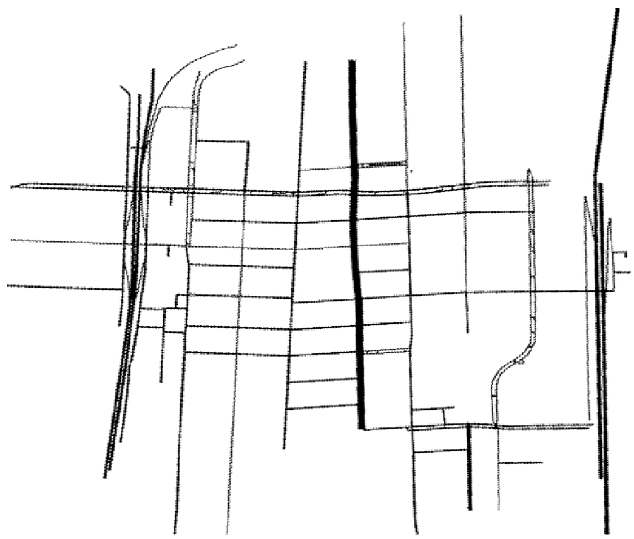

Figure 3.11: Urban network

As shown in Figure 3.11, the urban network consists of freeway I-75 and city roads in midtown Detroit, and it spans an area of $\sim$ 3km $\times$ 3km. In the urban network, vehicle speed ranges from 40km/h (i.e., 25mph) on small city streets to 120km/h (i.e., 75mph) on I-75. As shown in Figure 3.12, the freeway network consists of vehicles moving at a speed of $\sim$120km/h along opposite directions of I-75, and it spans an I-75 road segment of length 3.5km. We use the freeway network to understand protocol behavior in fast-varying network settings. Our study considers normal vehicle traffic flow conditions; the average bumper-to-bumper distance in the

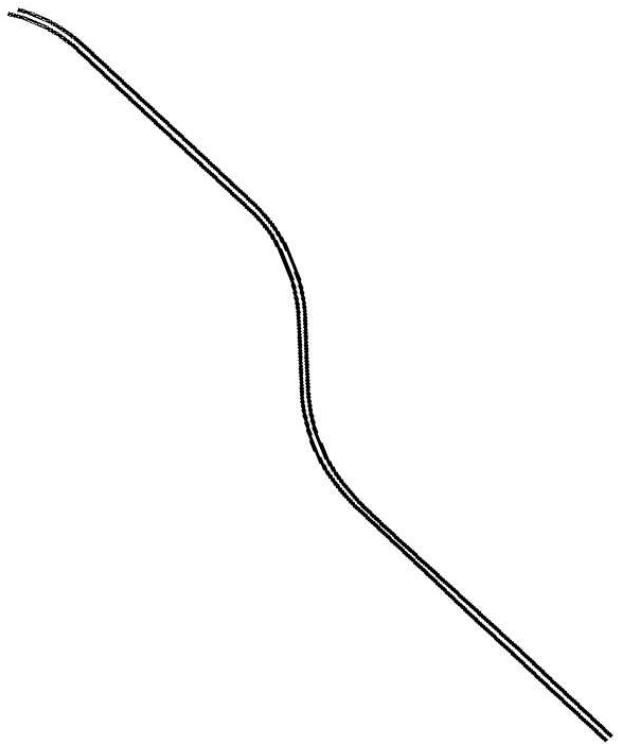

Figure 3.12: Freeway network

urban network ranges from ∼1 meter to ∼20 meters, and the average bumper-to-bumper distance in the freeway network is ∼20 meters.

We set the desired broadcast communication range as 150 meters and the desired broadcast reliability as 95%. For protocols that do not use transmission power and rate control (i.e., protocols other than DCC), the transmission power to set at a value that ensures that the signal-to-noise ratio (SNR) in the absence of interference is 6dB above the SNR for ensuring 95% communication reliability for links of length 150 meters, and the transmission rate is set as 6Mbps. For understanding supportable network throughput while satisfying the broadcast reliability requirement, we consider the saturated broadcast transmission scenario where every vehicle always has packets to transmit and the size of each data packet is 1,500 bytes.

3.4.2 Experimental Results

Urban network. For the urban network, Figure 3.17 shows the boxplot of communication reliability from each vehicle to its receivers, Figure 3.18 shows the number of concurrent transmissions in the network, Figure 3.19 shows the network throughput that is computed as the number of pack-

ets successfully delivered to receivers in every time-slot duration (i.e., 5ms), and Figure 3.20 shows the packet delivery delay when packet retransmission is used to ensure the application-required reliability for protocols that would be unable to ensure the application-required reliability otherwise (i.e., protocols other than CPS).

Enabling accurate, agile identification of interference relations among vehicles, our gPRK-based cyber-physical approach to interference modeling and transmission scheduling ensures predictable interference control and application-required broadcast reliability, as shown in Figure 3.17. Implicitly assuming a protocol interference model and using a contention-based approach to medium access control, 802.11p and DCC do not ensure predictable control of interference and thus do not ensure application-required communication reliability. Through congestion, power, and rate control, DCC improves the reliability of 802.11p, but the broadcast reliability is still quite low in DCC (i.e., being $\sim$6% in our study). Assuming an inaccurate protocol interference model and unable to address the challenge of high vehicle mobility to TDMA scheduling, the TDMA protocols AMAC and VDDCP cannot ensure predictable interference control, and the communication reliability from senders to receivers tend to be quite unpredictable, ranging from very low to very high and varying over time. In AMAC and VDDCP, the slot reservation tends to be unreliable in the presence of vehicle mobility and inter-vehicle interference, thus the concurrency in AMAC and VDDCP tends to be quite low too, as shown in Figure 3.18. The fact that the reliability is unpredictable while the concurrency is low in AMAC and VDDCP demonstrates the importance of accurately identifying inter-vehicle interference relations in an agile manner in the presence of vehicle mobility, as is accomplished in our CPS framework.

The concurrency in 802.11p and DCC is the highest among all the protocols, but their throughput is quite low due to the low communication reliability in both protocols, as shown in Figures 3.19 and 3.17. Due to the low concurrency and the unpredictable, often-low communication reliability in AMAC and VDDCP, the throughput is low in both protocols. Ensuring application-required reliability while maximizing channel spatial reuse, CPS enables significantly higher throughput than other protocols do.

To improve communication reliability, retransmission is needed in other protocols, which significantly increases the communication delay, as shown in Figure 3.20. The low concurrency and the unpredictable communication reliability in AMAC and VDDCP make their communication delay the largest among all the protocols.

Freeway network. For the freeway network, Figures 3.13, 3.14, 3.15, and 3.16 show the reliability, concurrency, throughput, and delay in different protocols. The overall behavior of different protocols are similar to those in the urban network. CPS ensures predictable communication reliability in the presence of high vehicle mobility, while the communication reliability tends to be unpredictable and often-low in other protocols. The predictable communication reliability in CPS also enables high network throughput and low communication delay.

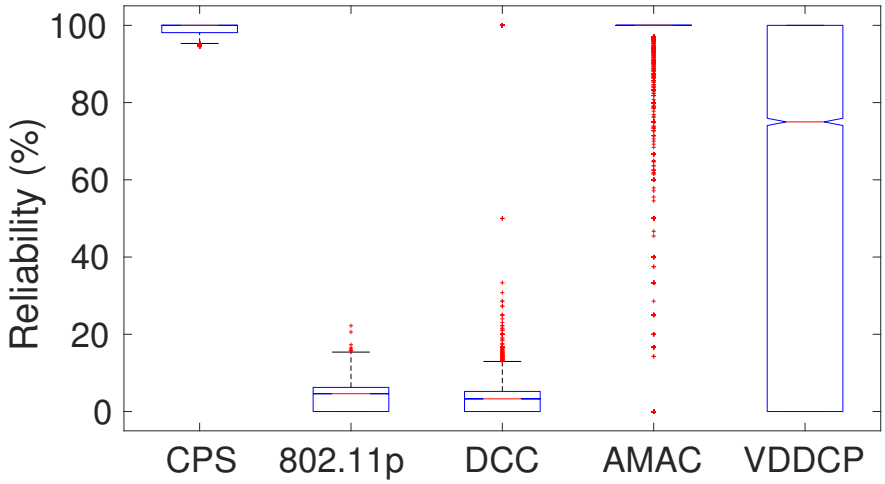

Figure 3.13: Reliability: freeway

Effectiveness of Set-Cover-Based Approach to Minimum Overhead Control Signaling. We have presented the set-cover-based approach to minimum overhead signaling of sender ERs in Section 3.3.3. For the urban network and freeway network discussed in Section 3.4, Figure 3.21 shows the empirical cumulative-distribution-function (CDF) of the percentage of overhead reduction in signaling sender ERs as a result of the set-cover-based approach to selecting the minimum number of receiver ERs to signal. We see that the overhead reduction is significant, with the median and maximum reduction up to 75% and 97.37% respectively. In addition, the overhead reduction is

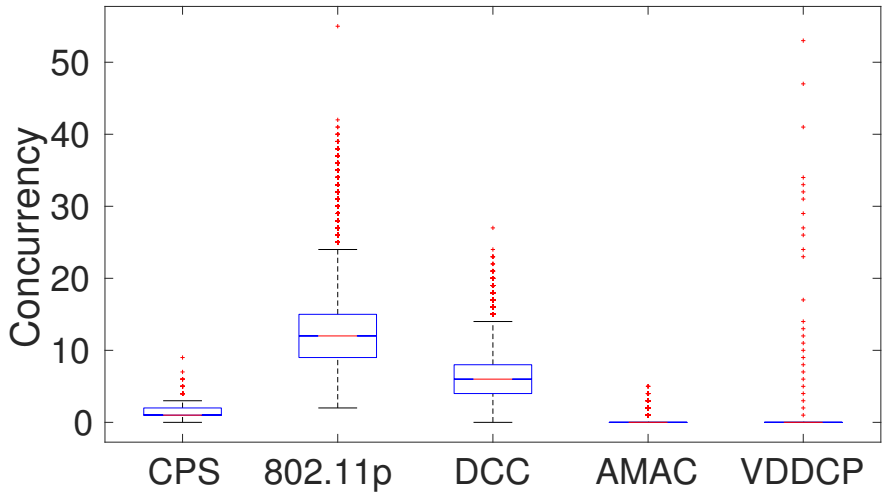

Figure 3.14: Concurrency: freeway

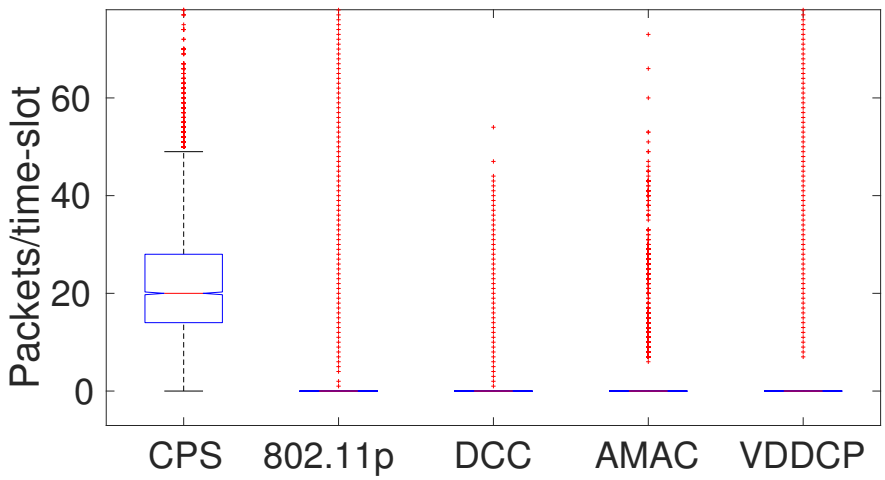

Figure 3.15: Throughput: freeway

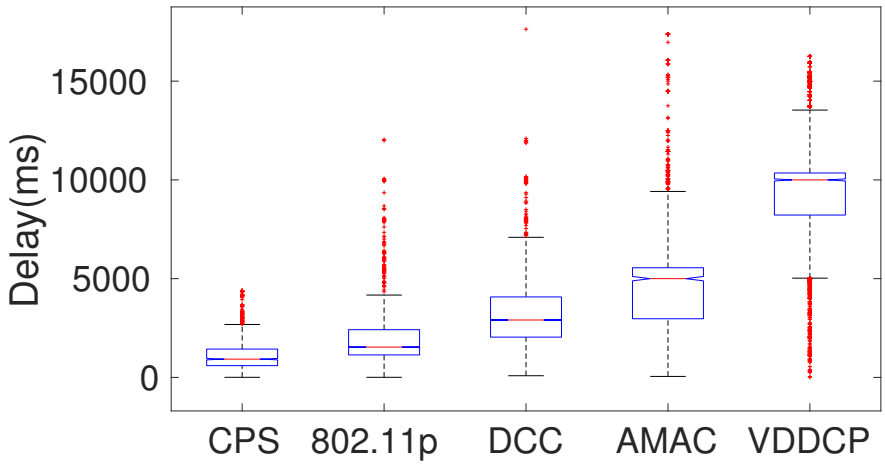

Figure 3.16: Delay: freeway

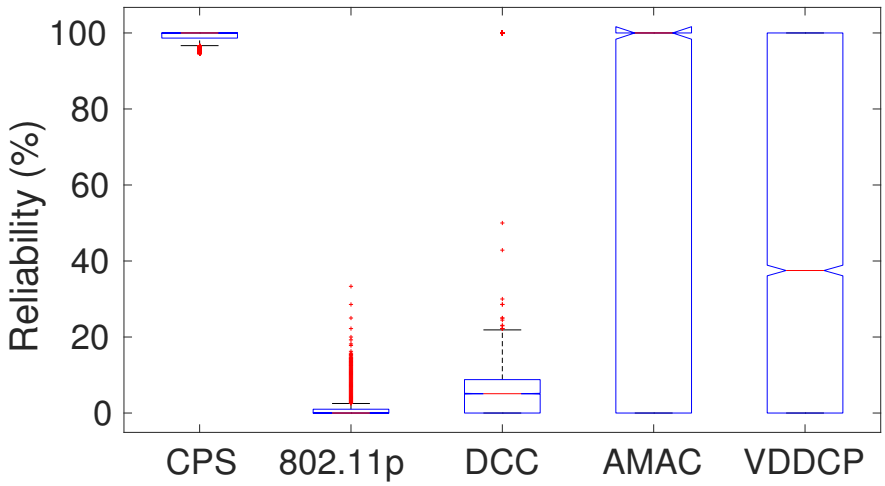

Figure 3.17: Reliability

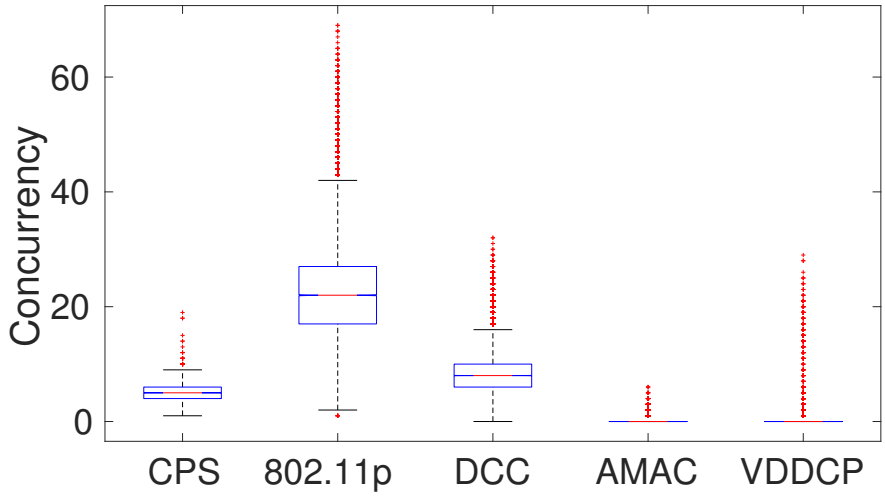

Figure 3.18: Concurrency

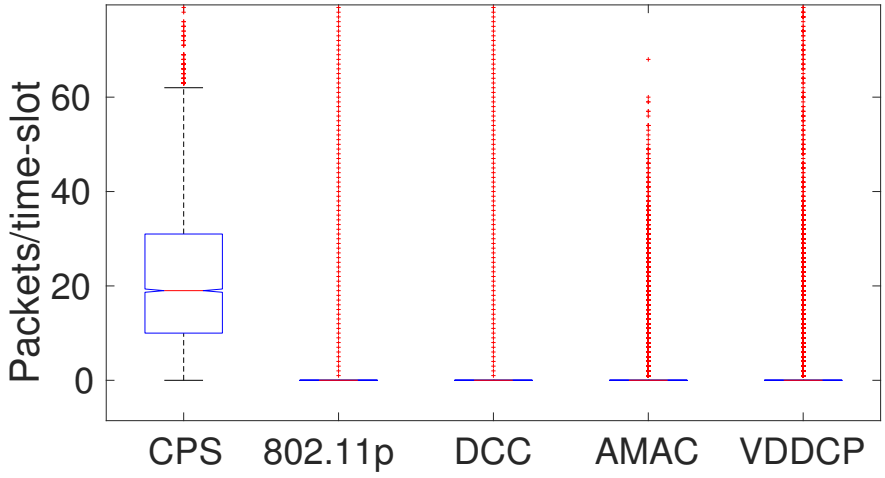

Figure 3.19: Throughput

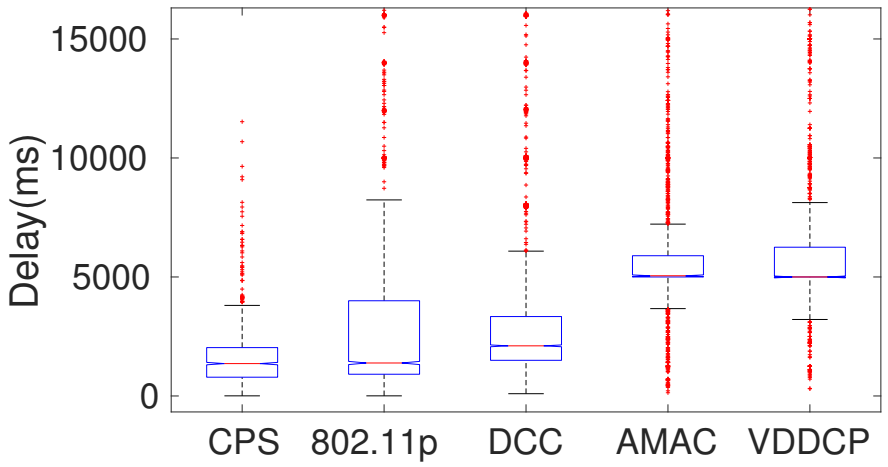

Figure 3.20: Delay

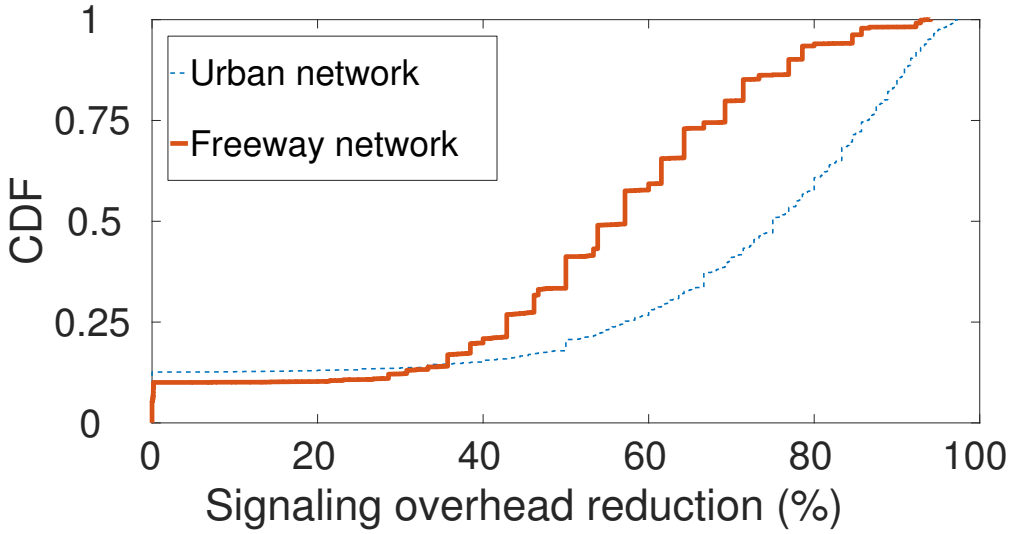

Figure 3.21: Control overhead reduction in sharing sender ERs

also more significant in networks of denser vehicle spatial distribution (e.g., in the urban network), where such savings in control signaling overhead are also more critical.

$\Delta I_U(\cdot)$ **analysis** For experimental study scenarios, we inspect the details of $\Delta I_U(\cdot)$ which denotes the changes of interference from beyond a link's exclusion region. As Figure 3.22 shows, the changes of $\Delta I_U(\cdot)$ falls in an interval that contains zero. Furthermore, Figure 3.23 shows $\Delta I_U(\cdot)$ of a typical link in a stable vehicle cluster in a traffic flow. Our detailed analysis shows that the mean of $\Delta I_U(\cdot)$ is 0.3528dB, and its 95% confidence interval is [-0.0261dB, 0.7318dB]. Thus the mean of $\Delta I_U(\cdot)$ is statistically equal to 0dB at the 95% confidence interval.

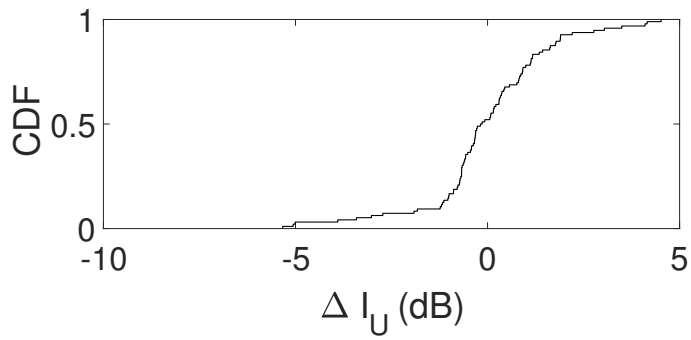

Figure 3.22: CDF of $\Delta I_U(.)$

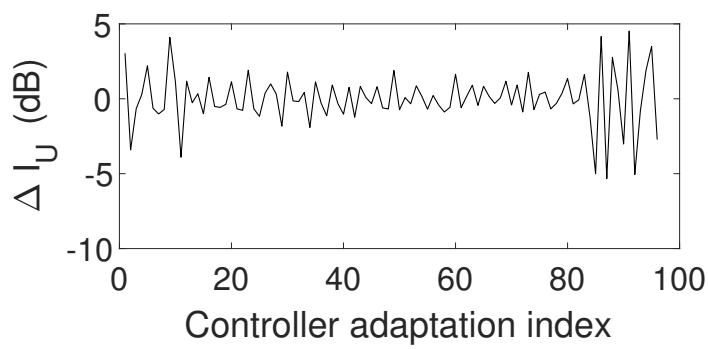

Figure 3.23: Time series of $\Delta I_U(.)$

Location tracking with GPS errors To understand how the CPS framework can adapt with vehicle mobility, we collect data to show neighbor vehicle location update intervals and neighbor vehicle location track errors. For location tracking error, we first collect the ground truth location for each vehicle, then every vehicle also reports its location tracking error whenever it receives location updates form neighbors.

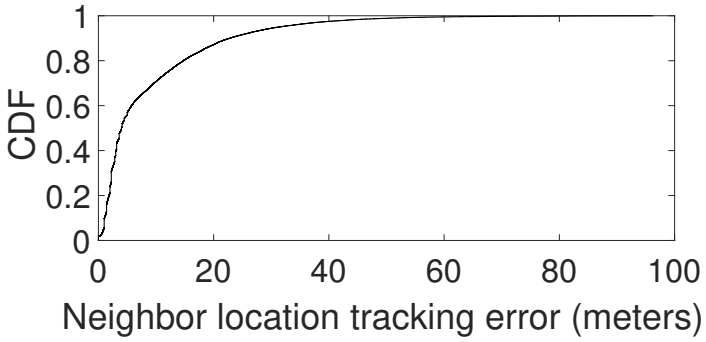

Figure 3.24: Neighbor location tracking errors

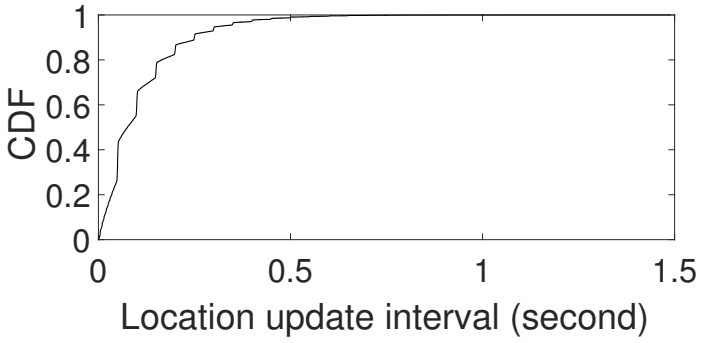

Figure 3.25: Neighbor location update intervals

Note that ground truth locations have 4-8 meters of inaccuracy due to imperfect GPS location service. Figure 3.24 shows a CDF of location tracking errors reported by all vehicles in our evaluation scenario. As we can see, location tracking error are mostly smaller than 30 meters. To overcome such errors and utilize history states of individual links, we have selected 30 meters as a distance buffer. Thus, link state data get persisted as long as the length of a link is smaller than $d_0 + 30$ in our evaluation.

We also have figure 3.25 to show a CDF of location update intervals reported by all vehicles in our test scenario. As the figure shows, the intervals are generally small.

Controller adaptation interval Figure 3.26 shows the CDF of controller adaptation interval in terms of seconds for *each* link. Even though, we consider broadcast, we still view broadcast sender and each of its receiver as a link. We see that almost all controller adaptation happens within 15 seconds. With more than 70% of consecutive controller adaptation happens within in 10 seconds.

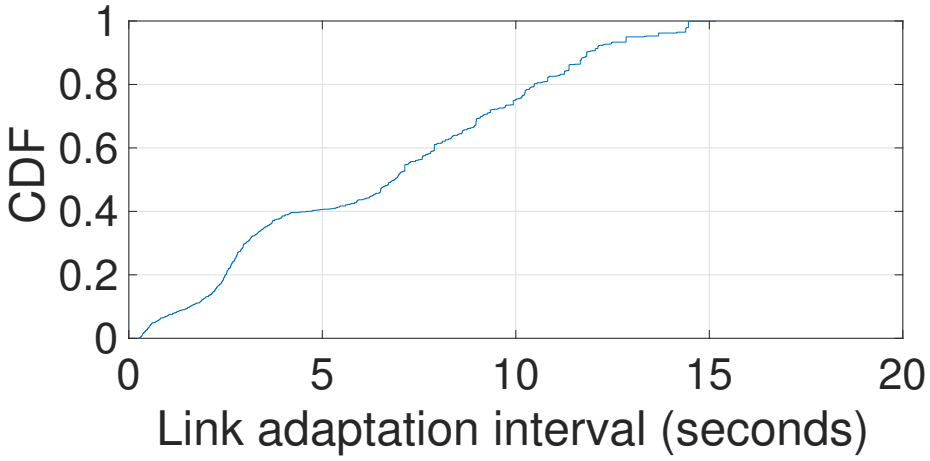

Figure 3.26: Controller adaptation interval

This time frame could be too long for transient links in different traffic flow, especially in freeways, but it's good enough for vehicles within the same traffic flow.

Different PDR requirements In Figure 3.27, we show the ranged PDR comparison in CPS. We define ranged PDR as follows: 1) We divide link distance into five groups. Each group can have 30 meters. Thus, we have links with sender receiver distance 0-30 meters as one group, 30-60 meters as another group, etc, until 120-150 meters as a group. In our evaluation, the maximum

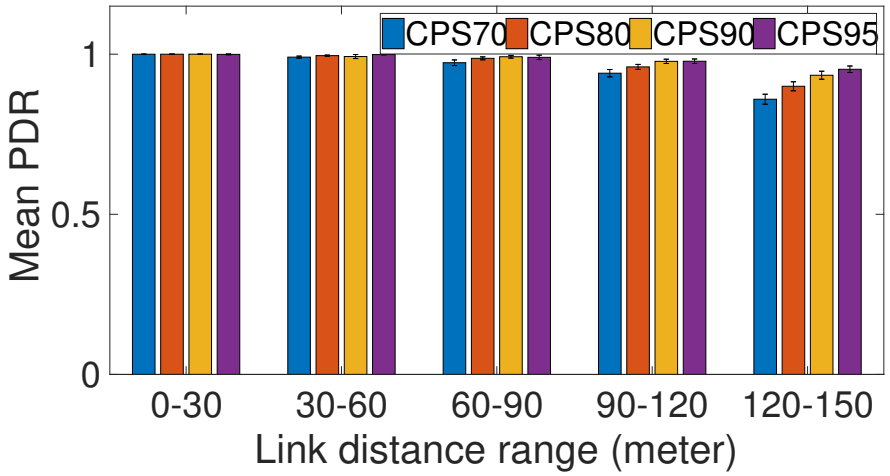

Figure 3.27: Mean ranged PDR comparison in CPS

link distance we consider is 150 meters. 2) Node mobility may cause link distance to change, as long as link distance of a link changes within the same group, we consider number of packets transmitted as a group of samples, and calculate the ratio of packets that are received by receivers.

In Figure 3.27, we show link *average* reliability in bar graph. we notice that when link distance is small, link reliability is generally better than that of links with longer distance. The group we pay special attention is the distance group 120-150 meters. In this group, we see a clear trend of PDR increase as application required reliability increases. There are still links whose average reliability is lower than application requirements as we will show data in Chapter 4.

Concurrency comparison with iOrder In Figure 3.28, we show concurrency comparison with iOrder when link reliability is 70%, 80%, 90%, and 95%. We define concurrency as the number of simultaneous transmitters in a time slot. The figure shows the mean concurrency collected in CPS and calculated in iOrder. We extended iOrder to a broadcast communication paradigm in our evaluation and added the channel model we used in ns-3 in our revised iOrder implementation. The figure shows concurrency in CPS is close to iOrder when application reliability requirement is

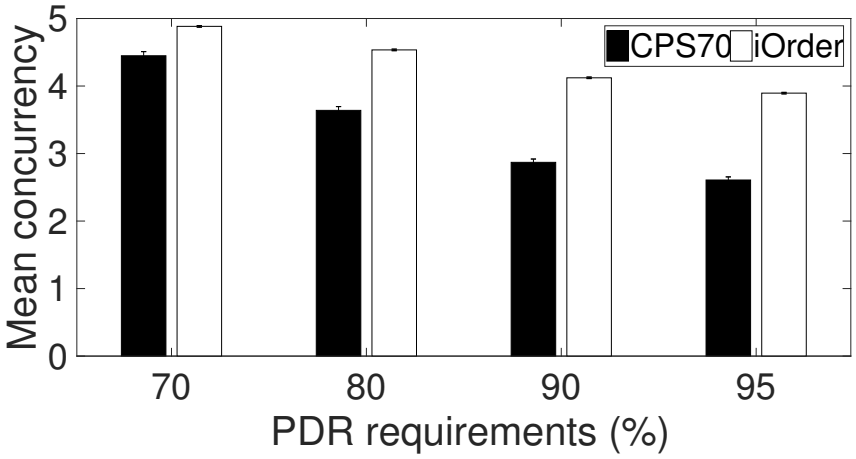

Figure 3.28: Mean concurrency comparison between CPS and iOrder

low. When application reliability requirement becomes higher, we experience more concurrency loss compared to iOrder.

CPS vs. OCPS. Figure 3.29 shows the empirical cumulative distribution function (CDF) of the communication reliability from each vehicle to its receivers in CPS and OCPS. We see that OCPS achieves a much higher communication reliability than other existing protocols, with the minimum communication reliability being 75% and the reliability being no less than the required 90% for about 85% of the links from a broadcast sender to its receivers. Nonetheless, the communication

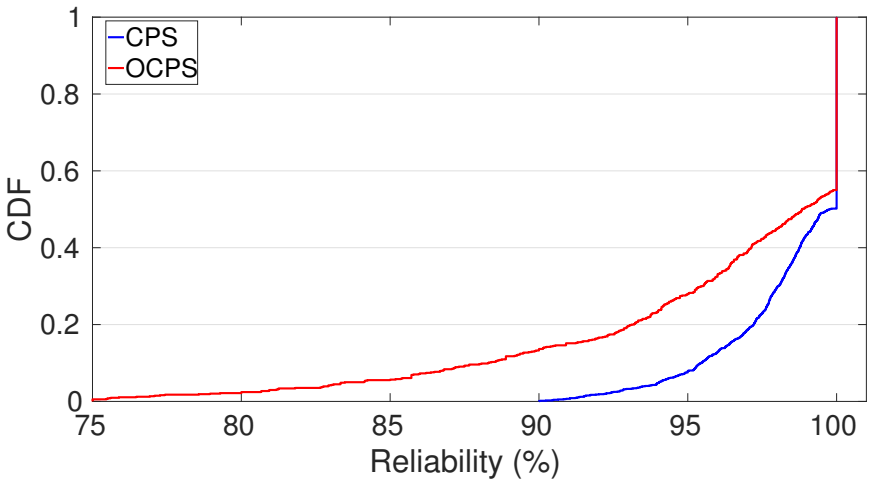

Figure 3.29: CPS vs. OCPS

reliability of about 15% of the links is less than the required 90% in OCPS, while CPS ensures the required reliability for all the links. The reason for this is because, in OCPS, even though the existence of an oracle addresses the signaling overhead challenge in PRK-based scheduling, it is still difficult to precisely track the highly-dynamic signal power from one vehicle to another in the presence of vehicle mobility, which makes it difficult to precisely track inter-vehicle interference relations and thus difficult to ensure predictable communication reliability. In CPS, the gPRK model and the tracking of vehicle movements through well-understood vehicle dynamics enable precise tracking of inter-vehicle interference relations and thus enable predictable interference control and predictable communication reliability, showing the benefits of using the geometric approximation of the PRK model in V2V networks.

3.5 Related Work

IEEE 802.11p is a well-studied industry standard specifying the medium access control mechanisms for inter-vehicle communication. Inheriting basic Wi-Fi mechanisms such as CSMA and thus unable to ensure predictable interference control, 802.11p-based solutions do not ensure predictable link reliability, for instance, even unable to ensure a broadcast reliability of 30% when information exchange load is high [53, 6]. To improve the reliability of inter-vehicle communications, schemes that control information exchange load as well as packet transmission power and rate have been proposed [66]. Not addressing the fundamental limitations of CSMA in interfer-

ence control, these schemes lead to the loss of network throughput and increase in communication delay while still being unable to ensure predictable communication reliability [6], as we have also observed in Section 3.4.

TDMA schemes [67, 69] have also been proposed for inter-vehicle communications. Based on the protocol interference model which is inaccurate and cannot ensure predictable interference control, however, these schemes cannot ensure predictable communication reliability. Multi-scale schemes have also been proposed to first allocate non-overlapping sets of time slots to different roads and then let vehicles on each road compete for channel access in a TDMA manner [70, 71, 72]. Assuming a protocol interference model in both road-level scheduling and vehicle-level scheduling, however, these schemes do not ensure predictable communication reliability. Schemes have also been proposed to first partition space into geographic regions such as rectangles or hexagons and then schedule transmissions based on geographic regions [73, 74]. Assuming a protocol interference model, however, these schemes do not ensure predictable communication reliability either. Resource allocation mechanisms have also been proposed to improve communication throughput between vehicles as well as between vehicles and transportation infrastructures [75]. Focusing on network throughput, these work do not consider ensuring predictable, controllable reliability in vehicular communication, and, due to throughput-reliability tradeoff [5], the high throughput usually comes at the cost of low communication reliability.

3.6 Concluding Remarks

For predictable reliability of inter-vehicle communications, we formulate and apply the geometric PRK (gPRK) interference model to predictable interference control in V2V networks. Our approach to gPRK-based interference modeling effectively leverages cyber-physical structures of V2V networks such as the spatial interference correlation, temporal link reliability bounds, correlated receiver ER adaptation, and set-cover-based control signaling in the cyber-domain as well as the vehicle locations and microscopic vehicle dynamics in the physical domain. Leveraging the cyber-physical, gPRK-based approach to interference modeling, our cyber-physical scheduling (CPS) framework enables predictable reliability of inter-vehicle communications. Enabling pre-

dictable interference control and communication reliability in the presence of vehicle mobility, our cyber-physical approach to interference modeling and data transmission scheduling is expected to enable the development of mechanisms for predictable real-time, throughput, and their tradeoff with reliability in inter-vehicle communications. While our focus in this study is on inter-vehicle communications, the basic methodologies can be extended to enable predictable communication reliability between vehicles and transportation infrastructures such as traffic lights. These are future directions worth pursuing.

CHAPTER 4: ENABLING SHORT-TERM RELIABILITY IN INTER-VEHICLE COMMUNICATION WITH POWER CONTROL

4.1 Introduction

With the efforts described in both Chapter 2 and Chapter 3, we are able to achieve an *average* link reliability that is no lower than an application required reliability $T_{S,R}$ for each link, yet *short-term* link reliability for each estimation interval may well be below the link reliability requirement. Fundamentally, this is due to the fact that the control objective for the controller running at each link is to guarantee average link reliability. To ensure performance guarantee in WSC systems with inter-vehicle communications settings, predictable per-packet successful reception probability is a must. Our previous work in Chapter 3 has addressed the scheduling problem with the help of the distributed solution ONAMA which provides us with a good foundation of average packet reception probability guarantee at MAC layer. In this chapter, we will focus on controlling network dynamics in inter-vehicle communication networks. ONAMA, by design, aims at providing average link reliability. The reason behind this fact is that the network conflict graph which is ONAMA's input is not generated with a goal of providing per-packet reception probability guarantee. If we provide ONAMA with proper network conflict graph, it can be reused for our problem in this chapter. With a more challenging goal, our solution needs to be able to adapt to network condition changes in a more agile manner. To this end, in addition to exclusion region and controller adaptations, we also leverage power control to achieve short-term link reliability in inter-vehicle communications.

Distributed power control in wireless networks is pioneered by the work [76] which employed an iterative method to adjust transmission power in cellular networks. Iterative power control approaches soon become infeasible in highly mobile wireless networks like those with inter-vehicle commutation settings due to fast topology changes, but these methods are well adopted by problems with static network settings to provide solutions. Following the iterative power control approach in [76], Weber et al. [77] proposed an iterative power control scheme called channel inversion (CI) power control. In [77], the transmission power for a link i is controlled by the

following scheme:

$$P_i = \frac{p}{\mathbf{E}[H^{-1}]} H_{ii}^{-1} \tag{4.1}$$

where p is the normal transmission power level, H is the channel fading matrix and H_{ii} denotes the fading factor from sender of link i to the receiver of link i. CI power control guarantees that the receive power at each link is the same for all links, and the expected transmission power $\mathbf{E}[P_i] = p$. Based on CI power control, Jindal et al. relaxed the power control scheme into the following:

$$P_i = \frac{p}{\mathbf{E}[H^{-s}]} H_{ii}^{-s} \tag{4.2}$$

The parameter s varies from $[0, 1]$. When $s = 0$, the control scheme represents constant power control (i.e., no power control); when $s = 1$, the control scheme represents CI power control scheme. This more generalized form is called fractional power control (FPC). FPC performs better compared to both no power control scheme and CI power control scheme.

While CI and FPC are both designed for continuous power control, Liu et al. [78] focused on discrete power control (DPC) in which power levels are not continuous. Liu et al. showed that by carefully choosing power levels, DPC is guaranteed to be better than cases when no power control scheme is used for wireless ad hoc networks. When only discrete power levels are available, they also show that DPC outperforms both CI power control and FPC.

The above-mentioned distributed power control schemes are all theoretical solutions, and they make assumptions that may not hold in practice. For example, [76] assumes the H matrix is known instantaneously; [77, 79, 78] assume network nodes distribution follows Poisson point process (PPP) or Poisson cluster process (PCP), which may not hold in practice, especially in inter-vehicle communications in which vehicles can only be located on roads, leaving much of the 2-D space unoccupied.

Motivation In this chapter, we use similar system settings as we did in Chapter 3 where vehicles periodically share their status to close-by neighbors in support of upper-layer applications, e.g., active safety applications. Vehicle status data are destined to vehicles within a certain geographic

distance. Since communication range in DSRC could be several hundreds of meters, we consider a one-hop broadcast communication paradigm in this chapter with DSRC settings such that the geographic distance can be covered by a single broadcast transmission. The communication links in Chapter 2 and Chapter 3 may experience periods of time during which their instantaneous link reliabilities are lower than application requirements. During these periods, system performance cannot be guaranteed, regardless of network node mobility. It makes our solutions in Chapter 2 and Chapter 3 unable to provide predictable guarantee in message delivery in a relatively short period of time.

More specifically, our link plant model only adapts its system parameter when the link has a new estimation of link reliability. With the default bandwidth in vehicle network communication technology, we expect link reliability estimation interval falls in between [2, 20] seconds, depending on the underlying scheduling algorithm. This time interval is clearly too long for links with fast link quality changes, for example, two vehicles moving in opposite directions on freeways. According to our previous frameworks, network dynamics cannot be addressed by a link unless it has a new link reliability estimation. This constraint may well result in degraded link reliability and causes instantaneous packet reception probability to be lower than higher-level application requirements.

Specifically, for a receiver R, let random variable $\mathbf{\Theta}$ denote its controller adaptations. For two consecutive controller adaptations Θ_n and Θ_{n+1}, the actual interference relations can change from Θ_n to Θ_{n+1}. In static networks, these changes do not come from changes in R's internal status, since R has not adapted its exclusion region which redefines interference relations. As a result, any changes between Θ_n and Θ_{n+1} are not addressed unless R conducts a new controller adaptation. That is, R does not have the ability to overcome these changes due to the lack of one or more additional controller adaptations between Θ_n and Θ_{n+1}. Mobility makes things worse since the controller adaptations may not be frequent enough to capture significant network condition changes.

Without power control, CPS or PRKS can suffer from concurrency loss in some special cases, e.g., sparse network. Suppose two transmitters S and S_1. If S_1 is located at the edge of the exclusion region of S, S_1 cannot transmit concurrently with S because $\langle S, R\rangle$, $\mathcal{P}_r(S_1, R) = K_{S,R,T_{S,R}}\mathcal{P}_r(S, R)$. If the transmission power at S_1 can be reduced such that

$$\mathcal{P}_r(S_1, R) < K_{S,R,T_{S,R}}\mathcal{P}_r(S, R), \tag{4.3}$$

S and S_1 can transmit concurrently according to the PRK interference model, thus improving spatial reuse as long as the packet success reception probability at the receivers of S_1 is still higher than application requirements.

Challenges To accomplish the goal of short-term reliable broadcast communication in inter-vehicle communications, we need to overcome the following challenges:

- *Communication paradigm.* Existing power control schemes in *ad hoc* networks generally target on unicast communication where the sender of a link only has to guarantee its corresponding receiver to have a signal to interference ratio (SIR) no lower than a threshold value $\gamma^0_{R,d}$ assuming sender receiver distance is d, and receiver is R. Our problem settings differ from these schemes in the sense that we consider power control mechanisms for a broadcast problem in inter-vehicle communications that aim at providing short-term link reliability for *each* individual receiver of a broadcast sender; A power control decision at a transmitter side is a fused result by inspecting power level recommendations from all receivers.
- *Packet reception model.* Existing power control schemes assume once the SIR at the target receiver is higher than $\gamma^0_{R,d}$, the packet is guaranteed to be decoded correctly, which is not true in practice. A more accurate model is a probabilistic model in which a probability distribution is associated with the success rate of packet decoding for different SINR values.
- *Mobility and node distribution.* Mobility has always been the primary challenge compared to scheduling in static wireless ad hoc networks. Due to mobility, network node distribution may not have closed-form mathematical representations especially when vehicles' mobility

is confined by roads, and features of roads may well be irregular in terms of widths, directions as well as traffic regulation signs. The commonly used PPP or PCP assumptions generally do not hold in these specific settings. In our work, we do not assume any of such node distributions.

- *Control target.* In the previous two chapters, we focus on average link reliability guarantee. In this chapter, we should revisit our controller design to enable fast recovery from short-term link reliability performance degradation.

Contributions We summarize our contributions as follows:

- We use Cantelli's inequality to estimate an interference plus noise quantile and use it as input to the link plant model to achieve *probabilistic* interference plus noise upper bound with an error rate of $1 - \rho$. In this chapter, we set $\rho = 0.95$.
- We design a field-deployable power control algorithm that is based on realistic assumptions and is aware of short-term packet reception probability. Besides, it works in highly mobile inter-vehicle communication networks.
- We integrate our power control algorithm with the distributed scheduling framework discussed in Chapter 3 to make use of probabilistic interference plus noise upper bound and guarantee performance.

4.2 System model and problem definition

Given a map $\mathbb{M}$ with freeways, local roads and traffic regulation signs, consider a network with vehicles as network nodes on $\mathbb{M}$. In our future discussions, we use vehicle and node interchangeably. Let us denote the vehicular network as $G = (\boldsymbol{V}, \boldsymbol{E})$, where $\boldsymbol{V}$ denotes the set of vehicles on $\mathbb{M}$. For any vehicle S and R, if $D(S, R) \leq d_0$, we say link $\langle S, R\rangle$ belongs to the edge set $\boldsymbol{E}$, i.e., $\langle S, R\rangle \in \boldsymbol{E}$, where $D(S, R)$ denotes the distance between vehicle S and vehicle R, and d_0 is a system parameter. If not emphasized, d is used to denote the distance between S and R, i.e., $d = D(S, R)$, to simplify our notations in this chapter. We omit time slot in notations d or $D(S, R)$ unless we wish to differentiate d by time slots. Due to mobility and GPS errors, d changes over time.

To ease our discussion, we call our solution to the problem we will define in this section **C**yber-**P**hysical **S**cheduling and **P**ower control (**CPSP**). In CPSP, we consider reliable communication for all elements in $\boldsymbol{E}$. More specifically, let $\mathbb{S}$ denote packet reception success event, $\mathbb{F}$ denote packet reception failure event, and $(\Omega, \mathcal{F}, P)$ be a probability space, where $\Omega = \{\mathbb{S}, \mathbb{F}\}$, $\mathcal{F} = \{\{\mathbb{S}\}, \{\mathbb{F}\}\}$. We also suppose P is known for given hardware configurations. The goal is to perform joint power control and scheduling at the MAC layer to guarantee for any time slot τ and for any receiver R and its senders $S \in \boldsymbol{S}_{R,d}$ such that if $d \leq d_0$, Pr$\{\mathbb{S}|\tau\} \geq p_{R,d}$ with a maximum outage probability of $1 - \rho_{R,d}$ while maximizing spatial reuse, where $p_{R,d}$ is a distance-based requirement. That is, we want to have

$$\text{Pr}\{\text{Events of Pr}\{\mathbb{S}|\tau\} \geq p_{R,d}\} \geq \rho_{R,d}. \tag{4.4}$$

Notice that $p_{R,d}$ implies that for receiver R, the packet decode probabilities across different values of d can be different. Notation $\rho_{R,d}$ implies that outage probability of R for different values of d can also be different. We will discuss $\boldsymbol{S}_{R,d}$ in details in section 4.2.2.

4.2.1 Why distance-based?

Traditionally, people have been defining problems using IDs or addresses of senders and receivers in wireless communication systems. Due to reasons we will discuss in this section, our problem has been defined based on distance. Before we discuss these reasons, we emphasize that guaranteeing packet reception probability for each receiver with a unique ID within d_0 distance away is the same as guaranteeing packet reception probability for receivers with d distance away if d can be any value in $[0, d_0]$. Thus, it makes no difference to differentiate using ID based or distance based problem definition in terms of outcome.

Our solution to CPSP involves estimating a probabilistic upper bound of interference plus noise at each receiver's side. Once CPSP gets the estimation, CPSP does power control for performance improvement. More details on the solution are given in Section 4.3. In what follows, we discuss key reasons that drive us to use distance-based problem definition.

Interference estimation challenge In this work, we choose to use gPRK model to control interference plus noise for each link at its receiver's side. In what follows, we use a typical link $\langle S, R\rangle$ for discussion. According to the gPRK model, we have a parameter $K_{S,R,T_{S,R}}$ and a link distance $d = D(S, R)$. The circular area with radius $K_{S,R,T_{S,R}} \times d$ centered at the location of R is the exclusion region area defined by the link's gPRK model. In inter-vehicle communication networks, d changes with high frequency, which means the exclusion region area of the link $\langle S, R\rangle$ changes quite frequently. In static network like the one considered in Chapter 2, if link $\langle S, R\rangle$ has its PRK model parameter fixed, its exclusion region area tends to be stable. This is due to unchanged PRK model parameter until the next controller adaptation, and we noticed average signal attenuation between a fixed distance changes in slower frequency, e.g., minutes. Thus, the interference plus noise R can experience while receiving data is upper bounded. With a well-designed scheduling algorithm, the upper bound is usually achieved when a maximum amount of allowable concurrent transmissions happen while nodes in the exclusion region do not transmit. In vehicular network, on the contrary, since d can change extremely fast (e.g., two vehicles moving southbound and northbound on a two-way freeway respectively), the link has an unstable exclusion region, regardless of the area covered by its exclusion region or nodes fall in its exclusion region. Although in reality, $d \neq 0$, the changing exclusion region makes it extremely difficult to estimate the upper bound of interference plus noise. We noticed that in gPRK model, exclusion region is defined by distance and the gPRK model parameter. With changing distance, the history samples of interference plus noise cannot provide meaningful guidance in interference plus noise estimation. For per-packet reception probability, if we cannot estimate interference upper bound accurately, a data reception can easily get corrupted due to unexpected strong interference. This usually happen when d has decreased too much.

Signal attenuation estimation challenge As we will see later in 4.3.4, signal attenuation between nodes is an important input for power assignment. Following the node ID- or address-based problem definitions, we have the similar challenge in estimating statistics of signal attenuation between two nodes in vehicular networks. Let us assume node S is moving south-

bound, and node R is moving northbound on a two-way freeway. If they both move at a speed of 70 MPH ($\approx$ 31.3m/s), the distance between S and R can change roughly 60 meters per second. While distance is not a good indicator for signal strength attenuation, it is still safe to say a distance change rate like this large certainly implies large signal attenuation variations. Since distance between S and R may not be recurring, samples of signal strength attenuation between S and R provide no meaningful guidance for future signal attenuation estimation.

When both interference plus noise and signal strength attenuation between two nodes in the network cannot be effectively estimated in node ID- or address-based problem definition, it is infeasible to provide per-packet reception probability guarantee.

Benefits of distance-based problem definition With distance-based problem definition, we propose to group interference plus noise by a constant distance at a receiver R. For instance, interference plus noise sampled with sender receiver distance d' and d'' belong to different groups when $d' \neq d''$. Since exclusion region is defined by both link distance and gPRK model parameter, we also propose to define a distance based packet reception probability concept, see Section 4.2.2 for details. With distance-based packet reception probability, exclusion regions we will get through exclusion region adaptations become valid for distance d at the receiver R. As long as we group exclusion regions by distance d and gPRK model parameter, we have homogeneous interference plus noise samples in the sense that they are sampled when the node exclusion regions are of the same size. Statistics computed from these homogeneous samples are more trustworthy.

Similarly, if we group signal attenuation by distance, all samples within the same group represent signal attenuations from a fixed distance away. While distance is not a perfect indicator for signal strength attenuation, it does provide some guidance on signal strength attenuation. When distance is fixed, the estimated statistics can provide much better implications on signal attenuations between nodes.

4.2.2 Packet reception probability estimation

The problem we consider requires that every sender $S \in \boldsymbol{S}_{R,d}$ of receiver R should have per-packet reception probability no lower than $p_{R,d}$. Due to mobility, consecutive packets from the

same sender S to R are sent with different values of d with high probability. Further, for the same reason, the link $\langle S, R\rangle$ may never be able to collect enough packet reception samples if the relative speed between S and R is too large. Large relative speed results in links with very short life time. Thus, we propose a *distance-centric* estimation method as follows:

For the same receiver R, and a distance d', as R's one hop neighbors transmit packets in different time slots, R maintains a set of triples (S, τ, d') which should be identified by d' and τ, where S is a sender, τ is a time slot, and d' is a distance independent of sender S. With d', we define a sender set at R as

$$\{\boldsymbol{S}_{R,d'} | \forall s, \text{ such that } D(s, R) = d'\}. \tag{4.5}$$

For any $s \in \boldsymbol{S}_{R,d'}$, the receiver R collects the packets been received and puts them in a set $\boldsymbol{\Phi}_{R,d'}$, where $\boldsymbol{\Phi}_{R,d'}$ denotes packets received while sender receiver distance is d'. According to the problem definition, whenever a sender receiver pair has distance d', they need to satisfy packet reception probability $p_{R,d'}$. Receiver R estimates packet reception probability based on SINR samples obtained while R was receiving packets that belong to $\boldsymbol{\Phi}_{R,d'}$ for distance d'. Notice that for a different distance d'', the receiver R should maintain another packet set, i.e., $\boldsymbol{\Phi}_{R,d''}$.

For each packet $\eta \in \boldsymbol{\Phi}_{R,d''}$, the receiver R has an SINR sample recorded. When estimating packet reception probability for the packet η, CPSP inspects the mapping δ. For instance, let us assume the SINR value R recorded for packet η is $\gamma_\eta(\tau)$ assuming the packet was been transmitted in time slot τ, then the packet reception probability is $\delta\big(\gamma_\eta(\tau)\big)$.

The benefits of estimating packet reception probability in this way are the following:

- In inter-vehicle communications, many applications are defined by distance between vehicles pairs, such as active safety application, instead of the actual sender receiver pairs.
- Using $\boldsymbol{\Phi}_{R,d'}$ to estimate packet reception probability, we base the estimation on packets that experienced similar signal attenuations and interference statistics, please refer to Section 4.3 for details. Furthermore, once we guarantee the reception probability of every packet $\eta \in \boldsymbol{\Phi}_{R,d'}$, where $d' \in [0, d_0]$, we then have solved the problem we consider.

- Exclusion region adaptations control packet reception probability from senders of a certain distance away. Once we have an exclusion region, regardless of vehicle mobility, the exclusion region is valid since it does not depend on senders, but only distances.
- Per-packet reception probability is still guaranteed via $p_{R,d}$. Notice that $p_{R,d}$ is inherently defined at the receiver R's side because only receivers can collect received packets and calculate PDR or packet reception probability without any feedback involved.
- For power control, we have a better foundation in the sense that signal strength attenuations are similar. We could then estimate the attenuation statistics. With the help of interference upper bound estimation discussed in Section 4.3.7, receivers are able to choose a power level that satisfies minimum SINR constraints and request its senders to use a power level no smaller than the chosen one through feedback. .
- Since packets are grouped by link distance, and exclusion region adaptation decisions are using distance-grouped packets, a receiver will only have one gPRK model parameter for a distance. This provides us with a good foundation for interference distribution estimation in the sense that the estimation is not sensitive to node distributions. Samples from history can be easily utilized to form larger interference sample sets. As network exists longer, our interference distribution estimation will become more accurate.

Notice that we do not care about node densities within or without exclusion regions since the gPRK as well as the original PRK model have been defined in a node density-independent context. In discussions below, we no longer use $K_{S,R,T_{S,R}}$ to denote gPRK model parameter. Instead, we use $K_{D(S,R),p_{R,D(S,R)}}$ with an emphasis on distance between S and R and the receiver R. We further simplify the notation with $K_{p_{R,d}}$ since the the distance and the receiver are in the notation $p_{R,d}$.

In future discussions, we add receiver and distance information in our Θ_n notation, thus for receiver R and sender receiver distance d, the nth controller adaptation is denoted as $\Theta_{n,R,d}$.

4.2.3 Assumptions

There are several assumptions we make for CPSP. We intentionally divide them into essential ones and evaluation ones. For essential assumptions, we have the following ones listed:

- Vehicles are equipped with a single radio. MIMO is not considered in this work,

- Wireless channels are *asymmetric* and experience fading and shadowing,
- Each vehicle has a GPS unit on board,
- Vehicles are able to adjust packet transmission powers, both data and control packets,
- Time is slotted, and synchronized by GPS,
- Packet reception is probabilistic, even for large SINR values,
- Energy is assumed to be unlimited as long as vehicles are turned on,
- Background noise is assumed to be a zero-mean random variable.

For assumptions that are we manually set in evaluation and independent of solution design, we have the following assumptions:

- Vehicles mobility uses car-following model in our experiment evaluation,
- Errors for GPS range from 4 to 8 meters.

4.2.4 Use gPRK model instead of PRK model

One of the fundamental problems in addressing reliable communication is interference modeling and control. In this chapter, we use a variant of the PRK interference model, gPRK, to model interference in inter-vehicle communication networks. Please refer to Chapter 3 for more discussions on the gPRK model and the benefits of using it. The adaptive nature of the gPRK model requires each receiver to run a local controller for *reliability-aware* interference control.

4.3 CPSP: cyber-physical scheduling and power control

In this section, we first give an overview of the CPSP system. We then discuss reasons that motivate us to use a two-step approach to solve the problem we defined in Section 4.2. We describe the algorithm running at each controller that helps achieve probabilistic interference plus noise upper bound in Section 4.3.3. We then discuss details on power level assignment policy, interference sampling, signal map maintenance, exclusion region adaptation logics and how we do quantile estimation. For reference purpose, we list all notations used in this section in Table 4.1.

Notation	Meaning
$D(S,R)$	distance between node S and node R
τ	time slot
$\gamma_R(\tau)$	SINR value at receiver R in time slot τ
$K_{p_{R,d}}$	gPRK model parameter for receiver R and node distance d with requirement $p_{R,d}$
$\rho_{R,d}$	quantile parameter of random variables for receiver R and distance d
$p_{R,d}$	the packet reception probability requirement for receiver R and distance d
$\widetilde{\boldsymbol{I}}$	generic notation for interference plus noise
$\boldsymbol{S}_{R,d}$	sender set recorded at receiver R when distance between elements in the set and R is d
$\Theta_{n,R,d}$	the nth controller adaptation at receiver R for distance d
$\mathcal{Q}^{\boldsymbol{X}}_{\rho_0}$	the ρ_0 quantile value for random variable $\boldsymbol{X}$
$\Delta\mathcal{Q}^{\widetilde{\boldsymbol{I}}_{R,d}}_{\rho_{R,d}}(\Theta_{n,R,d})$	The amount of extra quantile value of $\widetilde{I}$ exclusion region adaptation should accommodate at controller adaptation $\Theta_{n,R,d}$
δ	the SINR to PDR mapping
$\widetilde{\boldsymbol{I}}_{R,d}(\Theta_{n,R,d})$	interference plus noise samples after controller adaptation $\Theta_{n,R,d}$ at receiver R for distance d
$\boldsymbol{\mathcal{N}}_{R,d}(\Theta_{n,R,d})$	noise samples after controller adaptation $\Theta_{n,R,d}$ at receiver R for distance d
$\Delta\boldsymbol{I}_{U,(R,d)}(\Theta_{n,R,d})$	changes of interference beyond exclusion region at R for d
$\mathcal{P}_{r,(R,d)}(\Theta_{n,R,d})$	receive power samples after controller adaptation $\Theta_{n,R,d}$ at receiver R for distance d
$\mathcal{P}_{t,(R,d)}(\Theta_{n,R,d})$	transmit power samples after controller adaptation $\Theta_{n,R,d}$ at receiver R for distance d
ω	packet reception probability estimation window
$\gamma^i_{R,d}(\Theta_{n,R,d})$	the SINR value of the ith packet received at receiver R for distance d after controller adaptation $\Theta_{n,R,d}$
$\boldsymbol{\Phi}_{R,d}$	the packet set at R when sender receiver distance is d
$\Delta\widetilde{\boldsymbol{I}}_{g,(R,d)}(\Theta_{n,R,d})$	the difference between $\rho_{R,d}$ quantile controller wishes to achieve and the actual interference plus noise quantile value
ϵ	an extra amount of SINR in controller to help stabilize network
$\mathcal{Q}^{\widetilde{\boldsymbol{I}}_{R,d}}_{\rho_{R,d}}(K_{p_{R,d}},d)$	long-term estimation of interference plus noise quantile, regardless of time slot at R for d
$\boldsymbol{\mathcal{A}}_{R,d}$	samples of signal strength attenuation at R for nodes distance d away
$\mathcal{P}_{rc,(R,d)}$	R generated sender transmission power recommendation for distance d
$\widetilde{\boldsymbol{I}}_{\text{gray band}}$	computed interference plus noise values from neighbors in a circular band

Table 4.1: Notations in use in CPSP

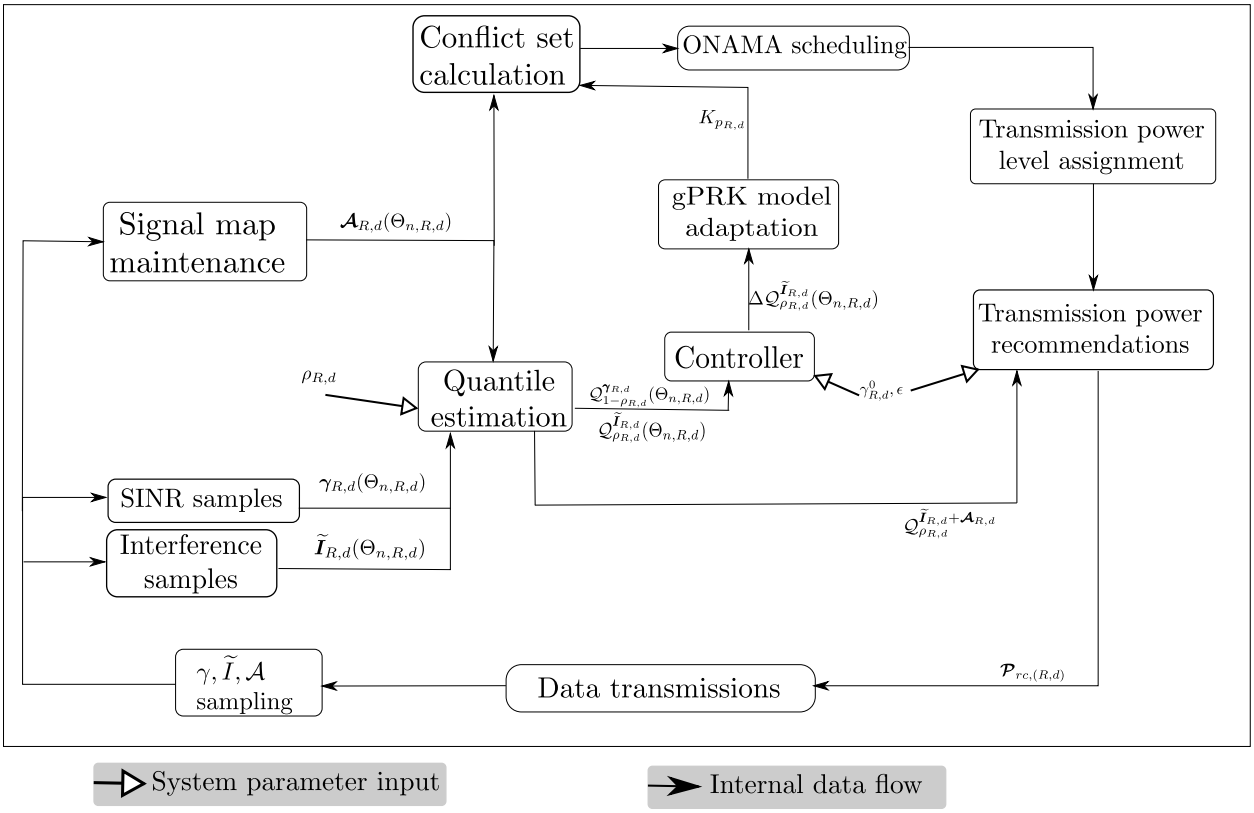

Figure 4.1: System diagram of CPSP

4.3.1 CPSP system overview

In this section, we briefly describe CPSP as a complete system with its system diagram shown in Figure 4.1. To guarantee probabilistic packet reception, we solve the problem defined in Section 4.2 from two aspects of a wireless communication system. They are interference plus noise control and power control. Following gPRK- or PRK-based scheduling, each network node runs a distributed MAC scheduling algorithm. In this chapter, we use ONAMA as shown at the top of Figure 4.1. ONAMA scheduling requires a conflict graph as input. ONAMA then takes the input and calculate maximal independent sets (MIS) using pipelined calculation. We will discuss how to calculate conflict graph later in this overview section. Each node transmits data packets according to results generated by ONAMA. Before sending out a data packet, the node needs to decide which transmission power level it should use. The decision process is discussed in Section 4.3.4. Basically, a sender inspects feedback information from its receivers. The feedback information is a transmission power each of its receivers has requested the node to use to guarantee minimum SINR requirement. Once a data packet is been sent out, receivers of the packet samples location, SINR, interference plus noise and signal strength attenuation from the sender. These sampled data are later used to drive decision processes in CPSP. For the control algorithm, as we will see in Section 4.3.3, it needs a quantile of sampled interference plus noise, a quantile of sampled SINR values to generate an amount of interference plus noise the receiver that runs the algorithm should allow or prevent to provide performance guarantee for future packets it tries to receive. When running the control algorithm, the receiver also needs system parameters $\gamma^0_{R,d}$ and ϵ, which will be covered in Section 4.3.3. All quantile values are generated using a single method discussed in Section 4.3.9. After the control algorithm has generated output, the receiver invokes an exclusion region adaptation process described in Section 4.3.8 to re-instantiate the parameter of its gPRK model. The output of the gPRK model parameter re-defines conflict relations of surrounding nodes. Thus, it becomes part of the input for conflict graph calculation. When calculating conflict graphs, nodes in CPSP use gPRK model parameters. Only nodes that are located outside of the exclusion region defined by the gPRK model are regarded as not conflicting. The sampled signal

strength attenuations together with sampled interference plus noise are the input of the process of calculating the minimum transmission power required to meet minimum SINR requirement at receivers' side. We call this minimum transmission power a transmission power recommendation from receivers' perspective. This will be discussed in detail in Section 4.3.4 .

4.3.2 Motivation for a two-step approach

In this section, we focus our discussion on a receiver R and its sender S with distance $d = D(S, R)$ when time slot is τ. That is, $S \in \boldsymbol{S}_{R,d}$. To perfectly guarantee $\Pr\{\mathbb{S}|\tau\} \geq p_{R,d}$ for τ and link $\langle S, R\rangle$, the sender S would need to know the exact SINR values at R, i.e., $\gamma_R(\tau)$, in a decision-making phase that is prior to packet reception. In Section 4.2, we have assumed for given hardware configurations, the packet reception probability for a given SINR is known. For each time slot, with realistic assumptions as listed in section 4.2.3, however, we are unable to assume $\gamma_R(\tau)$ is known since the exact interference power at R is unknown *in advance*.

There are several reasons that contribute to this fact:

- A sender cannot tell where the *non-local* simultaneous transmitters are located, and it is unable to estimate the interference caused by them individually with high accuracy. We say two nodes in a network are *non-local* when there is no direct communication in between.
- Due to network dynamics, e.g., node mobility, asymmetric and non-deterministic wireless channel, a vehicle cannot get the exact interference introduced by a concurrent transmitter.
- With power control, the exact transmission power levels of concurrent transmitters are also non-deterministic.

The goal of guaranteeing the condition $\Pr\{\mathbb{S}|\tau\} \geq p_{R,d}$ for link $\langle S, R\rangle$ is too strong when $p_{R,d}$ is large. For the same link configuration, if $\langle S, R\rangle$ has satisfied the condition at the current time slot, it may well violate the condition at the next time slot due to changes in its concurrent transmitter set as well as their transmission power levels. To make things worse, mobility and channel characteristics in inter-vehicle communications also make link configurations different even in consecutive time slots. Therefore, we assume for time slot τ and $\tau + 1$, link qualities for the same link $\langle S, R\rangle$ identified by node addresses of its sender S and receiver R are different. For each

time slot, the approach CPSP employs is to conservatively protect per-packet reception probability by studying interference introduced by concurrent transmitting neighbors and then estimating a probabilistic upper bound of sampled interference plus noise using a *non-parametric quantile estimation* method, see Section 4.3.9 for details. The quantile value serves as a probabilistic upper bound.

This proactive method can be quite effective due to the following reasons:

- Assuming $d = D(S, R)$, the receiver R inspects statistics of interference plus noise and $K_{p_{R,d}}$ that are associated with distance d. As we will discuss in Section 4.3.7, interference plus noise samples only depend on node distance d and $K_{p_{R,d}}$, thus the receiver R can accumulate interference plus noise samples as long as it exists in the network. A quantile from homogeneous interference plus noise samples becomes more accurate as the number of samples increases. When d changes, the quantile of interference plus noise R used for power control changes with d. However, the new interference plus noise quantile different from the previous quantile still represents a good probabilistic upper bound estimation. This is because of the long-term quantile estimation of interference plus noise we will discuss in Section 4.3.3. If the quantile estimation is not accurate, link $\langle S, R\rangle$ gets an outage. With large value of $\rho_{R,d}$, say 95%, this outage probability is expected to be low.
- Per-packet power control will handle link quality variations mainly due to node mobilities and guarantee $\Pr\{\mathbb{S}|\tau\} \geq p_{R,d}$. Power control is based on assuming interference plus nose and signal attenuations are the $\rho_{R,d}$ quantile of sampled values, thus will generate conservative decisions. We will discuss how CPSP gets signal attenuation samples in vehicular networks shortly.

For ease of discussion, we use $\widetilde{\boldsymbol{I}}$ to denote interference plus noise in future discussions. It becomes necessary to perform power control once $\widetilde{\boldsymbol{I}}$ is well-bounded if we want to improve network efficiency by allowing more nodes to transmit concurrently.

Given the probabilistically bounded $\widetilde{\boldsymbol{I}}$, and to achieve better concurrency and throughput, CPSP addresses the problem defined in Section 4.2 in a two-step approach as follows:

- *Step one*. Controller helps achieve probabilistically bounded $\widetilde{\boldsymbol{I}}$. In this work, $\rho_{R,d}$ is treated as a system parameter. Larger $\rho_{R,d}$ means more accurate probabilistic interference plus noise bound in general.
- *Step two*. Per-packet power control between two consecutive controller adaptations achieve fine-grained packet reception probability guarantee *while trying to maximize network concurrency*.

4.3.3 Step one: Interference plus noise quantile control

In this section, we focus our discussion on a receiver R with its senders $\boldsymbol{S}_{R,d}$. In addition, we still use d to denote the distance between a sender $S \in \boldsymbol{S}_{R,d}$ and the receiver R, i.e., $D(S, R)$, and assume time slot is τ.

Preliminaries We first define a ρ_0-quantile function. Let $\boldsymbol{X}$ be a random variable, and define $\mathcal{Q}_{\rho_0}^{\boldsymbol{X}}$ to be the function that takes the ρ_0-quantile value from the random variable $\boldsymbol{X}$. Let $\boldsymbol{\gamma}(\Theta_{n,R,d})$ be a random variable denoting the SINR (i.e., γ_R) values at R while R is receiving packets between $\Theta_{n,R,d}$ and $\Theta_{n+1,R,d}$. Let $\delta : \boldsymbol{\gamma} \rightarrow [0, 1]$ be the probability measure that maps packet reception SINR values to packet reception probability P. Notice that δ is assumed to be known as detailed in Section 4.2. Let random variables $\boldsymbol{I}_{R,d}(\Theta_{n,R,d})$, $\boldsymbol{\mathcal{N}}_{R,d}(\Theta_{n,R,d})$, $\boldsymbol{\mathcal{P}}_{r,(R,d)}(\Theta_{n,R,d})$, and $\boldsymbol{\mathcal{P}}_{t,(R,d)}(\Theta_{n,R,d})$ denote samples of interference, noise, data packet *reception* power at receiver R, and data packet *transmission* power at senders of R between $\Theta_{n,R,d}$ and $\Theta_{n+1,R,d}$ while sender receiver distance is d. In our later discussions, unless we explicitly mention, packets refer to data packets that are transmitted in data sub-slot.

With δ, $\boldsymbol{I}_{R,d}(\Theta_{n,R,d})$, $\boldsymbol{\mathcal{N}}_{R,d}(\Theta_{n,R,d})$, our goal is to guarantee, for receiver R , $\mathbf{Pr}\{\mathbb{S}|\Theta_{n,R,d}\} \geq p_{R,d}$ with an outage probability of $\rho_{R,d}$ for packet receptions towards $\Theta_{n+1,R,d}$. Let $\gamma_{R,d}^0 = \delta^{-1}(p_{R,d})$ be the *minimum* SINR that guarantees packet reception probability of $p_{R,d}$. $\gamma_{R,d}^0$ tends to be different for different d values. Suppose packet reception probability estimation window of receiver R is ω, then the goal is translated into controlling $\Pr\{\gamma_{R,d}^i(\Theta_{n,R,d}) \geq \gamma_{R,d}^0\} \geq \rho_{R,d}$ for $\forall i$, $i \in [1, \omega]$, where $\gamma_{R,d}^i(\Theta_{n,R,d})$ denotes SINR of the ith packet after $\Theta_{n,R,d}$ at R. Notice that packets considered here are those received while sender receiver distance is d, i.e., $\boldsymbol{\Phi}_{R,d}$.

Per-packet SINR variations after $\Theta_{n,R,d}$ compared to those before $\Theta_{n,R,d}$ are due to the following reasons:

- The adaptation amount $\Delta\mathcal{Q}_{\rho_{R,d}}^{\widetilde{\boldsymbol{I}}_{R,d}}(\Theta_{n,R,d})$ generated by the controller at R in $\Theta_{n,R,d}$ to address changes of interference plus noise within the current exclusion region. $\Delta\mathcal{Q}_{\rho_{R,d}}^{\widetilde{\boldsymbol{I}}_{R,d}}(\Theta_{n,R,d})$ denotes the amount adjusted for $\rho_{R,d}$ quantile of interference plus noise in controller adaptation $\Theta_{n,R,d}$. Variations of background noise $\Delta\boldsymbol{\mathcal{N}}_{R,d}(\Theta_{n,R,d})$ are considered in $\Delta\mathcal{Q}_{\rho_{R,d}}^{\widetilde{\boldsymbol{I}}_{R,d}}(\Theta_{n,R,d})$. Notice that $\boldsymbol{\mathcal{N}}_{R,d}(\Theta_{n,R,d})$ is modeled as a zero-mean random variable. $\mathcal{Q}_{\rho_{R,d}}^{\widetilde{\boldsymbol{I}}_{R,d}}(\Theta_{n,R,d}) + \Delta\mathcal{Q}_{\rho_{R,d}}^{\widetilde{\boldsymbol{I}}_{R,d}}(\Theta_{n,R,d})$ denotes the $\rho_{R,d}$-quantile interference plus noise the controller at R wishes to achieve at $\Theta_{n+1,R,d}$, and we use $\bar{\mathcal{Q}}_{\rho_{R,d}}^{\widetilde{\boldsymbol{I}}_{R,d}}(\Theta_{n+1,R,d})$ to denote this amount. Thus, we have

$$\bar{\mathcal{Q}}_{\rho_{R,d}}^{\widetilde{\boldsymbol{I}}_{R,d}}(\Theta_{n+1,R,d}) = \mathcal{Q}_{\rho_{R,d}}^{\widetilde{\boldsymbol{I}}_{R,d}}(\Theta_{n,R,d}) + \Delta\mathcal{Q}_{\rho_{R,d}}^{\widetilde{\boldsymbol{I}}_{R,d}}(\Theta_{n,R,d}). \tag{4.6}$$

  The actual quantile at $\Theta_{n+1,R,d}$ as a control result, i.e., $\mathcal{Q}_{\rho_{R,d}}^{\widetilde{\boldsymbol{I}}_{R,d}}(\Theta_{n+1,R,d})$, may differ. Therefore, we have

$$\bar{\mathcal{Q}}_{\rho_{R,d}}^{\widetilde{\boldsymbol{I}}_{R,d}}(\Theta_{n+1,R,d}) = \mathcal{Q}_{\rho_{R,d}}^{\widetilde{\boldsymbol{I}}_{R,d}}(\Theta_{n,R,d}) + \Delta\mathcal{Q}_{\rho_{R,d}}^{\widetilde{\boldsymbol{I}}_{R,d}}(\Theta_{n,R,d}) \approx \mathcal{Q}_{\rho_{R,d}}^{\widetilde{\boldsymbol{I}}_{R,d}}(\Theta_{n+1,R,d}). \tag{4.7}$$

- Dynamics of interference beyond the exclusion region when sender receiver distance is d, denoted by $\Delta\boldsymbol{I}_{U,(R,d)}(\Theta_{n,R,d})$. Notice that these senders form the set of $\boldsymbol{S}_{R,d}$.
- Changes of transmission power and attenuation among $\boldsymbol{S}_{R,d}$ and receiver R denoted by $\Delta\boldsymbol{\mathcal{P}}_{r,(R,d)}(\Theta_{n,R,d})$. Notice that we use reception power to represent dynamics in both signal attenuation and transmission power. Shadowing and fading effects are automatically captured by measured signal strength values.

Discussion on orthogonal decision-making With power control and exclusion region adaptations enabled, each receiver has to make decisions on which action to take according to its current packet reception probability statistics in order to provide probabilistic packet reception guarantee. A receiver can independently take two actions: exclusion region adaptation and power control. Intuitively,

- If the packet reception probabilities at receiver R are satisfied, R can reduce either its exclusion region or request transmission power level reduction from senders to make its packet reception probabilities as close to application requirements as possible.
- If the packet reception probabilities at R are not met, R can increase either its exclusion region or request transmission power level increase from senders to make sure its packet reception probability requirements are satisfied.

Note that each receiver strikes to make its packet reception probabilities as close to application required probabilities as possible, this is so that CPSP can improve network concurrency. For the receiver R, changing exclusion regions alone does not affect transmission power, thus its senders will *statistically* not introduce extra interference to neighbors. However, packet reception probability of neighbors will still be affected because network concurrency will change in general. Thus, the factor affected by changing exclusion region are concurrency and packet reception probability. On the other hand, if the receiver R chooses to request its senders to adjust transmission powers, the statistics of interference introduced by its senders seen by neighbors will change. As a result, packet reception probabilities at neighbor links will be affected. This action usually will not affect concurrency since exclusion regions are not altered. It is obvious that both actions affect packet reception probability in their own way.

In this work, we propose to make orthogonal decisions on exclusion region adaptation and power control such that they do not change at the same time. Let us consider the following case for an example. Suppose the receiver R has a very large exclusion region that makes interference plus noise very small, which results in too good packet reception probabilities. Now the sender of R, say S, observes the overshoot in packet reception probability and decides to reduce packet transmission power levels. In the meantime, receiver R decides to reduce its exclusion region because the interference plus noise values it experienced reflects that interference plus noise was over-protected. By reducing reception power and allowing extra amount of interference plus noise, the two *independent* actions at the link $\langle S, R\rangle$ would potentially make its packet reception probability be lower than application requirements. Furthermore, as we will see in future discussions

in Section 4.3.4, power control decisions are based on statistics of sampled results. Since taking samples also takes time, simultaneous decisions on exclusion region adaptations and power control are infeasible in our solution framework. We formally summarize this principle as follows:

Principle 4.1. *At any time for a receiver R and a distance d, the receiver R can only take one action in exclusion region adaptation and power control.*

Notice that when we say take action to do power control, we refer to statistically changing of inputs to the power control action.

Control goal In CPSP, the exclusion region adaptations are no longer aimed to control average interference plus noise. Instead, CPSP targets to control quantile of $\widetilde{\boldsymbol{I}}_{R,d}$ by changing the gPRK model parameter $K_{p_{R,d}}$.

Before we jump into details in controller design, let us define some additional notations. For each receiver R and sender $S \in \boldsymbol{S}_{R,d}$, we define $\mathcal{Q}_{\rho_{R,d}}^{\widetilde{\boldsymbol{I}}_{R,d}}(K_{p_{R,d}}, d)$ as a long-term estimation of the $\rho_{R,d}$ quantile of interference plus noise R has for gPRK model parameter $K_{p_{R,d}}$. The term long-term means a time duration longer than a controller adaptation interval. We also define $\epsilon \geq 0$ as an SINR margin such that when receiver R is receiving packets, and if the condition $\gamma_{R,d}^{0} \leq \gamma_{R,d}^{i} \leq \gamma_{R,d}^{0} + \epsilon$ holds, receiver R stops power control and exclusion region adaptations, where $i \in [1, \omega]$ is an integer. We introduce ϵ to improve network stability.

For decision-making at controller adaptation $\Theta_{n+1,R,d}$, we already have $\widetilde{\boldsymbol{I}}_{R,d}(\Theta_{n,R,d})$ and $\bar{\mathcal{Q}}_{\rho_{R,d}}^{\widetilde{\boldsymbol{I}}_{R,d}}(\Theta_{n,R,d})$. We then can compute $\mathcal{Q}_{\rho_{R,d}}^{\widetilde{\boldsymbol{I}}_{R,d}}(\Theta_{n,R,d})$ from $\widetilde{\boldsymbol{I}}_{R,d}(\Theta_{n,R,d})$ according to the method described in 4.3.9. Let

$$\Delta\widetilde{I}_{g,(R,d)}(\Theta_{n,R,d}) = \bar{\mathcal{Q}}_{\rho_{R,d}}^{\widetilde{\boldsymbol{I}}_{R,d}}(\Theta_{n,R,d}) - \mathcal{Q}_{\rho_{R,d}}^{\widetilde{\boldsymbol{I}}_{R,d}}(\Theta_{n,R,d}). \tag{4.8}$$

$\Delta\widetilde{I}_{g,(R,d)}(\Theta_{n,R,d})$ denotes the difference between ground truth interference plus noise quantile value and the target interference plus noise quantile value the controller at R has set in the latest controller adaptation, i.e., $\Theta_{n,R,d}$. The sign of $\Delta\widetilde{I}_{g,(R,d)}(\Theta_{n,R,d})$ denotes if the $\rho_{R,d}$ probabilistic

interference plus noise upper bound was successful or not. We further let

$$\Delta\gamma_{R,d}(\Theta_{n,R,d}) = \mathcal{Q}^{\boldsymbol{\gamma}_{R,d}}_{1-\rho_{R,d}}(\Theta_{n,R,d}) - \gamma^0_{R,d} - \epsilon. \tag{4.9}$$

The entire controller diagram for controlling interference plus noise probabilistic upper bound is given in Figure 4.2.

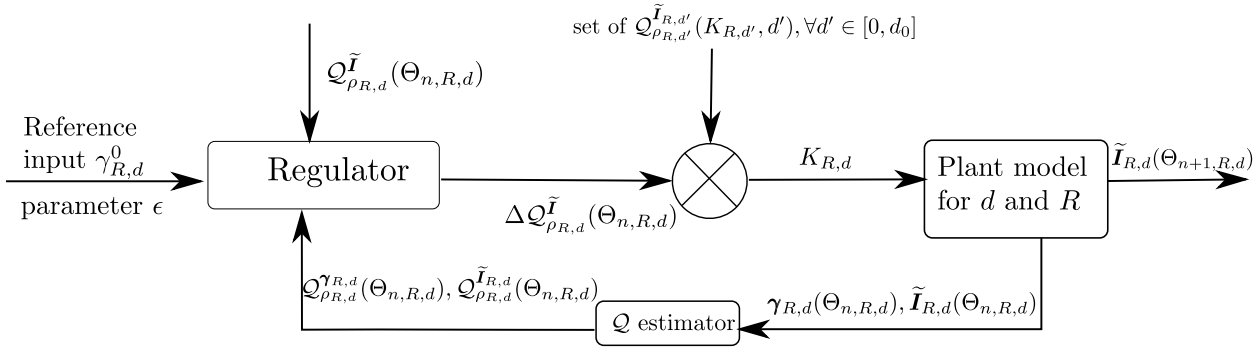

Figure 4.2: Controller diagram for CPSP

The algorithm running in the 'regulator' is briefly described as follows:

1. If $\Delta\widetilde{I}_{g,(R,d)}(\Theta_{n,R,d}) < 0$, interference plus noise is not well bounded. Since interference comes from outside of the coverage area of exclusion region, we definitely need to **increase** exclusion region. In this case, the samples in $\widetilde{\boldsymbol{I}}_{R,d}(\Theta_{n,R,d})$ after $\Theta_{n,R,d}$ and before $\Theta_{n+1,R,d}$ represent the most recent network conditions in terms of interference plus noise. Since the previous quantile was inaccurate in bounding $\widetilde{\boldsymbol{I}}_{R,d}(\Theta_{n,R,d})$, CPSP first uses $\widetilde{\boldsymbol{I}}_{R,d}(\Theta_{n,R,d})$ to update *long-term* quantile for the current gPRK model parameter $K_{p_{R,d}}$, which is $\mathcal{Q}^{\widetilde{\boldsymbol{I}}_{R,d}}_{\rho_{R,d}}(K_{p_{R,d}}, d)$. Then, CPSP uses only $\widetilde{\boldsymbol{I}}_{R,d}(\Theta_{n,R,d})$ samples to compute a different $\rho_{R,d}$ quantile of interference plus noise which denotes the current network conditions. These two quantile values usually should differ. We propose to let vehicles keep records on parameter $K_{p_{R,d}}$, link distance d, and interference plus noise quantile values in a hash map manner such that CPSP can search locally for a gPRK model parameter $K_{p_{R,d}}$ that has a $\rho_{R,d}$ quantile value closest to but greater than $\bar{\mathcal{Q}}^{\widetilde{\boldsymbol{I}}_{R,d}}_{\rho_{R,d}}(\Theta_{n+1,R,d})$. If no satisfactory records were found, CPSP adapts exclusion region for R and distance d and creates a new record

of an association among parameter $K_{p_{R,d}}$, distance d, and quantile of $\widetilde{\boldsymbol{I}}_{R,d}$. Please refer to Section 4.3.8 for details of exclusion region adaptation.

2. If $\Delta\widetilde{I}_{g,(R,d)}(\Theta_{n,R,d}) \geq 0$, we further differentiate the situations as follows:

   (a) If $-\epsilon \leq \Delta\gamma_{R,d}(\Theta_{n,R,d}) < 0$, CPSP recognizes the power assignments and exclusion regions as stable and will keep them fixed since $\Delta\gamma_{R,d}(\Theta_{n,R,d}) \in [0, \epsilon]$. We visualize

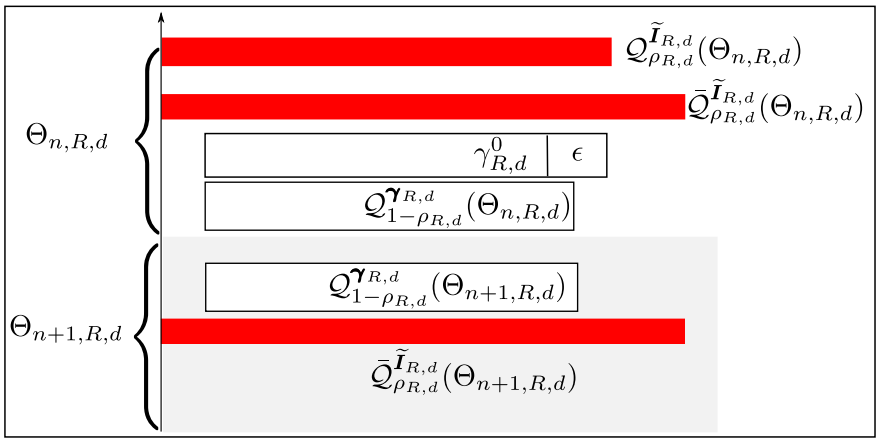

Figure 4.3: Case of stabilized exclusion region and power assignment

   this scenario in Figure 4.3. The figure shows interference plus noise is well-bounded since the actual quantile is smaller. We use longer bars to denote larger amount. This convention applies to both interference plus noise quantiles and SINR quantiles. In this case, the $1 - \rho_{R,d}$ quantile of SINR and the interference plus noise quantile in $\Theta_{n+1,R,d}$ are expected to be the same as in $\Theta_{n,R,d}$ as shown in the gray area.

   (b) If $\Delta\gamma_{R,d}(\Theta_{n,R,d}) < -\epsilon$, given that $\Delta\widetilde{I}_{g,(R,d)}(\Theta_{n,R,d}) \geq 0$ denotes interference plus noise is well-bounded, power control alone is adequate to guarantee packet reception probability. CPSP keeps exclusion region of receiver R regarding distance d fixed. We visualize this case in Figure 4.4. Again, interference plus noise is well-bounded, which denotes our previous exclusion region adaptation was successful. According to our two-step approach and Principle 4.1, we only use power control for performance guarantee, and power control will make sure $\mathcal{Q}_{1-\rho_{R,d}}^{\boldsymbol{\gamma}_{R,d}}(\Theta_{n+1,R,d})$ is no smaller than $\gamma_{R,d}^{0}$.

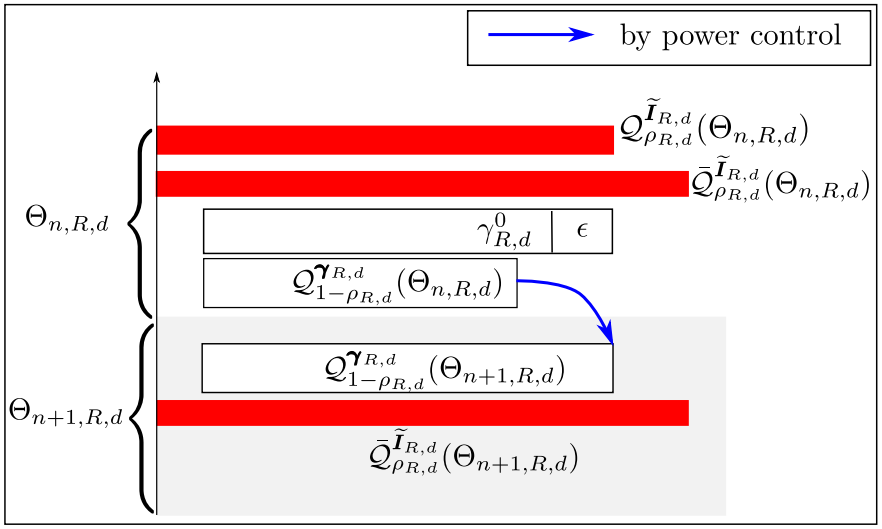

Figure 4.4: Case of unsatisfied SINR constraints when $\widetilde{\boldsymbol{I}}$ is well-bounded

(c) If $\Delta\gamma_{R,d}(\Theta_{n,R,d}) \geq 0$, packet reception probability is satisfied. We have two options to make packet reception probability of R as close to application requirements as possible. These two options are listed as follows:

i. if $\Delta\widetilde{I}_{g,(R,d)}(\Theta_{n,R,d}) > \Delta\gamma_{R,d}(\Theta_{n,R,d})$, since interference plus noise is well-bounded, we **decrease** the exclusion region for receiver R and distance d by an amount of $\Delta\gamma_{R,d}(\Theta_{n,R,d}) - \gamma_{R,d}^{0}$. This amount makes sure when power assignment is not changed, the extra amount of positive $\Delta\gamma_{R,d}(\Theta_{n,R,d})$ disappears due to increased background interference. As visualized in Figure 4.5, the quantile of sampled in-

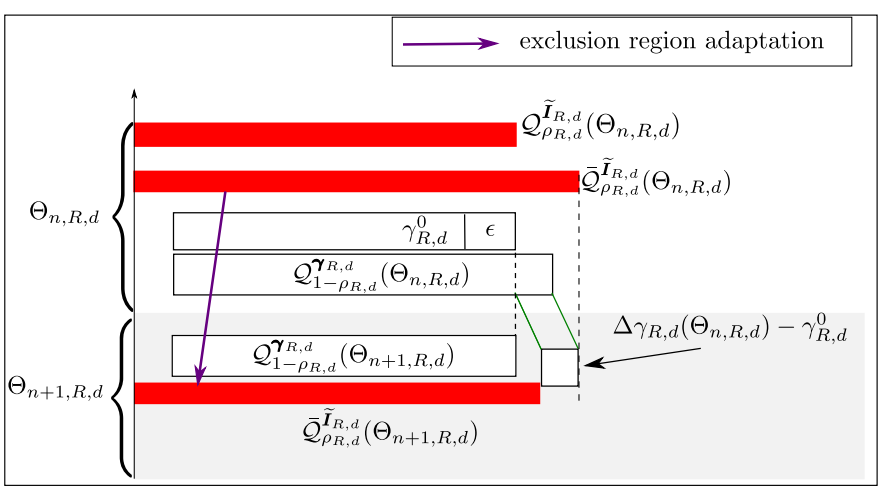

Figure 4.5: Case of over-protected quantile of interference plus noise

terference plus noise is much smaller than controller controlled quantile, we can still reduce the interference plus noise quantile value to achieve a receiver side SINR quantile closest to $\gamma^0_{R,d}$ while interference quantile control is effective. Notice that for SINR, we have $\gamma_{R,d}(\tau) = \mathcal{P}_{t,(R,d)}(\tau) - \mathcal{A}_{R,d}(\tau) - \widetilde{I}_{R,d}(\tau)$, where $\mathcal{P}_{t,(R,d)}(\tau)$ and $\widetilde{I}_{R,d}(\tau)$ are in unit of dBm, $\mathcal{A}_{R,d}(\tau)$ is in unit of dB, and τ is a time slot. The amount of interference we increase will result in the amount of SINR we decrease, statistically. Thus, we have set the amount to be $\Delta\gamma_{R,d}(\Theta_{n,R,d}) - \gamma^0_{R,d}$, and $\mathcal{Q}^{\boldsymbol{\gamma}_{R,d}}_{1-\rho_{R,d}}(\Theta_{n+1,R,d})$ will be no smaller than $\gamma^0_{R,d}$.

ii. if $\Delta\widetilde{I}_{g,(R,d)}(\Theta_{n,R,d}) \leq \Delta\gamma_{R,d}(\Theta_{n,R,d})$, CPSP keeps exclusion region of R for d fixed. Power control alone will be enough to guarantee packet reception probability. As visualized in Figure 4.6, we have interference plus noise well bounded,

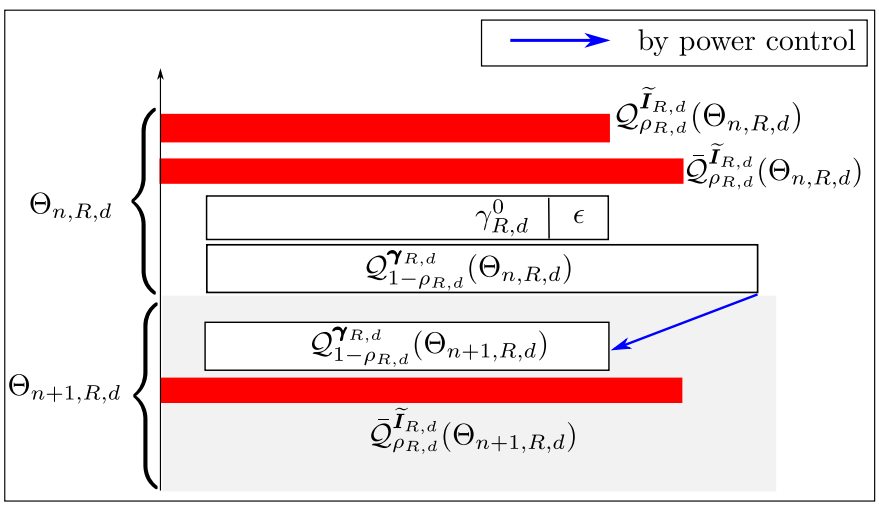

Figure 4.6: Case of too large transmission power level used

and SINR values are much larger than threshold. In fact, the SINR difference with respect to $\gamma^0_{R,d}$ is too large comparing to interference plus noise bound. In this case, we propose to only use power control to reduce SINRs.

The output of the 'regulator' is $\Delta\mathcal{Q}^{\widetilde{\boldsymbol{I}}_{R,d}}_{\rho_{R,d}}(\Theta_{n,R,d})$ as Figure 4.2 shows. From the controller's perspective, it updates $\bar{\mathcal{Q}}^{\widetilde{\boldsymbol{I}}_{R,d}}_{\rho_{R,d}}(\Theta_{n+1,R,d})$ according to Equation 4.7.

Discussion As we have described, a receiver will try to make its packet reception probabilities as close to application requirements as possible for all distance $d' \in [0, d_0]$, due to the nature of broadcast, receivers with smaller sender receiver distance will have better packet reception probabilities as long as their senders try to guarantee packet reception probabilities for all their receivers. The CPS work has shown if a sender guarantees PDR for receivers further away, receivers close-by will automatically have better PDR guaranteed, please refer to Figure 3.27 for details. This observation can give us some guidance on how to share control information, i.e., CPSP can only share information for longer links; if no such links exist, then CPSP shares information for shorter links instead.

4.3.4 Step two: power feedback and assignment

In our previous works on PRK-based scheduling, transmission power levels are fixed for each transmitter. No feedback is need for power level assignment. In CPSP, a receiver needs to provide feedback information to its senders for them to choose transmission power levels. For receiver R to estimate transmission powers $\mathcal{P}_{t,(R,d)}(S, R)$ for its sender S, it needs to know signal attenuation values from distance $d = D(S, R)$ away. Let us use $\boldsymbol{\mathcal{A}}_{R,d}$ to denote these attenuation values. Receiver R also needs to know interference plus noise at R, i.e., $\widetilde{\boldsymbol{I}}_{R,d}$, and the target SINR R wishes to achieve, which is $\gamma^0_{R,d}$. If we consider all of them in unit of dBm or dB, we have $\mathcal{P}_{t,(R,d)} - \boldsymbol{\mathcal{A}}_{R,d} - \widetilde{\boldsymbol{I}}_{R,d} = \gamma^0_{R,d}$. As we will discuss in Section 4.3.7, R will be able to differentiate $\mathcal{A}_{R,d}(\tau)$ and $\widetilde{I}_{R,d}(\tau)$ for a time slot τ. When making decisions on which power level receiver R requests its senders of distance d away to use, R uses Equation 4.10 to compute a transmission power recommendation $\mathcal{P}_{rc,(R,d)}$:

$$\mathcal{P}_{rc,(R,d)} = \gamma^0_{R,d} + \mathcal{Q}^{\widetilde{\boldsymbol{I}}_{R,d}+\boldsymbol{\mathcal{A}}_{R,d}}_{\rho_{R,d}}. \tag{4.10}$$

Since R also has statistics summary of signal attenuations from neighbors for distance d, it explores these neighbor feedbacks by taking EWMA of all *conflicting* neighbors with coefficient e, the neighbors that are closer to R have more weight. For instance, if $e = 0.8$, R_1 is 200 meters away,

but R_2 is 100 meters away from R, then feedback from R_1 is taken into EWMA first, then R_2, and finally R itself. In our evaluation, we set e to be 0.8.

When a sender S is allowed to transmit in a time slot, it inspects transmission power recommendations from all its receivers and choose the maximum transmission power of all recommendations to provide performance guarantee for all its receivers.

4.3.5 Timing of statistics usage

In this section, we sort out the timing of using various sample statistics in CPSP. As we have discussed in Section 4.3.2, senders obtaining instantaneous SINR at receivers side is impossible. Similar arguments applies to signal strength attenuation and interference plus noise too. As a result, we use statistics of samples for decision-making in CPSP. This implicitly indicates delay in using measured data. We show the relation of timing of each sampled data in Figure 4.7. First, we need to realize each node in the network G can be either transmitting node or receiving node as long as it does not send and receive in the same time slot. In Figure 4.7, we use the upper portion of the figure to demonstrate how a node, say R, when acting as a receiver should use sampled data. Let us focus on the controller adaptation $\Theta_{n,R,d}$ in our discussion. Before node R performs the controller adaptation $\Theta_{n,R,d}$, it has sampled packet reception SINR values, and the corresponding interference plus noise and signal strength attenuations from its senders. All these data are used in controller adaptation $\Theta_{n,R,d}$ which happens in a future time with respect to the sampling time instants. Similarly, when a node acts as a sender (as indicated in the bottom portion of the figure), it needs to share its own power recommendations to its future senders in its data packets. As discussed in Section 4.3.4, the node needs statistics of interference plus noise and signal strength attenuation. Since it is infeasible to get any accurate instantaneous samples or estimation of interference plus noise and signal strength attenuation for the sending time slot, CPSP lets the node to use previously obtained samples and the statistics from them. Notice that in power level recommendation calculations, signal strength attenuation and interference plus noise sampled after $\Theta_{n,R,d}$ make no contributions. This decision follows Principle 4.1.

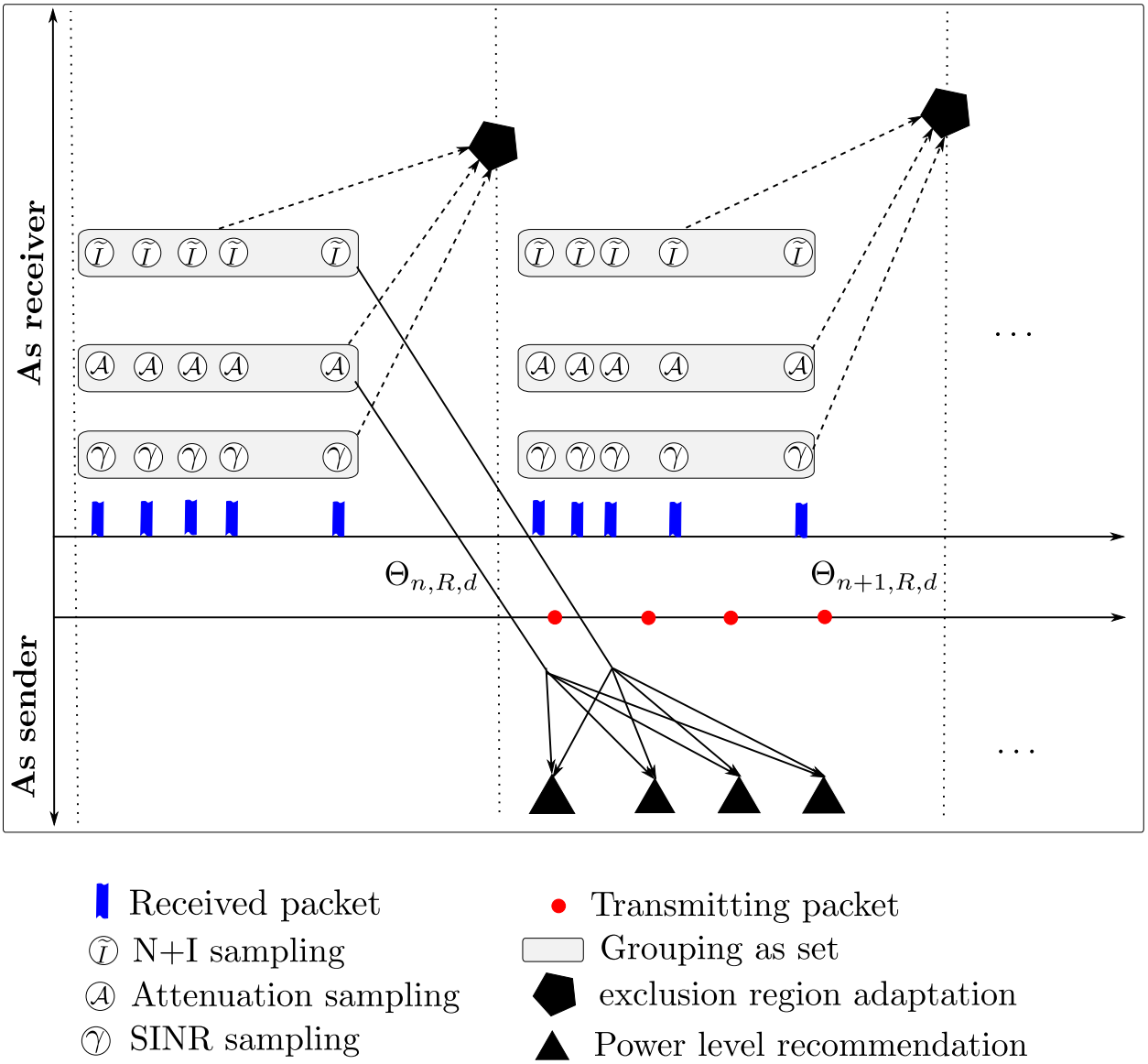

Figure 4.7: Timing of statistics usage of sampled data

In terms of timing of statistics usage, we summarize a principle CPSP follows and give it as follows:

Principle 4.2. *Nodes only use statistics of samples prior to the latest controller adaptations. Data sampled after the latest controller adaptation are used for future decision-making only.*

4.3.6 Link signal strength attenuation sampling

Signal strength attenuation sampling and statistics are important in both distributed scheduling and power control in CPSP, yet the signal map scheme we had in CPS cannot provide us with enough samples due to the following reasons:

- In PRKS or CPS, all signal map records maintain the latest estimation of the *average* signal attenuations among R and its neighbors. Signal maps in our previous works do not have the ability to preserve history records. However, history records are important in estimating signal attenuation statistics.
- Due to information exchange delay and node mobility, the distance between R and any of its senders $S \in \boldsymbol{S}_{R,d}$ changes very fast. The receiver R cannot guarantee the 'current' signal map records are still valid in terms of representing signal attenuations between S and R.
- Signal map records at R only represent communications between R and its neighbors. There are more pairs of nodes that can communicate directly via normal data transmission or control signaling that do not involve R. The signal map maintained by R that only involves R is quite limited. Notice that in CPS, we no longer share signal map records to neighbors due to their overwhelming bandwidth usage.

To be able to estimate link signal strength to overcome node mobilities, we propose to leverage *statistics* from neighbor signal maps and *historical* signal maps. The goal, as we see in Section 4.3.4, is to estimate an upper bound of the sum of signal attenuations and interference plus noise of distance d away. With the help of spatial and temporal signal map records, our estimation can be more accurate. Note that a vehicle should only consider signal map statistics from conflicting neighbors.

As we will discuss in details in Section 4.3.9, we use Cantelli's inequality to compute a probabilistic upper bound of $\boldsymbol{\mathcal{A}}_{R,d} + \widetilde{\boldsymbol{I}}_{R,d}$. To use Cantelli's inequality, we need sample mean,

standard deviation. Therefore, we propose to let each neighbor share its sampled attenuation mean and standard deviation together with distance d. Notice that the information sharing process is selective in the sense that nodes will only share statistics for longer distances unless data for longer distances are unavailable. If data for longer distance is indeed unavailable, nodes will share values for shorter distances instead.

4.3.7 Interference plus noise sampling

For receiver R, it has a gPRK model parameter $K_{p_{R,d}}$ when its its sender is distance d away. For each $S \in \boldsymbol{S}_{R,d}$, when S transmits, R also samples interference plus noise by inspecting SINR and RSSI and solving the following system while it is receiving packets from S:

$$\begin{cases} \mathcal{P}_{r,(R,d)}(S,R) + \widetilde{I}_{R,d} & = RSSI \\ \dfrac{\mathcal{P}_{r,(R,d)}(S,R)}{\widetilde{I}_{R,d}} & = \gamma_R \end{cases} \tag{4.11}$$

In Equation 4.11, variables are in unit of Watt, and $\widetilde{I}_{R,d}$ denotes noise plus interference at R. Thus, the receiver R can create sample records for each gPRK model parameter $K_{p_{R,d}}$. That is, receiver R creates or appends a record in an interference table identified by $K_{p_{R,d}}$ and d locally. When estimating quantile of $\widetilde{I}_{R,d}$, receiver R extracts interference plus noise samples identified by $K_{p_{R,d}}$ and d and feeds interference samples to the quantile estimator in Section 4.3.9. Note that all sampled interference plus noise samples will be removed if they are too old. We propose to remove interference samples that were taken at locations that are now out side of the coverage of its maximum exclusion region.

4.3.8 Exclusion region adaptation

In CPSP, we manage interference plus noise samples as well as its quantile values by distance. With variant transmission power levels, we employ a different scheme for exclusion region adaptation. Since the goal of the controller design is to estimate quantile of interference plus noise given a receiver R and sender receiver distance d, we do not differentiate nodes in exclusion region adaptation. Instead, we take all conflicting neighbors that are of the 'same' distance away

as a whole and calculate their contribution to quantile of interference plus noise. We illustrate the exclusion region adaptation process in Figure 4.8. Suppose the current gPRK model parameter for

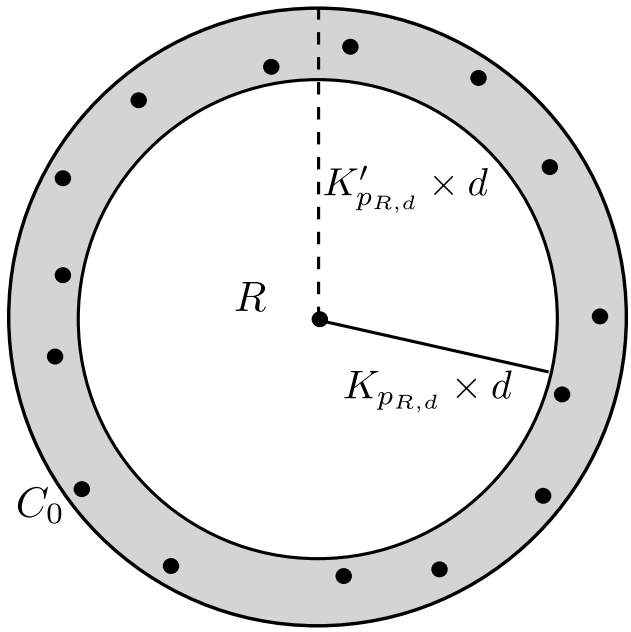

Figure 4.8: Illustration of exclusion region adaptation in CPSP

R with distance d is $K_{p_{R,d}}$, the corresponding quantile of interference plus noise is $\mathcal{Q}^{\widetilde{\boldsymbol{I}}_{R,d}}_{\rho_{R,d}}(\Theta_{n,R,d})$, and the output of the 'regulator' in Figure 4.2 is $\Delta\mathcal{Q}^{\widetilde{\boldsymbol{I}}_{R,d}}_{\rho_{R,d}}(\Theta_{n,R,d})$, receiver R adapts its exclusion region as follows. The receiver R queries addresses of nodes that fall in the gray band as shown in Figure 4.8 during the time from $\Theta_{n,R,d}$ to $\Theta_{n+1,R,d}$. Please keep in mind that the width of the gray band should be kept small, and nodes in the gray band generally may fall in the band at different time slots. In our evaluation, we set the width of the gray band to be one meter. To enable quantile estimation, R also records the data transmission power levels of each node in the gray band, and their corresponding time slots and signal attenuation samples. Let us take C_0 in Figure 4.8 as an example. When C_0 transmits a packet and if R overhears the packet, R decodes the packet and makes a copy of the data transmission power levels C_0 shared in the packet if the transmission power levels are for time slots in which R received data packets. Notice that since C_0 and R could be quite far away from each other, we are referring to control packets here in general. With data transmission power levels and signal attenuation samples, R computes an interference plus noise

for each overheard data transmission power level using the following formula:

$$\widetilde{I}_{R,D(C_0,R)} = \mathcal{P}_{t,(R,D(C_0,R))} - \mathcal{Q}_{\rho_{R,d}}^{\boldsymbol{\mathcal{A}}_{R,D(C_0,R)}}. \tag{4.12}$$

Let $\widetilde{\boldsymbol{I}}_{R,D(C_0,R)}$ denote the set of $\widetilde{I}_{R,D(C_0,R)}$ values computed from data transmission power levels shared by C_0. With all nodes in the gray band, and all such transmission power levels shared from them, R can create a set of interference samples as follows:

$$\widetilde{\boldsymbol{I}}_{\text{gray band}} = \{\widetilde{\boldsymbol{I}}_{R,D(c,R)} | c \text{ falls in gray band}\}.$$

The receiver R then calculates $\mathcal{Q}_{\rho_{R,d}}^{\widetilde{\boldsymbol{I}}_{\text{gray band}}+\widetilde{\boldsymbol{I}}_{R,d}}(\Theta_{n,R,d})$. Then, R assumes the $\rho_{R,d}$ quantile of interference plus noise is this amount. Now, if by considering all nodes in the gray band CPSP still cannot address the adaptation amount $\Delta\mathcal{Q}_{\rho_{R,d}}^{\widetilde{\boldsymbol{I}}_{R,d}}(\Theta_{n,R,d})$, R continues to increase $K'_{p_{R,d}}$ to a slightly larger value until $\Delta\mathcal{Q}_{\rho_{R,d}}^{\widetilde{\boldsymbol{I}}_{R,d}}(\Theta_{n,R,d})$ is accounted for. This explains the situation of exclusion region increase. The exclusion region decrease case is similar in the sense that R considers smaller new $K'_{p_{R,d}}$ values as compared to the original $K_{p_{R,d}}$.

4.3.9 Nonparametric quantile estimation

The goal of interference quantile estimation is to create a mapping $\sigma : (d, K_{p_{R,d}}) \rightarrow \mathcal{Q}_{\rho_{R,d}}^{\widetilde{\boldsymbol{I}}_{R,d}}$ such that for each pair of distance d and gPRK model parameter $K_{p_{R,d}}$, there is a single quantile value of interference plus noise for it. This mapping will be used in exclusion adaptations and transmission power recommendation calculations. Notice that there is no time slot involved in this association since this mapping is evolving and represents the latest estimation. That is, we incorporate history estimation results into our latest samples and update our estimation.

In this chapter, we use Cantelli's inequality to provide one-sided quantile estimation for random variables. Give a random variable $\boldsymbol{X}$ and a real number $k > 0$, the Cantelli's inequality implies

$$\Pr\big(\boldsymbol{X} - \mu(\boldsymbol{X}) \geq k\big) \leq \frac{\sigma(\boldsymbol{X})^2}{k^2 + \sigma(\boldsymbol{X})^2}. \tag{4.13}$$

where $\mu(\boldsymbol{X})$ denotes expectation, and $\sigma(\boldsymbol{X})$ denotes standard deviation of the random variable $\boldsymbol{X}$. For quantile parameter $\rho_{R,d}$, we solve the following equation for k.

$$\frac{\sigma(\boldsymbol{X})^2}{k^2 + \sigma(\boldsymbol{X})^2} = \rho_{R,d}. \tag{4.14}$$

Once we get the value for k, the $\rho_{R,d}$ quantile value for random variable $\boldsymbol{X}$ is obviously $k + \mu(\boldsymbol{X})$.

4.4 Evaluation

We use the same experiment settings as we did in Chapter 3 for urban scenario as depicted in Figure 3.11. We compare our experiment results to CPS in this section. In our evaluation, we set $p_{R,d}$ as 90% with its corresponding expected SINR guarantee $\gamma^0_{R,d}$ as 18.77 dB for all receivers.

4.4.1 Metrics

In the following, we list out the metrics we will use to evaluate CPSP in our evaluation.

- *PDR*. The goal of CPSP is to show how well CPSP can guarantee probabilistic packet successful decode guarantee compared to CPS. As a first step, we compare link-level reliability as we did before, namely PDR.
- *SINR*. As we discussed, we have transformed our problem into SINR guarantee. To better understand our solution, we need to show the SINR values while packet reception, regardless of success or failure of packet reception.
- *Concurrency*. Concurrency is defined as the number of nodes that transmit concurrently in a time slot. Due to more strict requirements on packet reception probability, we expect some loss of concurrency.
- *Transmission power*. We are only interested in data transmission power in this section. We have set our normal transmission power as 16 dBm.
- $\widetilde{\boldsymbol{I}}_{R,d}$ *quantile bound failure rate*. We evaluate the percentage of $\widetilde{\boldsymbol{I}}_{R,d}$ quantile bound failure as a way to show if our fundamental assumption of interference upper bound holds.

4.4.2 CPSP behaviors

In this section, we evaluate the SINR guarantee while nodes are receiving packets. We record SINR values whenever a packet is been received, regardless of packet reception success or

failure. Figure 4.9 shows the difference of the SINR value for each packet η , i.e., $\gamma_{R,d}(\eta)$, and the target SINR value $\gamma^0_{R,d}$. In our evaluation, $\gamma^0_{R,d} = 18.77$ dBm. As the figure shows, most of the SINR values are above the target SINR value $\gamma^0_{R,d}$. Notice that the extremely large SINR values are because of very short distance between a sender and its receiver. Our calculation shows the percentage of $\gamma_{R,d}(\eta) - \gamma^0_{R,d} < 0$ is only 1.571%. We also show the effectiveness of probabilistic

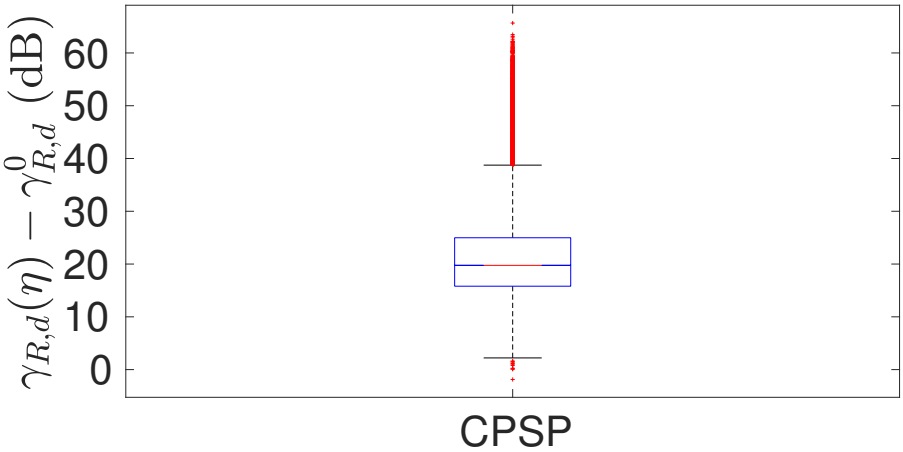

Figure 4.9: SINR guarantee in CPSP

upper bound of $\widetilde{\boldsymbol{I}}_{R,d}$ in Figure 4.10. In our evaluation, we let $\rho_{R,d} = 0.95$. Figure 4.10 shows around 93% of SINR samples are under the quantile bound. Notice that data shown in Figure 4.10 is calculated by $\mathcal{Q}^{\widetilde{\boldsymbol{I}}_{R,d}}_{\rho_{R,d}}$ minus measured $\widetilde{\boldsymbol{I}}_{R,d}$, thus positive difference means effective bound. In

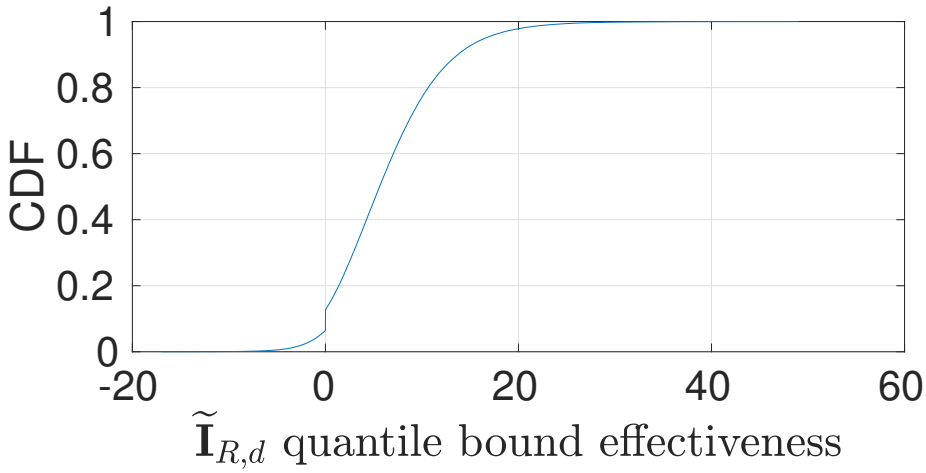

Figure 4.10: Probabilistic upper bound of $\widetilde{\boldsymbol{I}}_{R,d}$ in CPSP

addition, Figure 4.11 shows the transmission power level used by node in data transmission. Notice that in our simulation, transmission power levels are integer levels. The actual transmission power in dBm is the transmission power level plus 16 dBm. We notice that more than 50% of time, normal data transmission power is good enough to guarantee per-packet reception probability as indicated by power level zero in Figure 4.11. However, to overcome unexpected interference due to network dynamics, there are still a large portion of situations where nodes do have to use higher than normal transmission power levels to guarantee packet reception probability. Notice the bottom part of the CDF where power level is negative. This represents situations where a transmitter's receivers are all quite close to itself. As a result, even the standard 16 dBm transmission power is more than enough to guarantee packet reception probability. The probability is quite low, and can represent sparse network situations. In our simulation, this usually happens at places where vehicles are born. As vehicles move, they tend to choose potentially effective roads in the network as decided by SUMO's routing algorithm. Such 'sparse network situation' soon becomes rare since vehicles all choose good roads and are close to each other.

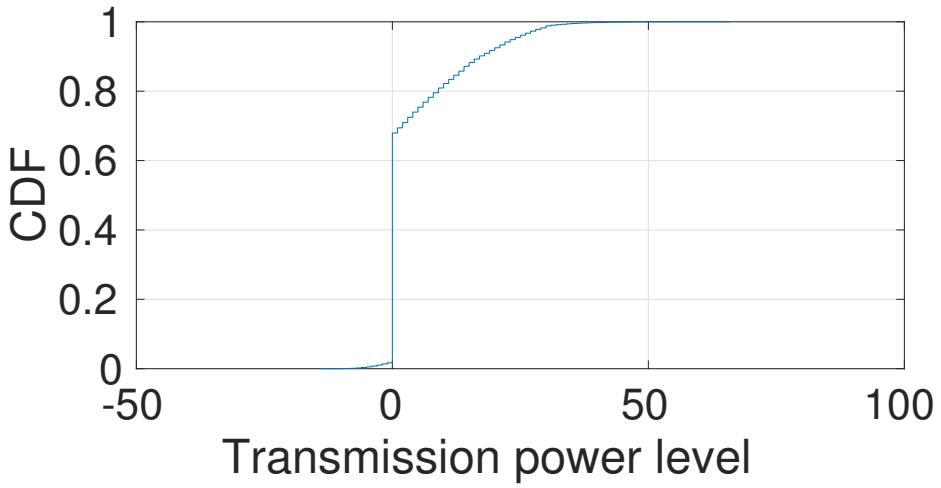

Figure 4.11: Transmission power levels in CPSP

4.4.3 Comparison with CPS

In this section, we compare two key metrics in CPS with those in CPSP. In this section, we set PDR requirement as 90%. When PDR is 90%, the averaged SINR is 18.77dBm. Figure 4.12

shows the CDF of link reliability for both CPS and CPSP. We see that in CPS, there are more than 10% of links whose link reliability requirement cannot be met. In CPSP, while link reliability is met, the achieved link reliability is much higher than application requirement. Figure 4.13 shows the concurrency comparison between CPS and CPSP. We can clearly see the performance loss compared to CPS in terms of concurrency. We also notice that the number of time slots in which there is only one transmitter is larger. Notice that, in our concurrency comparison study, we pair time slots in CPS and CPSP, making sure the comparison is fair.

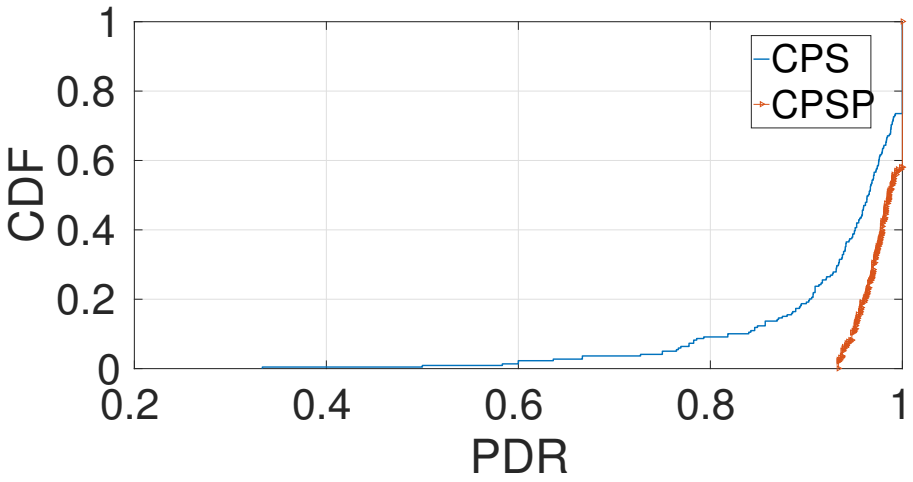

Figure 4.12: PDR comparison between CPS and CPSP

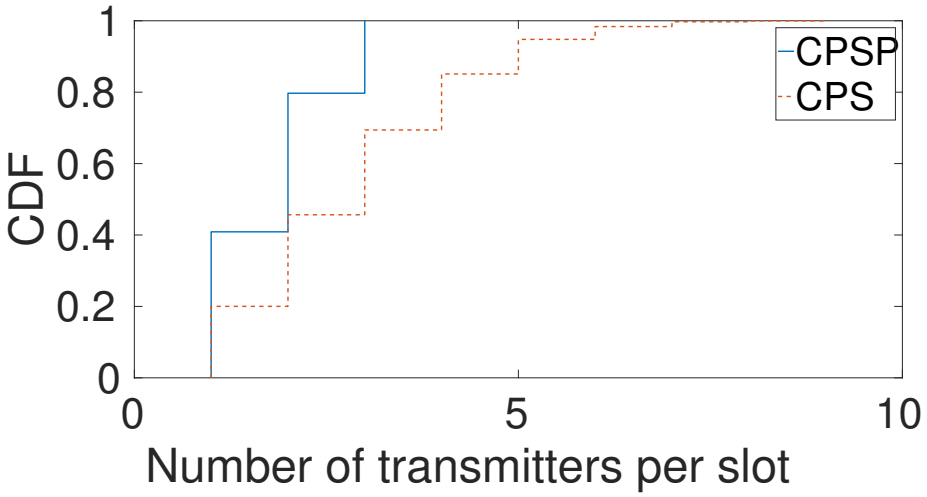

Figure 4.13: Concurrency comparison between CPS and CPSP

4.5 Concluding remarks

This chapter shows that with MAC layer scheduling and per-packet power control, PRK based scheduling framework is able to achieve short-term link reliability in inter-vehicle communication networks. Due to asymmetric wireless channel, non-deterministic concurrent transmitter set and distributed power assignment policy, we conservatively protect packet receptions, thus resulting in lower network concurrency. CPSP has no assumptions for wireless channel model, radio model as well as underlying networks. As a result, it is more realistic than those theoretical analysis works.

CHAPTER 5: CONCLUSION

In this dissertation, we present our research accomplishments in reliable communication in traditional wireless sensor networks and more challenging inter-vehicle communication networks. We employ the PRK interference model for accurate interference relation identification and design a distributed controller to control average link communication reliability in traditional wireless sensor networks. We also give reasons why using the PRK interference model in vehicular networks can be less feasible. We then propose a variant of the PRK interference model called gPRK interference model. We then design a distributed MAC scheduling protocol using the gPRK model. With average link reliabilities guaranteed, we further design a joint power control and scheduling solution to provide more challenging per-packet reception probability guarantee. By achieving per-packet reception probabilities, we expect our techniques described in this dissertation to be a basis for real-time communication solutions that can further be specifically tailored for each wireless networked sensing and control systems for performance optimization.

APPENDIX

Conference Publications

C1. Hongwei Zhang, Xiaohui Liu, Chuan Li, Yu Chen, Xin Che, Feng Lin, Le Yi Wang, George Yin, "Scheduling with Predictable Link Reliability for Wireless Networked Control." *IEEE/ACM International Symposium on Quality of Service (IWQoS)*, 2015

C2. Yuehua Wang, Yu Chen, Chuan Li, Hongwei Zhang, Jayanthi Rao, TJ Giuli, Patrick Gossman, Xiangying Yang, Jing Zhu, "VInsight: Enabling Open Innovation in Networked Vehicle Sensing and Control." *IEEE Network*

C3. Abhimanyu Gosain, Mark Berman, Marshall Brinn, Thomas Mitchell, Chuan Li, Yuehua Wang, Hai Jin, Jing Hua, Hongwei Zhang, "Enabling Campus Edge Computing using GENI Racks and Mobile Resources." *IEEE/ACM Symposium on Edge Computing (SEC)*, 2016

C4. Chuan Li, Hongwei Zhang, Jayanthi Rao, Le Yi Wang, George Yin, "Cyber-Physical Interference Modeling for Predictable Reliability of Inter-Vehicle Communications." *ACM/IEEE International Conference on Internet-of-Things Design and Implementation (IoTDI)*, 2018

REFERENCES

[1] J. Baillieul and P. J. Antsaklis, "Control and communication challenges in networked real-time systems," *Proceedings of the IEEE*, vol. 95, no. 1, pp. 9–28, 2007.

[2] S. Srinivasa and M. Haenggi, "Throughput-delay-reliability tradeoffs in multihop networks with random access," in *Communication, Control, and Computing (Allerton), 2010 48th Annual Allerton Conference on*. IEEE, 2010, pp. 1117–1124.

[3] ns-3. http://www.nsnam.org.

[4] J. Mittag, S. Papanastasiou, H. Hartenstein, and E. G. Ström, "Enabling accurate cross-layer phy/mac/net simulation studies of vehicular communication networks," *Proceedings of the IEEE*, vol. 99, no. 7, pp. 1311–1326, 2011.

[5] H. Zhang, X. Che, X. Liu, and X. Ju, "Adaptive instantiation of the protocol interference model in wireless networked sensing and control," *ACM Transactions on Sensor Networks (TOSN)*, vol. 10, no. 2, p. 28, 2014.

[6] H. Zhang, X. Liu, C. Li, Y. Chen, X. Che, F. Lin, L. Y. Wang, and G. Yin, "Scheduling with predictable link reliability for wireless networked control," in *Proceedings of the IEEE/ACM International Symposium on Quality of Service (IWQoS'15)*, 2015.

[7] C. Li, H. Zhang, J. Rao, L. Y. Wang, and G. Yin, "Cyber-physical interference modeling for predictable reliability of inter-vehicle communications," *arXiv preprint arXiv:1708.04318*, 2017.

[8] X. Liu, H. Zhang, Q. Xiang, X. Che, and X. Ju, "Taming uncertainties in real-time routing for wireless networked sensing and control," *IEEE Transactions on Smart Grid*, vol. 4, no. 1, pp. 288–301, 2013.

[9] H. Zhang, A. Arora, Y.-r. Choi, and M. G. Gouda, "Reliable bursty convergecast in wireless sensor networks," *Computer Communications*, vol. 30, no. 13, pp. 2560–2576, 2007.

[10] H. Zhang, A. Arora, and P. Sinha, "Link estimation and routing in sensor network backbones: Beacon-based or data-driven?" *IEEE Transactions on Mobile Computing*, vol. 8, no. 5, pp. 653–667, 2009.

[11] J. R. Moyne and D. M. Tilbury, "The emergence of industrial control networks for manufacturing control, diagnostics, and safety data," *Proceedings of the IEEE*, vol. 95, no. 1, pp. 29–47, 2007.

[12] G. Brar, D. M. Blough, and P. Santi, "The scream approach for efficient distributed scheduling with physical interference in wireless mesh networks," in *Distributed Computing Systems, 2008. ICDCS'08. The 28th International Conference on*. IEEE, 2008, pp. 214–224.

[13] A.-H. Mohsenian-Rad, V. W. Wong, and R. Schober, "Optimal sinr-based random access," in *INFOCOM, 2010 Proceedings IEEE*. IEEE, 2010, pp. 1–9.

[14] L. B. Le, E. Modiano, C. Joo, and N. B. Shroff, "Longest-queue-first scheduling under sinr interference model," in *Proceedings of the eleventh ACM international symposium on Mobile ad hoc networking and computing*. ACM, 2010, pp. 41–50.

[15] Y. Yi, G. De Veciana, and S. Shakkottai, "On optimal mac scheduling with physical interference," in *IEEE INFOCOM 2007-26th IEEE International Conference on Computer Communications*. IEEE, 2007, pp. 294–302.

[16] G. Zhou, T. He, J. A. Stankovic, and T. Abdelzaher, "Rid: Radio interference detection in wireless sensor networks," in *Proceedings IEEE 24th Annual Joint Conference of the IEEE Computer and Communications Societies.*, vol. 2. IEEE, 2005, pp. 891–901.

[17] M. Sha, G. Xing, G. Zhou, S. Liu, and X. Wang, "C-mac: Model-driven concurrent medium access control for wireless sensor networks," in *INFOCOM 2009, IEEE*. IEEE, 2009, pp. 1845–1853.

[18] R. Maheshwari, S. Jain, and S. R. Das, "A measurement study of interference modeling and scheduling in low-power wireless networks," in *Proceedings of the 6th ACM conference on Embedded network sensor systems*. ACM, 2008, pp. 141–154.

[19] J. I. Choi, M. Jain, M. A. Kazandjieva, and P. Levis, "Granting silence to avoid wireless collisions," in *Network Protocols (ICNP), 2010 18th IEEE International Conference on*. IEEE, 2010, pp. 82–91.

[20] A. Gupta, X. Lin, and R. Srikant, "Low-complexity distributed scheduling algorithms for wireless networks," *IEEE/ACM Transactions on Networking (TON)*, vol. 17, no. 6, pp. 1846–1859, 2009.

[21] J. Ni, B. Tan, and R. Srikant, "Q-csma: queue-length-based csma/ca algorithms for achieving maximum throughput and low delay in wireless networks," *Networking, IEEE/ACM Transactions on*, vol. 20, no. 3, pp. 825–836, 2012.

[22] X. Che, H. Zhang, and X. Ju, "The case for addressing the ordering effect in interference-limited wireless scheduling," *Wireless Communications, IEEE Transactions on*, vol. 13, no. 9, pp. 5028–5042, 2014.

[23] J. L. Hellerstein, Y. Diao, S. Parekh, and D. M. Tilbury, *Feedback control of computing systems*. John Wiley & Sons, 2004.

[24] X. Liu, "Predictable real-time wireless networking for sensing and control," *Wayne State University Dissertations*, vol. 1149, 2015.

[25] J. Huang, S. Liu, G. Xing, H. Zhang, J. Wang, and L. Huang, "Accuracy-aware interference modeling and measurement in wireless sensor networks," in *Distributed Computing Systems (ICDCS), 2011 31st International Conference on*. IEEE, 2011, pp. 172–181.

[26] I. MEMSIC. (2015) Telosb sensor node. http://www.memsic.com.

[27] X. Ju, H. Zhang, and D. Sakamuri, "Neteye: a user-centered wireless sensor network testbed for high-fidelity, robust experimentation," *International Journal of Communication Systems*, vol. 25, no. 9, pp. 1213–1229, 2012.

[28] J. Polastre, J. Hill, and D. Culler, "Versatile low power media access for wireless sensor networks," in *Proceedings of the 2nd international conference on Embedded networked sensor systems*. ACM, 2004, pp. 95–107.

[29] M. Doddavenkatappa, M. Chan, and A. Ananda, "Testbeds and research infrastructure. development of networks and communities," 2012.

[30] (2015) Scheduling with predictable link reliability for wireless networked control. Wayne State University, Tech. Rep. DNC-TR-15-01. https://sites.google.com/site/dnctrs/DNC-TR-15-01.pdf.

[31] K. K. Leung, C. W. Sung, W. S. Wong, and T.-M. Lok, "Convergence theorem for a general class of power-control algorithms," *IEEE Transactions on Communications*, vol. 52, no. 9, pp. 1566–1574, 2004.

[32] L. Bao and J. Garcia-Luna-Aceves, "A new approach to channel access scheduling for ad hoc networks," in *Proceedings of the 7th annual international conference on Mobile computing and networking*. ACM, 2001, pp. 210–221.

[33] W. Ye, J. Heidemann, and D. Estrin, "An energy-efficient mac protocol for wireless sensor networks," in *INFOCOM 2002. Twenty-First Annual Joint Conference of the IEEE Computer and Communications Societies. Proceedings. IEEE*, vol. 3. IEEE, 2002, pp. 1567–1576.

[34] M. Z. n. Zamalloa and B. Krishnamachari, "An analysis of unreliability and asymmetry in low-power wireless links," *ACM Trans. Sen. Netw.*, vol. 3, no. 2, Jun. 2007. [Online]. Available: http://doi.acm.org/10.1145/1240226.1240227

[35] G. Zhou, T. He, S. Krishnamurthy, and J. A. Stankovic, "Models and solutions for radio irregularity in wireless sensor networks," *ACM Transactions on Sensor Networks (TOSN)*, vol. 2, no. 2, pp. 221–262, 2006.

[36] G. Brar, D. M. Blough, and P. Santi, "Computationally efficient scheduling with the physical interference model for throughput improvement in wireless mesh networks," in *Proceedings of the 12th annual international conference on Mobile computing and networking*. ACM, 2006, pp. 2–13.

[37] O. Goussevskaia, Y. A. Oswald, and R. Wattenhofer, "Complexity in geometric sinr," in *Proceedings of the 8th ACM international symposium on Mobile ad hoc networking and computing*. ACM, 2007, pp. 100–109.

[38] L. X. Cai, L. Cai, X. Shen, J. W. Mark, and Q. Zhang, "Mac protocol design and optimization for multi-hop ultra-wideband networks," *IEEE transactions on wireless communications*, vol. 8, no. 8, pp. 4056–4065, 2009.

[39] A. Hasan and J. G. Andrews, "The guard zone in wireless ad hoc networks," *IEEE Transactions on Wireless Communications*, vol. 6, no. 3, pp. 897–906, 2007.

[40] L. B. Jiang and S. C. Liew, "Improving throughput and fairness by reducing exposed and hidden nodes in 802.11 networks," *IEEE Transactions on Mobile Computing*, vol. 7, no. 1, pp. 34–49, 2008.

[41] H. Ma, H. M. Alazemi, and S. Roy, "A stochastic model for optimizing physical carrier sensing and spatial reuse in wireless ad hoc networks," in *IEEE International Conference on Mobile Adhoc and Sensor Systems Conference, 2005.* IEEE, 2005, pp. 8–pp.

[42] K.-J. Park, L. Kim, and J. C. Hou, "Adaptive physical carrier sense in topology-controlled wireless networks," *IEEE Transactions on Mobile Computing*, vol. 9, no. 1, pp. 87–97, 2010.

[43] L. Fu, S. C. Liew, and J. Huang, "Effective carrier sensing in csma networks under cumulative interference," *IEEE Transactions on Mobile Computing*, vol. 12, no. 4, pp. 748–760, 2013.

[44] L. E. Li, R. Alimi, D. Shen, H. Viswanathan, and Y. R. Yang, "A general algorithm for interference alignment and cancellation in wireless networks," in *INFOCOM, 2010 Proceedings IEEE*. IEEE, 2010, pp. 1–9.

[45] Y. Wu, J. A. Stankovic, T. He, and S. Lin, "Realistic and efficient multi-channel communications in wireless sensor networks," in *INFOCOM 2008. The 27th Conference on Computer Communications. IEEE*. IEEE, 2008.

[46] R. T. Al-Zubi and M. Krunz, "Interference management and rate adaptation in ofdm-based uwb networks," *IEEE Transactions on Mobile Computing*, vol. 9, no. 9, pp. 1267–1279, 2010.

[47] S. Lin, J. Zhang, G. Zhou, L. Gu, J. A. Stankovic, and T. He, "Atpc: adaptive transmission power control for wireless sensor networks," in *Proceedings of the 4th international conference on Embedded networked sensor systems*. ACM, 2006, pp. 223–236.

[48] F. Tobagi and L. Kleinrock, "Packet switching in radio channels: Part ii-the hidden terminal problem in carrier sense multiple-access and the busy-tone solution," *IEEE Transactions on communications*, vol. 23, no. 12, pp. 1417–1433, 1975.

[49] S. Louis and Missouri. (2008) Re-port: Cyber-physical systems sum-mit[r]. http://varma.ece.cmu.edu/Summit/CPSSummitReport.pdf.

[50] R. Johri, J. Rao, H. Yu, and H. Zhang, "A multi-scale spatiotemporal perspective of connected and automated vehicles: Applications and wireless networking," *arXiv preprint arXiv:1508.05344*, 2015.

[51] L. Xu, L. Y. Wang, G. Yin, and H. Zhang, "Impact of communication erasure channels on the safety of highway vehicle platoons," *Intelligent Transportation Systems, IEEE Transacti ons on*, vol. 16, no. 3, pp. 1456–1468, 2015.

[52] ——, "Communication information structures and contents for enhanced safety of highway vehicle platoons," *Vehicular Technology, IEEE Transactions on*, vol. 63, no. 9, pp. 4206–4220, 2014.

[53] X. Ma, J. Zhang, and T. Wu, "Reliability analysis of one-hop safety-critical broadcast services in vanets," *Vehicular Technology, IEEE Transactions on*, vol. 60, no. 8, pp. 3933–3946, 2011.

[54] "Ieee standard for wireless access in vehicular environments (wave)–multi-channel operation," *IEEE Std 1609.4-2010 (Revision of IEEE Std 1609.4-2006)*, pp. 1–89, Feb 2011.

[55] J. R. L. Y. W. C. Li, H. Zhang and G. Yin. (2015) Cyber-physical interference modeling for predictable reliability of inter-vehicle communications. Wayne State University, Tech. Rep. DNC-TR-16-01. https://sites.google.com/site/dnctrs/DNC-TN-16-01.pdf.

[56] S. Y. Han, N. B. Abu-Ghazaleh, and D. Lee, "Double regression: Efficient spatially correlated path loss model for wireless network simulation," in *INFOCOM, 2013 Proceedings IEEE*. IEEE, 2013, pp. 1824–1832.

[57] X. Chang, J. Huang, S. Liu, G. Xing, H. Zhang, J. Wang, L. Huang, and Y. Zhuang, "Accuracy-aware interference modeling and measurement in wireless sensor networks," *IEEE Transactions on Mobile Computing*, vol. 15, no. 2, pp. 278–291, 2016.

[58] R. Jain, *The art of computer systems performance analysis: techniques for experimental design, measurement, simulation, and modeling*. John Wiley & Sons, 1990.

[59] M. Treiber and A. Kesting, "Traffic flow dynamics," *Traffic Flow Dynamics: Data, Models and Simulation, Springer-Verlag Berlin Heidelberg*, 2013.

[60] E. A. Wan and R. Van Der Merwe, "The unscented kalman filter for nonlinear estimation," in *Adaptive Systems for Signal Processing, Communications, and Control Symposium 2000. AS-SPCC. The IEEE 2000*. Ieee, 2000, pp. 153–158.

[61] V. Chvatal, "A greedy heuristic for the set-covering problem," *Mathematics of operations research*, vol. 4, no. 3, pp. 233–235, 1979.

[62] X. Liu, Y. Chen, and H. Zhang, "A maximal concurrency and low latency distributed scheduling protocol for wireless sensor networks," *International Journal of Distributed Sensor Networks*, vol. 2015, p. 153, 2015.

[63] D. Krajzewicz, J. Erdmann, M. Behrisch, and L. Bieker, "Recent development and applications of sumo–simulation of urban mobility," *International Journal On Advances in Systems and Measurements*, vol. 5, no. 3&4, 2012.

[64] S. Kokalj-Filipovic, L. Greenstein, B. Cheng, and M. Gruteser, "Methods for extracting v2v propagation models from imperfect rssi field data," in *Vehicular Technology Conference (VTC Fall), 2015 IEEE 82nd*. IEEE, 2015, pp. 1–5.

[65] F. Bai, D. D. Stancil, and H. Krishnan, "Toward understanding characteristics of dedicated short range communications (dsrc) from a perspective of vehicular network engineers," in *Proceedings of the sixteenth annual international conference on Mobile computing and networking*. ACM, 2010, pp. 329–340.

[66] S. Subramanian, M. Werner, S. Liu, J. Jose, R. Lupoaie, and X. Wu, "Congestion control for vehicular safety: synchronous and asynchronous mac algorithms," in *Proceedings of the ninth ACM international workshop on Vehicular inter-networking, systems, and applications*. ACM, 2012, pp. 63–72.

[67] F. Borgonovo, A. Capone, M. Cesana, and L. Fratta, "Adhoc mac: new mac architecture for ad hoc networks providing efficient and reliable point-to-point and broadcast services," *Wireless Networks*, vol. 10, no. 4, pp. 359–366, 2004.

[68] K. Lam, "Design of a medium access control protocol that exploits the structures of vehicular networks," Ph.D. dissertation, General Motors Company, 2011.

[69] F. Farnoud and S. Valaee, "Reliable broadcast of safety messages in vehicular ad hoc networks." in *INFOCOM*, vol. 9, 2009, pp. 226–234.

[70] R. K. Lam and P. Kumar, "Dynamic channel reservation to enhance channel access by exploiting structure of vehicular networks," in *Vehicular Technology Conference (VTC 2010-Spring), 2010 IEEE 71st*. IEEE, 2010, pp. 1–5.

[71] H. Omar, W. Zhuang, and L. Li, "Vemac: A tdma-based mac protocol for reliable broadcast in vanets," *Mobile Computing, IEEE Transactions on*, vol. 12, no. 9, pp. 1724–1736, 2013.

[72] Y.-C. Lai, P. Lin, W. Liao, and C.-M. Chen, "A region-based clustering mechanism for channel access in vehicular ad hoc networks," *Selected Areas in Communications, IEEE Journal on*, vol. 29, no. 1, pp. 83–93, 2011.

[73] R. Mangharam, R. Rajkumar, M. Hamilton, P. Mudalige, and F. Bai, "Bounded-latency alerts in vehicular networks," in *2007 Mobile Networking for Vehicular Environments*. IEEE, 2007, pp. 55–60.

[74] S. Viqar and J. L. Welch, "Deterministic collision free communication despite continuous motion," in *Algorithmic Aspects of Wireless Sensor Networks*. Springer, 2009, pp. 218–229.

[75] R. Zhang, X. Cheng, Q. Yao, C.-X. Wang, Y. Yang, and B. Jiao, "Interference graph-based resource-sharing schemes for vehicular networks," *Vehicular Technology, IEEE Transactions on*, vol. 62, no. 8, pp. 4028–4039, 2013.

[76] G. J. Foschini and Z. Miljanic, "A simple distributed autonomous power control algorithm and its convergence," *IEEE transactions on vehicular Technology*, vol. 42, no. 4, pp. 641–646, 1993.

[77] S. Weber, J. G. Andrews, and N. Jindal, "The effect of fading, channel inversion, and threshold scheduling on ad hoc networks," *IEEE Transactions on Information Theory*, vol. 53, no. 11, pp. 4127–4149, 2007.

[78] C.-H. Liu, B. Rong, and S. Cui, "Optimal discrete power control in poisson-clustered ad hoc networks," *IEEE Transactions on Wireless Communications*, vol. 14, no. 1, pp. 138–151, 2015.

[79] N. Jindal, S. Weber, and J. G. Andrews, "Fractional power control for decentralized wireless networks," *IEEE Transactions on Wireless Communications*, vol. 7, no. 12, pp. 5482–5492, 2008.

ABSTRACT

PREDICTABLE RELIABILITY IN INTER-VEHICLE COMMUNICATIONS

by

CHUAN LI

May 2018

Advisor: Dr. Hongwei Zhang

Major: Computer Science

Degree: Doctor of Philosophy

Predictably reliable communication in wireless networked sensing and control systems (WSC) is a basic enabler for performance guarantee. Yet current research efforts are either focus on maximizing throughput or based on inaccurate interference modeling methods, which yield unsatisfactory results in terms of communication reliability. In this dissertation, we discuss techniques that enable reliable communication in both traditional wireless sensor networks and highly mobile inter-vehicle communication networks. We focus our discussion on traditional wireless sensor networks in Chapter 2 where we discuss mechanisms that enable predictable and reliable communications with no centralized infrastructures. With the promising results in Chapter 2, we extend our methods to inter-vehicle communication networks in Chapter 3. We focus on the broadcast communication paradigm and the unique challenges in applying the PRK interference model into broadcast problems in highly mobile inter-vehicle communication networks. While Chapter 2 and Chapter 3 focus on average reliability, we switch our problem to a more challenging aspect: guaranteeing short-term per-packet reception probability in Chapter 4.

Specifically, we describe the PRKS protocol in Chapter 2 which considers unicast transmission paradigm in traditional static wireless sensor networks. PRKS uses the PRK interference model as a basis for interference relation identification that captures characteristics of wireless communications. For communication reliability control, we design a controller that runs at each link receiver and is able to control the average link reliability to be no lower than an application requirement as well as minimizing reliability variation. We further evaluate PRKS with extensive

ns-3 simulations. The CPS protocol described in Chapter 3 considers an one-hop broadcast problem in multi-hop inter-vehicle communication networks. We analyze the challenges of applying the PRK model in this particular setting and propose an approximated PRK model, i.e., gPRK model, that addresses the challenges. We further design principles that CPS uses to instantiate the gPRK model in inter-vehicle communications. We implement the CPS scheduling framework in an integrated platform with SUMO and ns-3 to evaluate our design.

In Chapter 4, we conservatively estimate the background interference plus noise while nodes are receiving packets. In the meantime, receivers decide minimum power levels their sender should use and feedback their decisions to their senders. Senders fuse feedbacks and choose a power level that guarantees expected packet reception probability at each receivers' side. We notice in our evaluation that guaranteeing short-term reliability causes extra concurrency loss.

AUTOBIOGRAPHICAL STATEMENT

Chuan Li is a Ph.D. candidate in the Computer Science Department at Wayne State University. He received his Bachelor's degree in Computer Science and Technology from Chongqing University (CQU), Chongqing, China in 2008. He also received his Master's degree in Computer System Architecture from CQU. His research interests include ad hoc wireless networks, wireless sensor networks, vehicular ad hoc networks.